ROLES OF *MANDUCA SEXTA* SERPIN-8 AND HEMOLYMPH PROTEINASE-1 IN THE PROPHENOLOXIDASE ACTIVATION SYSTEM

By

FAN YANG

Bachelor of Science in Food Science and Engineering
East China University of Science and Technology
Shanghai, China
2004

Master of Science in Microbial and Biochemical Pharmacy
East China University of Science and Technology
Shanghai, China
2007

Submitted to the Faculty of the
Graduate College of the
Oklahoma State University
in partial fulfillment of
the requirements for
the Degree of
DOCTOR OF PHILOSOPHY
December, 2012

ROLES OF *MANDUCA SEXTA* SERPIN-8 AND

HEMOLYMPH PROTEINASE-1 IN THE

PROPHENOLOXIDASE ACTIVATION SYSTEM

Dissertation Approved:

Dr. Haobo Jiang

Dissertation Adviser

Dr. Jack Dillwith

Dr. Deborah Jaworski

Dr. Andrew Mort

Dr. Sheryl Tucker

Dean of the Graduate College

ACKNOWLEDGEMENTS

I would like to thank my major advisor Dr. Haobo Jiang for his guidance, advice and support during my Ph.D.'s study.

I thank all my committee members, Dr. Jack Dillwith, Dr. Deborah Jaworski, and Dr. Andrew Mort for their instruction, suggestions and encouragement in my research.

I would like to thank members of Dr. Jiang's laboratory for their helpful suggestions. They are Dr. Picheng Zhao, Niranji Sumathipala, Shuguang Zhang, Yingxia Hu, Xiufeng Zhang, Xiaolong Cao, Yan He and Dr. Kai Li. A special thank goes to Yang Wang, Senior Research Specialist, who keeps the laboratory functional, teaches me techniques, and supports my research.

I would like to thank the Department of Entomology and Plant Pathology for the opportunity to study and research at Oklahoma State University. I thank every faculty member in the department for offering useful courses and providing a stimulating environment. I thank Dr. Steve Hartson and Janet Rogers from the DNA/protein Core Facility for mass spectrometry.

I thank my friends for their encouragement. I especially would like to mention long-time friends Yang Shi and Rulan Shangguang, as well as Jiameng Wang.

Finally, I would like to thank my family for their love and support.

Name: FAN YANG

Date of Degree: DECEMBER, 2012

Title of Study: ROLES OF *MANDUCA SEXTA* SERPIN-8 AND HEMOLYMPH PROTEINASE-1 IN THE PROPHENOLOXIDASE ACTIVATION SYSTEM

Major Field: ENTOMOLOGY

Abstract:

Melanization (prophenoloxidase activation) is a major innate immune response in insects, which produces highly toxic and reactive compounds around the wounding or infection. It involves an extracellular serine proteinase pathway which rapidly amplifies responses to infection and stimulate killing of pathogens. Inhibitory regulation of the proteinases by serine proteinase inhibitors (serpins) is important for ensuring a localized defense response.

One immune responsive serpin and one clip domain hemolymph proteinase (HP) from *M. sexta* were investigated. RT-PCR was used to examine gene expression. Proteins were expressed using baculovirus/insect cell system, and purified with various types of columns. Western immunoblotting was performed to analyze protein levels and protein-protein interactions in vitro and in vivo.

M. sexta serpin-8 mRNA and protein levels increased significantly after immune challenge. Similar to *Drosophila* serpin Necrotic, serpin-8 has an N-terminal extension and a Leu at the predicted P1 site. The serpin-8 core domain (serpin-8-ΔN) was expressed and purified. Serpin-8-ΔN has a specificity being able to inhibit elastase- and chymotrypsin-like proteinases and formed inhibitory complexes with chymotrypsin, Cathepsin G, and elastase. Addition of recombinant serpin-8-ΔN to *M. sexta* plasma suppressed proPO activation. *M. sexta* hemolymph proteinase, HP19 and HP14 are highly possible physiological targets of serpin-8.

Two isoforms of hemolymph proteinase-1 (HP1) are present in *M. sexta* hemolymph. The two proteins share 90% amino acid sequence similarity. Recombinant HP1 zymogens and catalytic domains were expressed and purified. Addition of zymogens or catalytic domains of HP1 into plasma resulted in proPO activation. Proteolytic cleavage of proHP6 was observed, when catHP1a alone was added into plasma. ProHP6 cleavage occurred within the catalytic domain when proHP6 was incubated with proHP1a in the presence of detergent. Some hemolymph factor(s) may contribute to the cleavage of proHP6 at its correct activation site, although the identity of such factor(s) is not yet known. HP1 was found to be regulated by *M. sexta* serpin-4 and serpin-5, and the serpin-proteinase complexes formed in an uncommon way.

TABLE OF CONTENTS

Chapter Page

LIST OF TABLES

Table Page

LIST OF FIGURES

Figure Page

Chapter II

Chapter III

Chapter IV

Figure Page

CHAPTER I

INTRODUCTION

Insects are one of the most successful groups of living organisms, accounting for nearly one million species (Hoffmann 1995). During evolution, insects developed a complex and effective innate immune system different from the adaptive immune system of vertebrates to cope with a large variety of pathogens. It has been established that the innate immune system provides an essential first line defense and plays a key role in stimulating and orienting the following adaptive immune responses (Vilmos et al., 1998). It is proven that the innate immune mechanisms of insects share many fundamental characteristics with the innate immune system of vertebrates (Hoffmann et al., 1996).

The innate immune responses of insects have three tightly interconnected reactions (Hoffmann et al., 1996). The first is the proteolytic cascades triggered by wounding or pathogen infection. This is the case of the coagulation cascade leading to blood clotting, and of the prophenoloxidase activating cascade. The second is the cellular immune responses, which mainly consist of phagocytosis and encapsulation of invading microorganisms (Hoffmann 1995). The third is the synthesis of a variety of antimicrobial peptides by fat body and other tissues.

Melanization (prophenoloxidase activation) is an important innate immune defense in many invertebrates. This immune reaction produces toxic quinone substances involved in formation of melanin that physically encapsulates invading pathogens (Cerenius et al., 2008). A complex extracellular serine proteinase cascade is involved in the proteolytic activation of prophenoloxidase (proPO), which is activated by host proteins recognizing conserved surface

components of microorganisms. More than 25 serine proteinase cDNAs have been isolated from *M. sexta* fat body and hemocytes in our laboratory (Jiang et al., 1999; Jiang et al., 2005). Identification of these hemolymph proteinases (HPs) is important to elucidate the roles of serine proteinases in insect innate immune responses. Prophenoloxidase-activating proteinases (PAPs) are among the few serine proteinases with known functions (Wang et al., 2001; Jiang et al., 2003). Two separate pathways leading to proPO activation have been proposed in *M. sexta*, which involves a few key HPs (Wang et al., 2006; An et al., 2009). Other than these HPs with clear functions, most of HPs are not well studied in *M. sexta*. cDNA of *M. sexta* HP1 was isolated earlier and it is reported that HP1 is highly expressed in hemocytes, but not in fat body. No significant change in HP1 mRNA level occurs after immune challenge (Jiang et al., 1999). Little is known about the activation, biochemical activity and biological functions of HP1.

ProPO activation is negatively regulated by **s**erine **p**roteinase **in**hibitors (serpins) of serpin superfamily. Serpins, identified in nearly all species, adopt a conserved tertiary structure and act as suicide substrates by binding covalently to their target proteinases. They regulate a variety of physiological processes and defense mechanisms, such as blood coagulation, inflammation and complement activation. Insect hemolymph contains high concentrations of serpins. They regulate endogenous proteinases generated during immune responses (Kanost, 1999). Several serpins have been well characterized in *M. sexta*. They either directly inhibit PAPs (Jiang et al., 1996; Zhu et al., 2003) or inhibit serine proteinases upstream of PAPs (Zou et al., 2005; Tong et al., 2005) to effectively limit the production of quinones and ensure a localized defense response. *M. sexta* serpin-8 is a newly discovered immune responsive serpin with an N-terminal extension. Its inhibitory specificity and biological function have not been investigated.

My research aims to: (1) express, purify and functionally characterize *M. sexta* serpin-8; (2) express and purify *M. sexta* HP1, and investigate its function in proPO activation system.

CHAPTER II

REVIEW OF LITERATURE

Insect immune system

The immune system provides organisms protection from invasion of a wide range of pathogens. In vertebrates, one component of immunity, the innate immune system fights infections from the very first moment when pathogens invade host organisms and it is considered as the fundamental defense weapon of hosts (Hoffmann 1995). The other component, acquired immunity, which is mediated by white blood cells, takes days to develop an enormous array of antibodies that are able to recognize pathogens that the host may never have encountered before (Kaufmann, 2008). Although innate and acquired immune systems were discovered at around the same time, the knowledge of mechanisms used by acquired immunity quickly outpaced the understanding of innate immunity. The measurement, chemical analysis, purification and structural determination of antibodies became available in the early 1980's (Kimbrell et al., 2001). Understanding of innate immunity requires different methods and perspectives and involves both invertebrates and vertebrates. Innate immunity evolved before the separation of vertebrates and invertebrates (Janeway, 1989), and some organisms exclusively depend on it.

Although they lack acquired immunity, insects are the most evolutionarily successful organisms and account for nearly 90% of all extant animal species. Insects are able to efficiently defend against an extremely large variety of potentially harmful microorganisms (Hoffman, 1995). Many innate immune mechanisms are conserved throughout the animal kingdom

(Kanost et al., 2004). The insect host defense system has many similarities to the basic characteristics of mammalian acute phase response. Consequently, insect innate immunity attracts substantial interests in recent years and studies have led to the discovery of several major interconnected reactions in the immune system.

The insect innate defense begins with the initiation of two proteolytic cascades. One of them leads to localized blood clotting (Iwanaga, 1993b), the other leads to melanization at the wounding site or around invading microorganisms (Söderhäll et al., 1996). Phagocytosis of bacteria by specialized cells and encapsulation of larger organisms by blood cells occur next. Concomitantly, a variety of antimicrobial peptides which are synthesized in the fat body and secreted into hemolymph, act synergistically to kill the invading microorganisms (Osaki et al., 1999).

Genetic study of *Drosophila* provides an opportunity to dissect the development and differentiation of this immune system at the level of transtriptional control (Hoffman, 2003). At the same time, innate immune responses of lepidopteran larvae have been studied for more than 40 years and used as models for biochemical research (Kanost et al., 2004). *Manduca sexta* is used to investigate hemocytes and hemolymph proteins, as the last instar larva reaches 10-12 g, and 1-2 ml of hemolymph can be collected from each individual. It is an ideal subject for protein purification or study of protein interactions that occur in hemolymph.

Recognition of invasive microorganisms

All types of invasive microbes need to be recognized and killed. How does an insect host recognize and destroy all of them? A multilayer defense is involved: the first line is a physical barrier, the exoskeleton or cuticle (Brey et al., 1993). Once this layer is breached, insects use the second layer of defense for recognition of infection. Microorganisms have various surface features that distinguish them from multicellular organisms, which are known as “microbial patterns” and their detectors are thus called “pattern recognition receptors or proteins” (Kang et

al., 1998). Those microbial patterns include β-1,3-glucan of fungi, peptidoglycans (PG), lipopolysaccharide (LPS), and lipoteichoic acid (LTA) of bacteria. Thus, some of the pattern recognition proteins are named as β-1,3-glucan recognition protein (βGRP), peptidoglycan recognition protein (PGRP), Gram-negative bacteria-binding protein (GNBP), hemolin, and lectins (*e.g*. mannose-binding protein) (Gillespie et al., 1997). Upon binding to their target "microbial patterns", pattern recognition proteins undergo a conformational change required for recruiting other plasma factors or hemocytes to eliminate microorganisms (Liu et al., 2001). However, little is known about how such structural changes activate the signaling pathways which result in blood clotting or melanization.

Hemolin is a member of the immunoglobulin superfamily and participates in protein complex formation with bacterial surfaces and is used to initiate phagocytosis (Su et al., 1998). Only lepidopteran hemolin has been identified (Rasmuson et al., 1979; Ladendorff et al., 1990; Lee et al., 2002). No ortholog has been discovered in the *Drosophila melanogaster* or *Anopheles gambiae* genomes. *M. sexta* hemolin is able to bind hemocytes and surface components of bacteria, such as LPS and LTA. Hemolin's ability to bind both hemocytes and bacteria helps to trap bacteria in hemocyte nodules and further clear bacteria from circulation in hemolymph (Ladendorff et al., 1990).

C-type lectins are calcium-dependent carbohydrate-binding proteins. They function as pattern recognition proteins in the vertebrate and invertebrate innate immune systems (Weis et al., 1998). *M. sexta* has at least four immunelectins (IML), immulectin1-4, all of which contain two tandem carbohydrate recognition domains and are highly similar in sequence to such domains in other C-type lectins from insects to mammals. In vitro encapsulation assays showed that *M. sexta* IML-1 and IML-3 enhance cellular encapsulation but not melanization. IML-2 and IML-4 enhance both encapsulation and melanization (Yu et al., 1999; Yu et al., 2000; Yu et al., 2002).

The βGRP family of recognition proteins include a β-1,3-glucanase-like domain in the carboxyl terminus. They bind to β-1,3-glucan but lack the amidase activity, due to amino acid

substitutions in the catalytic center (Ochiai et al., 1999). Up till now, two β-1,3-glucan recognition proteins (βGRPs) have been purified and cloned from *M. sexta* (Ma et al., 2000; Jiang, et al., 2004). They are similar in sequence to *B. mori* βGRP. The *M. sexta* βGRPs aggregate yeasts and bacteria through β-1,3-glucan and LTA (but not LPS). βGRPs have been demonstrated to stimulate the prophenoloxidase activation cascade in several arthropod species. Gram-negative bacteria-binding proteins (GNBPs), first identified in the silkworm (Lee et al., 2003) are other members of the family. *M. sexta* GNBP specifically binds to LTA, LPS, diaminopimelic acid-type peptidoglycans (DAP-PGs) from *E. coli* and *B. subtilis* (Wang et al., 2011).

PGRPs were first characterized in larger insect species, like silkworm through their ability to bind either to intact bacteria or to surface components of bacteria (Yoshida et al., 1996). They are similar in sequence to T7 lysozyme but lack a hydrolytic activity. The differences in structures of the PGRP domains may account for the discrimination between classes of microorganisms. *Drosophila* genome encodes 13 PGRP genes which have been classified to three groups according to its length, short-form, transmembrane long-form and cytoplasmic long-form (Gottar et al., 2002). In short PGRPs, a signal peptide is followed by the PGRP domain. *Drosophila* PGRP-SA and -SD are short secretory proteins binding to Gram-positive bacteria through Lys-type PG (Michel et al., 2001). The long PGRPs contain an N-terminal transmembrane region with a C-terminal PGRP domain. *Drosophila* PGRP-LC is a long form with a transmembrane domain. It recognizes DAP-type PG from Gram-negative bacteria (Ramet et al., 2002). *Drosophila* cytoplasmic PGRP-LE activates the immune deficiency (Imd) pathway when it is overexpressed. It was discovered that mice and humans have four genes encoding PGRP family members (Takehana 2002).

Insect cellular immune responses

The insect immune system consists of cellular and humoral components which work together to protect hosts from a variety of invaders. Cellular immunity refers to immune responses that do not involve antibodies or complement, but rather involve the activation of different types of immune cells. The cellular responses to infection in insects include phagocytosis, nodulation and encapsulation. Hemocytes exhibit changes in morphology from freely circulating cells to aggregates of adherent cells. They are believed to play signaling functions between distant immune responsive tissues via the production of cytokines (Evans et al., 2003).

Insect hemocytes are originated from lymph lobes (Jung et al., 2005). Proliferation and differentiation of *Drosophila* blood cells are under the control of several signaling pathways. The transcription factors involved in these pathways are highly similar to those in the regulation of mammalian hematopoiesis (Evans et al., 2003). Insect hemocytes are classified into a few groups according to their morphology and biological functions (Meister 2005). In *Drosophila*, there are three: plasmatocytes, lamellocytes and crystal cells. Plasmatocytes are phagocytic macrophage-like cells which consist of 90%-95% of the blood cells (Vilmos et al., 1998). They are primarily responsible for phagocytic removal of dead cells and microbial pathogens and tissue remodeling during insect metamorphosis. Unlike the mechanism of phagocytosis in vertebrates, little data is available about the molecular aspects of phagocytosis in insects. A small peptide named plasmatocyte-spreading peptide has been identified in several lepidopteran species (Wang et al., 1999; Skinner et al., 1991). It is present in plasma as an inactive precursor. Once it is activated upon wounding, it stimulates the adhesion of plasmatocytes to the body wall and reduces bleeding. Lamellocytes have a flattened shape and are capable of encapsulation of larger invaders (Rizki et al., 1894). Encapsulation is a multicellular defense mechanism in which a capsule of overlapping layers of hemocytes is formed around protozoans, nemotodes, and eggs or larvae of parasitic insects. Encapsulation may associate with melanization to kill invaders (Strand et al., 1995). Crystal cells constitute 5% of hemocytes. They are nonphagocytic cells involved in

melanizaion. Mature crystal cells express prophenoloxidase (proPO) which mediates the melanization process. They are fragile, ready to disrupt, and release their content into hemolymph upon activation (Rizki et al., 1994). Therefore, they function as storage cells for the large amount of proPO in their cytoplasm in crystallized form.

Insect humoral immune responses

The insect humoral responses parallel the mammalian acute phase responses which are stimulated by injury or bacterial challenge and characterized by the synthesis of acute phase proteins mainly in the liver and blood cells (Vilmos et al., 1998). In insects, humoral responses are also triggered by wound or pathogen infection. The proteolytic cascade leads to three immediate reactions: hemolymph clotting, melanization, and antimicrobial peptides synthesis.

Hemolymph clotting

Hemolymph clotting is an essential mechanism to limit the loss of hemolymph and heal wounds. In arthropods, two types of clotting mechanism have been studied. One was investigated in cockroach (*Leucophaea maderae*) (Bohn et al., 1984) and locust (*Locusta migratoria*) (Dushay 2009). The polymerization of clottable proteins such as lipophorin and vitellogenin-like proteins is catalyzed by a Ca^{2+} dependent transglutaminase released from hemocytes. The other type is well studied in the horseshoe crab (*Lymulus polyphemus*) (Iwanaga et al., 2005). The LPS or β-1,3-glucan mediated clotting is activated by a three-step serine protease cascade, where four serine proteases and one clottable protein (Factors C, G, B, proclotting enzyme and coagulogen) are involved. The last reaction in the cascade is to convert coagulogen to insoluble coagulin gel, resulting in gelation or cell agglutination. A structural homology occurs between the hemolymph clotting enzymes, the complement system and blood clotting of mammals. It is possible that the three proteolytic cascades share a common origin.

Melanization and prophenoloxidase (proPO) activation system

Melanization reaction in insects is associated with multiple host defense mechanisms leading to the sequestration and killing of invading microorganisms (Hultmark 1993). It is controlled by a cascade of serine proteinases that ultimately activates the inactive proPO to active PO which, in turn, catalyzes the formation of quinones. Quinines are precursors for cuticle sclerotization and melanin synthesis. Quinone compounds may also be involved in wound healing and encapsulation of parasites (Jiang et al., 2003).

The key enzyme in the melanization process is phenoloxidase (PO), which is present as a precursor form, prophenoloxidase (proPO), in the hemocytes or in the plasma. POs are probably necessary for insect survival and all insect genomes contain genes for POs (Cerenius et al., 2008). The number of PO genes ranges from 10 in the mosquito *Aedes aegypti* (Waterhouse et al., 2007) to a single PO gene in the honeybee *Apis mellifera* (Zou et al., 2006). POs are primarily produced by specific hemocytes such as crystal cells of *Drosophila*, and oenocytoids in many other insects and the granular hemocyte types in crustaceans (Rizki et al., 1985; Shrestha et al., 2008; Söderhäll et al., 1983). After release, it is either actively transported to cuticle (Ashida et al., 1997) or deposited around wounds and encapsulated parasites (Bidochka et al., 1997). All arthropod POs lack a signal peptide (Ling et al., 2005). It is thus unclear how POs are released from the cells. PO belongs to a class of metalloproteins with type-3 copper centers (Decker, 2007). Arthropod POs are more similar in amino sequence to arthropod hemocyanins which also belong to metalloproteins, than to fungal or mammalian tyrosinases, especially in their copper binding sites (Jiang et al., 1997).

PO is synthesized as an inactive zymogen, proPO which can be activated by proteolytic cleavage at a specific site near the amino terminus (Jiang et al., 2003). It is reported that proPO can also be activated by certain detergent (e.g. cetylpyridinium chloride) that do not cleave peptide bonds, perhaps by inducing a conformational change at the active site (Hall et al., 1995). Two proPOs have been cloned in *M. sexta*, proPO-1 and proPO-2 (Hall et al., 1995; Jiang et al.,

1997). They share 50% sequence similarity and form predominantly heterodimers in *M. sexta* plasma (Jiang et al., 1997). The crystal structure of *M. sexta* proPOs leads to a model for localized proPO activation in insects (Li et al., 2009).

Wounding or exposure to certain pathogens leads to the activation of proPO by a proteinase, named proPO-activating proteinase (PAP) in *M. sexta* (also known as proPO-activating factors or enzyme (PPAF/PPAE) in other insects. Three PAPs have been cloned and studied in *M. sexta*. PAP-1 was isolated from a cuticular extract of *M. sexta* (Wang et al., 2001). PAP-2 and PAP-3 were purified from *M. sexta* hemolymph (Jiang et al., 2003). PAP-2 and PAP-3 contain two amino-terminal regulatory clip domains followed by a carboxyl-terminal catalytic domain, whereas PAP-1 consists of one clip domain at its amino-terminus (Jiang et al., 2003). The solution structure of PAP-2 dual clip domain shows that it includes a probable substrate-binding site, a bacterial-interacting region and a remarkable charged surface for specific association with activator/cofactor (Huang et al., 2007). The three PAPs effectively activate proPO to PO only when in the presence of serine proteinase homologs (SPHs) which are considered as cofactors (Yu et al., 2003). SPHs are similar in amino acid sequence to serine proteinases, but they lack proteolytic activity because their active site serine residues are changed to glycine. Three PPAFs have been identified in the beetle, *Tenebrio. molitor*, and two of them have been crystallized providing details about the activation mechanism (Kan et al., 2008; Park et al., 2007; Lee et al., 2004). Structural evidence of PPAFs has shown that upon activation, PPAF-II (a SPH) oligomerises and its clip-domain is responsible for binding of PO. This interaction ensures that active PO is under tight control and that the active PO is not spread through the hemolymph in an uncontrolled manner, but stays in the local area of activation cascade (Piao et al., 2007).

Although PO-generated compounds are powerful weapons to fight against pathogens, they can also be harmful to host tissues and cells (Zhao et al., 2007). The need for a tight temporal and spatial control of its activity is obvious. Several critical steps in the proPO

activation pathway are carried out by specific serine proteinases and serine proteinase inhibitors (serpin) prevent premature and excessive activation. These inhibitors are present at high concentrations in insect hemolymph.

Synthesis of antimicrobial peptides

The hallmark of the humoral immune response is the systematic antimicrobial response. It corresponds to the challenge-induced synthesis of a variety of antimicrobial peptides (AMPs) by the fat body (Sondergaard, 1993) and release into the hemolymph where they readily reach their effective concentrations. Fat body, a functional equivalent of mammalian liver and adipose tissues, synthesizes most of AMPs, due to its large size and its location inside the open circulatory system. Other tissues, such as hemocytes, cuticular epithelial cells, gut, and salivary glands also produce AMPs (Boman, 1991; Brey et al., 1993). Injection of bacteria into the hemocoel induces the production of AMPs in the hemolymph of *Drosophila*. Some AMPs are very stable due to the presence of intramolecular disulfide bonds and are detectable in the hemolymph several weeks after the challenge. The number of insect AMPs is large: over 100 have been reported so far. Many AMPs have low molecular weights. Although they are diverse in structure, many AMPs are amphipatic, acting at membranes to kill microbes by lysis. According to their structures, AMPs are divided into a least two major classes: the cyclic peptides containing disulfide bonds, and the linear peptides lacking cysteines (Hoffman et al., 1996).

The most prominent peptides in the cyclic group are the 4 kDa anti-Gram-positive bacterial insect defensins and the 5 kDa antifungal peptide drosomycin. Insect defensins are cationic peptides containing six conserved cysteins engaged in three disulfide bridges (Cornet et al., 1995). About 30 defensins have been characterized in various insect species, such as *Aedes*, *Anopheles* and *Drosophila* (Lowenberger et al., 1995; Dimarcq et al., 1994). The sequence similarity is high among these insect defensins and the overall structure is strictly conserved. Insect defensins are not homologous to mammalian and plant defensins. Drosomycin contains 8

cysteines engaged in intramolecular disulfide bridges. It exhibits potent antifungal activity but is inactive against bacteria. Drosomycin, shows a significant homology with a family of 5 kDa cysteine-rich plant antifungal peptides isolated from seeds of *Brassicaceae*, indicating that plants and insects can rely on similar molecules in their innate host defense (Fehlbaum et al., 1994).

There are mainly three families in the linear group: cecropins, proline-rich peptides, and glycine-rich peptides. Cecropins (4 kDa) are strongly cationic, amphipatic and cause instantaneous lysis of bacterial cells through disintegration of their cytoplasmic membranes. Thus, cecropins have antibacterial activity against both Gram-positive and Gram-negative bacteria (Boman, 1994). Proline-rich peptides are those with molecular mass of 2-4 kDa, lacking cystein and containing at least 25% proline. They are primarily active against Gram-negative bacteria by increasing the membrane permeability (Hetru et al., 1994). The glycine-rich family includes several 9-30 kDa polypeptides, all of which have a high percentage of glycine residues (10-22%). They are mainly active against Gram-negative bacteria (Lee et al., 1995).

The identification of AMPs was followed by analysis of the challenge-induced control of their expression in the early 1990s. By the mid-to-late 1990s, it was discovered that the expression of AMP genes depends on two members of the nuclear factor-κB (NF-κB) family in *D. melanogaster*, DIF (dorsal-related immunity factor) and Relish. DIF and Relish are responsive to fungal and bacterial infection respectively through two distinct signaling pathways, known as the Toll and immune deficiency (Imd) pathways (Lemaitre et al., 2007).

The Toll pathway activation accounts primarily for response to fungi and Gram-positive bacteria. It involves several factors that were initially discovered in the control of dorsoventral patterning in the embryo and it is parallel to the mammalian signaling cascades downstream of the interleukin-1 receptor (IL-1R) and the Toll-like receptors (TLRs) (Hoffman, 2003). *Drosophila* Toll is a transmembrane receptor, consisting of an extracellular leucine-rich repeat and intracellular signaling domain. The key player in the activation of Toll pathway is a cysteine-knotted cytokine-growth factor-like polypeptide, spätzle which is activated at the end of a

proteolytic cascade (Lemaitre et al., 1996). The binding of spätzle to Toll activates the signaling pathway which leads to the dissociation of NF-κB-like protein, Dorsal, and Dif from their inhibitory protein, the IκB-like protein, Cactus.

The Imd pathway is similar to the tumor-necrosis factor-receptor (TNF-R) pathway in mammals (Hoffmann et al., 2002). It is primarily, although not exclusively, involved in defense against Gram-negative bacteria, and most AMPs controlled by this pathway are predominantly active against Gram-negative bacteria, such as cecropins, attacins, drosocin, diptericins. Initiation of the Imd pathway requires a transmembrane PGRP, PGRP-LC. However, the mechanisms by which PGRP-LC activates the Imd pathway remain unclear. Relish, the NF-κB-like protein involved in this pathway is not inhibited by Cactus, but has its own inhibitory domain in its carboxy-terminal region (Dushay et al., 1996). Activation of Relish requires a signal-induced proteolytic cleavage that dissociates the Rel-homology domain from its inhibitory domain and allows its nuclear translocation.

Although some immune-induced genes are clearly dependent on one pathway only, others can be induced by both cascades. *Drosomycin* gene is such an example. It is easily induced by the Toll pathway, but it also can be induced by the Imd pathway in the systemic response and is only activated by the Imd pathway in the local response (Tzou et al., 2000). Therefore, a question is whether the two pathways can synergistically increase the expresion of some immune-response genes. It is partially supported by a bioinformatics analysis which shows that κB binding sites are specific for either Toll or Imd pathway activation (Leulier et al., 2000).

Serine proteinases and serine proteinase pathways

Fat body and hemocytes produce and secrete a variety of plasma proteins with direct antimicrobial activity or with indirect functions in insect immune responses. One group of proteins plays an important role in signal transduction by forming a network of extracellular serine proteinase. Components of this network have a Ser residue in their active site.

Among them, *M. sexta* PAP-1, PAP-2 and PAP-3 belong to a subfamily of arthropod serine proteinases that contain at least one amino-terminal clip domain and a carboxyl-terminal proteinase domain. The clip domain was first identified in proclotting enzyme from the horseshoe crab (*Tachypleus tridentatus*) (Jiang et al., 2000). Typical clip-domain proteinases consist of an amino-terminal regulatory clip domain, a catalytic serine proteinase domain and a linker connecting the two domains. Clip domains are 37-55 amino acid residue sequences which are tethered together by three pairs of disulfide bonds to form a compact "paper clip-like" structure. The function of a clip domain is largely unclear, but it might play an important role in protein-protein interactions, since most of the clip-domain serine proteinases are involved in signal-amplifying cascade reactions (Jang et al., 2008). The clip-domain serine proteinases are synthesized as zymogens and need to be activated by a specific proteolytic cleavage between the clip domain and the catalytic domain. After cleavage, a pair of cysteine residues still links the two domains such that when the proteinase is activated, the catalytic heavy chain remains covalently attached by the disulfide bond to the light chain which includes the clip domain (Fig.1). The clip-domain serine proteinases have been found in different insect species and participate extensively in the immune reactions. In addition to clip-domain serine proteinases, other serine proteinases have also been identified as member of the cascade.

Sequential activation of extracellular serine proteinase cascades regulates important innate immune reactions, hemolymph clotting, melanization, and AMP synthesis as mentioned above. These proteolytic cascades have a functional core consisting of several serine proteinases that undergo zymogen activation, upon cleavage by an upstream proteinase. Biochemical studies performed in *T. molitor* and *M. sexta*, and genetic analysis in *D. melanogaster*, reveal striking similarities in the mechanisms underlying serine proteinase activation by microbial invaders (Fig. 2). All involve the sequential activation of an apical modular serine proteinase (that displays a certain level of autoactivation) and clip-domain proteinases (Buchon et al., 2009).

In *M. sexta*, HP14 is converted to the active form in the presence of β-1,3-glucan and βGRP1 or βGRP2 (Wang et al., 2006). Binding of β-1,3-glucan and recognition proteins triggers the autoactivation of proHP14 into HP14, which then processes proHP21 (Wang et al., 2007). In turn, HP21 cleaves proPAP-2 (or proPAP3) into PAP2 (or PAP3) that finally activates proPO in the presence of SPHs (Gorman et al., 2007). In *T. molitor*, binding of PG to the PGRP-SA/GNBP1 complex induces autoactivation of a *Tm*-modular serine proteinase zymogen (*Tm*-MSP) (Fig. 2). *Tm*-MSP in turn generates another serine proteinase *Tm*-SAE (SPE activating enzyme). Active *Tm*-SAE cleaves precursor of *Tm*-SPE (spätzle-processing enzyme), which results in the activation of spätzle and proPO (Kan et al., 2008).

The *Drosophila* Toll pathway establishes the dorsoventral axis during embyronic development (Fig. 2). A large mosaic protein named Nudel autoactivates and activates the zymogen form of Gastrulation defective (Gd), the upstream activating proteinase of Snake. The active Snake, a clip-domain serine proteinase cleaves to activate a downstream clip-domain protein, Easter. Easter is a serine proteinase which processes spätzle to become a functional Toll ligand that ventralizes the embryo (Lemaitre et al., 2007). A similar proteinase cascade occurs in *Drosophila* as in *T. molitor* such that, upon microbe challenge, binding of PG to the PGRP-SA/GNBP1 complex induces activation of a modular serine proteinase zymogen. *Dm*-MSP in turn activates another serine proteinase Grass to cleave *Dm*-SPE. *Dm*-SPE generates active spätzle and turns on the Toll-AMP intracellular pathway.

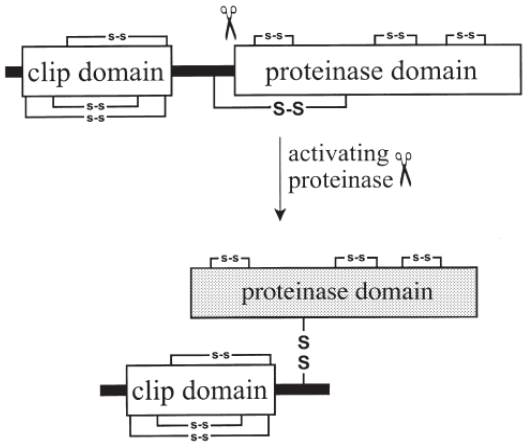

Figure 1. Domain organization of clip-domain proteinases. The proteinases contain at least one amino-terminal clip domain followed by a linker region of variable length and a carboxyl-terminal serine proteinase domain. A disulfide bond connects the linker region to the proteinase domain. When the proteinase zymogen is activated by a specific proteolysis, the clip domain and the proteinase domain remain covalently linked to each other (Jiang et al., 2000).

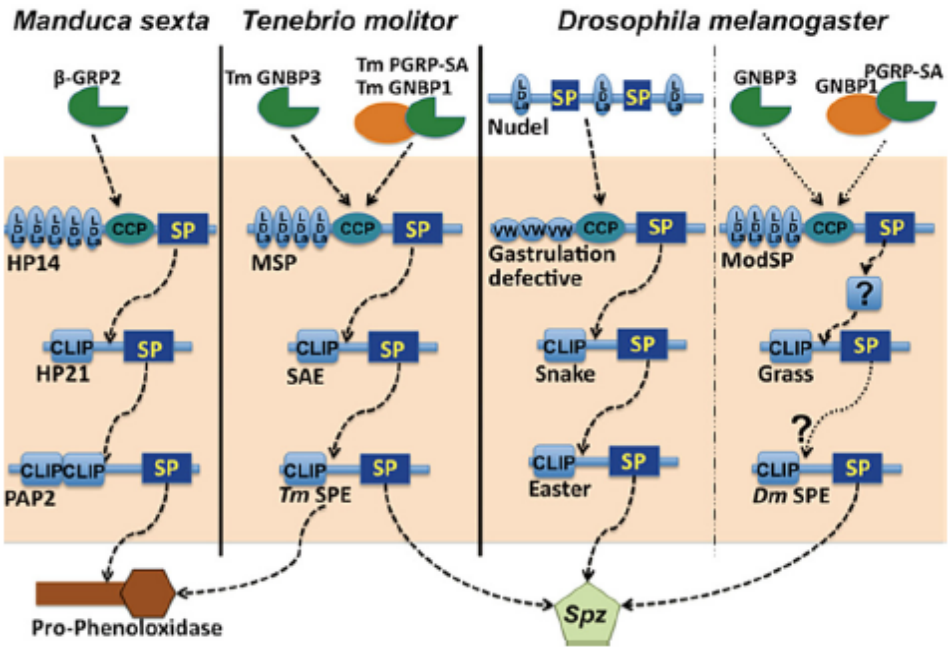

Figure 2. Extracellular cascades of serine proteinases in insects. Biochemical studies performed in *T. molotor* and *M. sexta*, and genetic analysis in *D. melanogaster*, reveal striking

similarities in the mechanisms underlying serine proteinase activation by pattern recognition proteins (Buchon et al., 2009).

Regulation of serine proteinases by serpins

Serpins are 50 kDa serine proteinase inhibitors present in nearly all species. They are suicidal inhibitors that form covalent acyl complex with their target proteinases. Serpins were first identified in humans and the most intensively-studied ones are human plasma proteins named antitrypsin and antithrombin. Serpins regulate a variety of physiological processes and defense mechanisms, such as blood coagulation, inflammation and complement activation. In humans, several serpin mutations are linked to diseases, for example emphysema and blood-coagulation disorders (Reichhart 2005).

Serpins, about 350-400 amino acids long, contain a single domain. Some serpins have an N-terminal or C-terminal extension, such as *Drosophila* serpin, Necrotic and *M. sexta* serpin-3. The serpin tertiary structure consists of three beta-sheets (A, B and C), and 7-9 alpha-helices. There is an exposed C-terminal reactive center loop (RCL) which acts as bait for the target proteinase (Gettins, 2002). The P1 residue located in the RCL determines primary specificity of inhibition. When a serpin binds to its target proteinase, the proteinase cleaves a scissile bond between residues P1 and P1' within the RCL and is trapped into the backbone carbonyl of the P1 residue via a covalent ester linkage with the active site Ser. The RCL then inserts into beta-sheet A in the serpin core structure and displaces the proteinase (Ye et al., 2001). The proteinase is dragged to the other side of the serpin with its active site distorted, while the RCL is completely inserted into beta-sheet A. Serpins are identified as inhibitory based on several specific residues in the hinge and RCL regions. Counting down toward P1 site, there is a consensus inhibitory pattern: P17 (E), P16 (E/K/R), P15 (G), P14 (T/S), P12-P9 (A/G/S), which is required for efficient insertion of the RCL into beta-sheet A in the serpin core structure (Reichhart 2005). Non-inhibitory serpins have divergent and shorter sequences in this region.

Insect hemolymph contains a high concentration of serpins. They may regulate endogenous proteinases generated during immune responses (Kanost, 1999). The proPO activation pathway, an effective way for wound healing and microbe killing, produces quinones that polymerize to form melanin. But quionones are toxic to hosts (Zhao et al., 2007) and should be highly regulated as a local, transient reaction against invaders. Several serpins have been identified in *M. sexta*. *M. sexta* serpin-1 is a mixture of 12 proteins resulting from mutually exclusive alternative splicing. These proteins differ in inhibitory selectivity because each of them contains a different reactive center loop (Jiang et al., 1996). Two of the 12 serpin-1 isoforms have been found to form complex with *M. sexta* serine proteinases. Serpin-1J can inhibit activation of proPO and form SDS-stable complex with PAP-3 in vitro (Jiang et al., 2003). Serpin-1I contributes to inhibition of HP14 (Wang et al., 2006). *M. sexta* serpin-2 is expressed in hemocytes and is located in the cytoplasma. The target proteinase of serpin-2 is unknown. *M. sexta* serpin-3 has been demonstrated to block proPO activation by inhibition of PAP-3 (Zhu et al., 2003). *M. sexta* serpin-6 also strongly inhibits PAP-3. There are other serpins which inhibit upstream proteases of the cascade (Zou et al., 2005). *M. sexta* sepin-4 is found to inhibit HP1, HP6 and HP21, and *M. sexta* serpin-5 is an inhibitor of HP1, HP6 and two other unknown proteinases (Tong et al., 2005).

In the *Drosophila* genome, there are 29 serpin genes (Irving et al., 2000). Analysis shows that 17 out of 29 have hinge and RCL regions that correspond to active, inhibitory serpins, and 19 out of 29 have a signal peptide. Among the 17 active inhibitors, 12 are secreted and five intracellular. Seven and five of the non-inhibitory serpins are extra- and intracellular respectively. Only a few *Drosophila* serpins have been studied in detail. *Drosophila* serpin43Ac (Necrotic) is reported to be responsible for the control of serine proteinases in the Toll pathway (Levashina et al., 2003). It negatively regulates one or more serine proteinases that participate in spätzle activation after infection. The *serpin43Ac* is located in a cluster of four serpin genes in chromosome 43A. Deletion of the three other transcripts, serpin43Aa, serpin43Ab and

serpin43Ad has no effect on the Toll pathway. The activation of the melanization process is regulated by *Drosophila* serpin27A, orthologous to *M. sexta* serpin-3. Loss-of function mutations in serpin27A lead to a high rate of spontaneous melanization and constitutively increased PO activity in the blood (Ligoxygakis et al., 2002). In addition to its function in immunity, serpin27A also plays a role during early embryogenesis. It directs dorso-ventral axis formation in early development by restricting the activation of a proteolytic cascade to the ventral part of the embryo. Similar to *M. sexta serpin-1* and *Drosophila serpin42Da* encodes at least 10 isoforms that differ at both the N-terminus and C-terminus (Kruger et al., 2002). One isoform, serpin42DaA forms an SDS-stable complex with human furin and with its *Drosophila* homolog, subtilisin-like PC2. The existence of non-inhibitory serpins strengthens the possibility of divergent functions. *Drosophila* serpin76A, one of the non-inhibitory serpins, may function in binding hydrophobic hormones and transport function in *Drosophila* (Coleman et al., 1995).

Table 1. List of abbreviations

AS	ammonium sulfate	NF-κB	nuclear factor-κB
AMP	antimicrobial peptide	PG	peptidoglycans
CPC	cetylpyridinium chloride	PGRP	peptidoglycan recognition protein
CH	control hemolymph	PO	phenoloxidase
clip-SP	clip domain serine proteinase	proPO	prophenoloxidase
DAP-PG	diaminopimelic acid-type peptidoglycan	PAP	PO-activating proteinase
DS	dextran sulfate	POI	phenoloxidase inhibitor
DIF	dorsal-related immunity factor	PPAF	proPO-activating factor
βGRP	β-1,3-glucan recognition protein	RCL	reactive center loop
GNBP	Gram-negative bacteria-binding protein	rpS3	ribosomal protein S3
HP	hemolymph proteinase	SP	serine proteinase
Imd	immune deficiency	SPH	serine proteinase homolog
IML	immunelectins	SERPIN	serine proteinase inhibitor
IH	induced hemolymph	SPE	spätzle-processing enzyme
IL-1R	interleukin-1 receptor	SAE	SPE activating enzyme
LPS	lipopolysaccharide	TNF-R	tumor-necrosis factor-receptor
LTA	lipoteichoic acid	TLR	Toll-like receptor
MSP	modular serine proteinase		

CHAPTER III

EXPRESSION, CHARACTERIZATION AND FUNCTIONAL STUDY OF *MANDUCA SEXTA* SERPIN-8

Introduction

Phenoloxidase (PO) is important in defense against pathogens and parasites in insects. PO catalyzes the hydroxylation of a monophenol to an *o*-diphenol, and the oxidation of *o*-diphenol to *o*-quinone. The toxic quinone intermediates and *o*-quinones polymerize to form melanin at the injury spot or around invading microorganisms (Hultmark 1993). The melanization process involves prophenoloxidase (proPO) activation, in which the inactive form of proPO is converted to the active enzyme PO (Kim et al., 2005). ProPO activation in insects is mediated by a serine proteinase cascade, similar to the blood clotting system and complement system in vertebrates (Ashida et al., 1997). In the presence of pathogens, components of this cascade become activated sequentially via limited proteolytic cleavage.

Due to the toxic nature of products of the melanization process (Zhao et al., 2007), plasma serpins regulate the proPO activation pathway. Serpins are serine proteinase inhibitors about 50 kDa with an exposed reactive center loop (RCL) near their carboxyl terminus. The P1 residue located in RCL determines the primary specificity of inhibition (Gettins, 2002). Several serpins from *M. sexta* have been characterized previously. *M. sexta* serpin-1 is a mixture of 12 proteins resulting from mutually exclusive alternative splicing (Jiang et al., 1996). Nine out of 12 isoforms of *M. sexta* serpin-1 have been separated

and identified in plasma using two-dimensional PAGE and MALDI-TOF/TOF analysis (Ragan et al., 2010). *M. sexta* serpin-3 was recently found to inhibit HP8 (Christen et al., 2012) besides PAP-3 (Zhu et al., 2003). *A. gambia* serpin-6 (AgSRPN6) controls melanization by forming a complex with *M. sexta* PAP-1, PAP-3 and HP6 (An et al., 2012).

Necrotic (Nec or Spn43Ac) is a *Drosophila* serpin that regulates the extracellular activation of the *Drosophila* Toll-mediated antifungal response (Levashina et al., 1999). Nec has a predicted P1-P1' Leu-Ser active site, suggesting that it has an antichymotrypsin inhibitory specificity (Robertson et al., 2006). Nec has an 88-100 residue N-terminal extension which is unusual among serpins. The extension contains regions rich in glutamines and prolines, including a 24-residue polyglutamine repeat (Robertson et al., 2003). A few other inhibitory serpins contain an N-terminal extension. The extension in antithrombin is involved in forming a heparin binding site, whereas the extension in heparin provides an additional proteinase binding site (Robertson et al., 2003). The N-terminus of Nec has little sequence homology with either of these proteins, which makes it difficult to investigate its function. However, it is established that the N-terminus is not required for inhibitory activity (Pelte et al., 2006). Persephone, a thrombin-like serine proteinase in *Drosophila*, may be inhibited by Nec *in vivo* (Ligoxygakis et al., 2002).

M. sexta serpin-8 is a newly discovered serpin with an N-terminal extension. More than 20 hemolymph proteinases are known in *M. sexta* (Jiang et al., 2005) and some of these are likely endogenous proteinase targets of serpin-8. The purpose of this study is to define the inhibitory selectivity of serpin-8, examine its regulatory role in the proPO activation pathway, and identify its target proteinase(s). To achieve this, we have expressed and purified the recombinant protein. Using this material we have been able to show serpin-8 acts as an inhibitor of some commercial proteinases and two proteinases in the *M. sexta* proPO activation system.

Materials and Methods

Insects

M. sexta eggs were originally purchased from Carolina Biological Supply, and the larvae were reared as described by Dunn and Drake (Dunn et al., 1983).

Collection of hemolymph, hemocytes, and fat body from *M. sexta* larvae

Control hemolymph was collected from cut prolegs of day 2, 5th instar larvae. Day 2, 5th instar larvae were injected with a mixture of formaldehyde-killed *E. coli* (1×10^8 cells/larvae) and 100 µg of *Micrococcus luteus* (Sigma) suspended in 100 µl of saline (0.9% w/v of NaCl). Hemolymph from three larvae was combined as one biological sample. Hemolymph was collected into microcentrifuge tubes at 0, 6, 12, and 24 h. A few crystals of diethyldithiocarbamate and phenylthiourea were added to the tubes before collection to prevent melanization of hemolymph. Hemocytes were collected and removed from hemolymph by centrifugation at 5,000×g for 15 min at 4°C. Hemolymph from the naïve and injected larvae were aliquoted and stored at -80°C.

RNA extraction and reverse transcription-PCR analysis

Total RNA samples were isolated from fat body and hemocytes of naïve and induced *M. sexta* larvae and different tissues (cuticle, midgut, salivary gland, muscle, nerve, trachea, Malpighian tubules) using the Micro-to Midi total RNA purification system (Invitrogen). Tissues from three larvae were combined to form one biological sample, except for salivary gland and nerve, which were from six larvae. 2-4 µg RNA sample, 10 pmol oligo(dT), and dNTPs (1 µl, 10 mM each) were mixed with diethylpyrocarbonate-treated H_2O in a final volume of 12 µl, denatured at 65°C for 5 min, and quickly chilled on ice for 3 min. Moloney murine leukemia virus reverse transcriptase (1 µl, 200 U/µl, Invitrogen), 5×buffer (4 µl), 0.1 M dithiothreitol (2 µl), and RNase OUT (1 µl, 40U/µl, Invitrogen) were added to the denatured RNA sample (12 µl) for first strand cDNA synthesis at 37°C for 50 min. *M. sexta* ribosomal protein S3 (rpS3) mRNA was

used as an internal control to normalize the cDNA samples using specific primers j037 (5'-CAT GAT CCA CTC CGG TGA CC-3') and j038 (5'-CGG GAG CAT GAT TTT GAC CTT AA-3'). Primers j117 (5'-CGA GCA ATC TGG GAA TCT CGC T-3') and j119 (5'-TGG AAG CAA TCC AGC TGT TGA-3') were used to amplify *M. sexta* serpin-8 cDNA, and primers j640 (5'-CAA TTG GTG GAA CTC CAA CAT-3') and j641 (5'-CTC GAG GTC ATA AAT GGA CTG-3') were used to amplify *M. sexta* HP19 cDNA under thermal cycling conditions empirically chosen to avoid saturation: 27 cycles of 94°C, 30s, 55°C, 30s, 72°C, 45s. After separation by 1% agarose gel electrophoresis, intensities of the PCR products were quantified and compared using Kodak Digital Science 1D Gel Analysis Software.

Expression and purification of *M. sexta* serpin-8 core region (serpin-8-ΔN) and HP19 catalytic domain (catHP19) from insect cells

The entire coding region for serpin-8-ΔN was amplified by PCR using forward primer j137 (5'-CCA TGG GAA TTC ATT CGG GGC CTG CAT C-3', *Eco*RI site underlined) and reverse primer j143 (5'-TCA AGC ATG CTC GAG TGT AGG ATC CAT TAT TCT TGC-3', *Xho*I site underlined). The amplified fragment was purified with Wizard PCR Preps DNA Purification System (Promega) and ligated into pGEM-T vector (Promega) to verify sequence. From the correct plasmid, the *Eco*RI-*Xho*I fragment was retrieved by restriction digestion and directionally inserted to the same sites of $pMFH_6$ (Lu et al., 2008) a plasmid vector modified from pFastBac1, to generate recombinant baculovirus according to the manufacture's instruction.

We have a project to express the catalytic domains of hemolymph proteinases in *M. sexta* (see appendices) and HP19 is one of those hemolymph proteinases. HP19 catalytic domain (catHP19) was amplified using forward primer j640 (5'-CAA TTG GTG GAA CTC CAA CAT-3', *Mfe*I site underlined) and reverse primer j641 (5'-CTC GAG GTC ATA AAT GGA CTG-3', *Xho*I site underlined). The recombinant plasmid, $pMFH_6$-serpin-8-ΔN or $pMFH_6$-catHP19 was

transformed into *E. coli* strain DH10Bac, which contains a bacmid and a helper plasmid. The recombinant bacmid obtained by transposition of $pMFH_6$-serpin-8-ΔN or $pMFH_6$-catHP19 donor plasmid was isolated. The insertion of serpin-8-ΔN or catHP19 frangment in the recombinant bacmid was confirmed by PCR using a serpin-8-ΔN or catHP19 gene-specific forward primer and a reverse primer located downstream of the transposition site on the bacmid.

For serpin-8 expression, the initial viral stock (V_0) was obtained by transfected *Spodoptera frugiperda* Sf9 cells with a bacmid-cellFECTIN mixture, and its titer was improved through serial infections. Sf9 cells (at 2.0×10^6 cells/ml) in 100 ml of Sf-900 II serum-free medium (Invitrogen) were infected with the baculovirus stocks at a multiplicity of infection of 10 and grown at 27°C for 96 h with gentle agitation (100 rpm). The expression of catHP19 was the same.

Serpin-8-ΔN purification was carried out using 500 ml of the cell culture medium. The cells were removed by centrifugation at 5,000×*g* for 15 min. The supernatant was mixed with an equal volume of distilled water (500 ml) with 1mM benzamidine at 4°C for 30 min. After centrifugation at 12,000×*g* for 30 min, the cleared supernatant (1000 ml) was applied to a dextran sulfate (DS)-Sepharose column (40 ml) (Nakamura et al., 1985) equilibrated with buffer A (10 mM potassium phosphate, pH 6.4, 1 mM benzamidine) and washed with 200 ml of buffer A, bound proteins were eluted with a linear gradient of 0-1.0 M NaCl in buffer A (100 ml).

The fractions (4 ml/tube) were collected and aliquots of the franctions (7 μl) were subjected to SDS-PAGE and immunoblot analysis using anti-His5 antibody (BioRad). Fractions containing serpin-8-ΔN were pooled and applied onto nickel-nitrilotriacetic-acid-agarose column (2 ml), equilibrated with buffer B (50 mM potassium phosphate, pH 8.0, 300 mM NaCl, 10 mM imidazole, 0.005% Tween-20) and washed with 10 ml of buffer B and bound proteins were eluted from the column with a linear gradient of 10-100 mM imidazole in buffer B (10 ml). Finally, tightly bound proteins were eluted with 5 ml of buffer B containing 250 mM imidazole. The fractions (1 ml/tube) were collected and aliquots of the franctions (7 μl) were subjected to SDS-

PAGE and immunoblot analysis using anti-His5 antibody (BioRad). Fractions containing serpin-8-ΔN were pooled and concentrated using Amicon ultracentrifugal 30K MWCO filter device (Millipore). Buffer of the concentrated protein was exchanged with 20 mM Tris-HCl, pH 7.5, 50 mM NaCl using the same filter and stored at -80°C in aliquots. About 600μg of serpin-8-ΔN was used as antigen for preparing a rabbit polyclonal antiserum. CatHP19 was purified from the conditioned medium (1 liter) by the same protocol.

Inhibitory activity assay and complex formation assay

Recombinant serpin-8-ΔN (200 ng/μl, 1 μl) was incubated with various commercial proteinases (100 ng/μl, 1 μl) in the buffer (8 μl, 20mM Tris-HCl, pH 8.0) at room temperature for 10 min. For the control, serpin-8-ΔN was replaced by the buffer. Then 150 μl of a suitable substrate was added, and the residual proteinase activity was measured by monitoring A_{405} in the kinetic mode on a plate-reader (Molecular Device). One unit activity is defined as ΔA_{405}/min=0.001. The proteinases and their substrates were diluted immediately before use in buffer (20 mM Tris-HCl, pH 8.0, 50 mM NaCl). The proteinases and their artificial substrates used in the assay were bovine pancreatic trypsin (Sigma) and N-acetyl-Ile-Glu-Ala-Arg-*p*-nitroanilide (IEAR*p*Na, 50 μM, Sigma); bovine α－chymotrypsin (Sigma) and N-succinyl-Ala-Ala-Pro-Phe-*p*-nitroanilide (100 μM Sigma); human neutrophil Cathepsin G (Sigma) and N-succinyl-Ala-Ala-Pro-Phe-*p*-nitroanilide (AAPF*p*Na, 100 μM, Sigma); porcine pancreatic elastase (Sigma) and N-succinyl-Ala-Ala-Pro-Leu-*p*-nitroanilide (AAPL*p*Na, 100 μM, Sigma); proteinase K (Sigma) and N-succinyl-Ala-Ala-Pro-Phe-*p*-nitroanilide (AAPF*p*Na, 100 μM, Sigma). For complex formation assay, the reactions were stopped by adding SDS-PAGE loading buffer and boiling for 5 min. The samples were separated by 10% SDS-PAGE and visualized by immunoblotting using serpin-8 antibody.

Serpin-proteinase association rate constant (k_a)

Various concentrations of purified serpin-8-ΔN (1 µl) was mixed with bovine α－chymotrypsin (2 µM, 1 µl), porcine pancreatic elastase (6 µM, 1 µl) and human neutrophil Cathepsin G (50 µM, 1 µl) in the buffer (8 µl, 20 mM Tris-HCl, pH 7.5) at a serpin/proteinase molar ratio of 20, incubated at room temperature for 15, 30, 45, 60, 75, 90 and 120 sec, and then the residual amidase activities of proteinases were measured using substrates, N-succinyl-Ala-Ala-Pro-Phe-*p*-nitroanilide (AAPF*p*Na, 100 µM, 150 µl, Sigma) and N-succinyl-Ala-Ala-Pro-Leu-*p*-nitroanilide (AAPL*p*Na, 100 µM, 150 µl, Sigma). With excessive serpin, the reactions are pseudo-first order. From the linear regression curve of ln(residue amidase activity) vs. incubation time (t), the half-life time ($t_{0.5}$) for inhibition was calculated. Association rate constants (k_a) were calculated using equation $k_a=0.693/(t_{0.5}*I^0)$, I^0 is the initial concentration of the serpin) (Beatty et al., 1979).

Assay of catHP19 residual amidase activity

Purified recombinant catHP19 (150 ng/µl, 2 µl,) was incubated with 6 mM cetylpyridinium chloride (CPC, 1 µl) in the buffer (7 µl, 20 mM Tris-HCl, pH 7.5, 50 mM NaCl) at room temperature for 5 min. The residual amidase activity was then measured using an artificial substrate, N-succinyl-Ala-Ala-Pro-Leu-*p*-nitroanilide (AAPL*p*Na, 100 µM, 150µl, Sigma) by monitoring A_{405} in kinetic mode on a plate-reader (Molecular Device). One unit activity is defined as ΔA_{405}/min=0.001. An average activity data were plotted as mean ± S.D. (n = 3) in the bar graph. CPC or catHP19 alone was used as controls.

ProPO activation and inhibition

One µl of hemolymph was incubated for 30 min at room temperature with *M. luteus* (1 µg/µl in saline, 1 µl) in the buffer (8 µl, 20 mM Tris-HCl pH 8.0, 1 mM $CaCl_2$, 0.001% Tween-

20). PO activity was measured by adding 150µl of 2 mM dopamine (in 100 mM sodium phosphate buffer, pH 7.5) as a substrate and monitoring A_{470} for 10 min on a microplate reader (Jiang et al., 2003a). Hemolymph samples which have low basal PO activity were selected for the assay.

To dertermine the role of catHP19 in proPO activation, naïve hemolymph (1 µl), *M. luteus* (1 µg/µl, 1 µl), and catHP19 (100 ng/µl, 1 µl) were incubated in the buffer (7 µl, 20 mM Tris-HCl pH 8.0, 1 mM $CaCl_2$, 0.001% Tween-20) at room temperature for 30 min. PO activity was measured using dopamine as described above. Activity data were plotted as mean ± S.D. (n = 3) in the bar graph. Control reactions were plasma only and *M. luteus* with plasma.

For inhibition assay, 1 µl of induced hemolymph was incubated for 5 min at room temperature with purified recombinant serpin-8-ΔN (1 µl) at varying concentrations in the buffer (7 µl, 20 mM Tris-HCl pH 8.0, 1 mM $CaCl_2$, 0.001% Tween-20). Then 1 µl of *M. luteus* (1 µg/µl) was added and incubated for another 10 min at room temperature before the PO activity (mean ± S.D., n = 3) assay as described above.

Determination of the cleavage site in *M. sexta* serpin-8

To determine the position of the scissile bond in the serpin-8, purified serpin-8-ΔN (150 ng/µl, 2 µl) was incubated with catHP19 (100 ng/µl, 2 µl) in the buffer (26 µl, 20 mM Tris-HCl, pH 7.5, 50 mM NaCl) at room temperature for 30 min. Half of the reaction mixture (15 µl) was subjected to 10% SDS-PAGE for detection of the serpin-proteinase complex, and half of the mixture was subjected to MALDI-TOF mass spectrometry (Jiang et al., 2003). The molecular mass of a newly appeared peak that was absent in the control spectra of serpin-8-ΔN and catHP19 alone was compared with calculated values of the carboxyl-terminal peptides to deduce the cleavage site in serpin-8-ΔN.

Immunoblot analysis

Cell-free hemolymph samples were collected as described above, and these plasma samples (10 μl) were mixed with 100% saturated ammonium sulfate (8.2 μl, pH 7.0) on a vortexer. The ammonium sulfate (A.S.) was adjusted to 45% saturation, and centrifuged to separate precipitate from the supernatant which contains storage protein. The pellet was saved and re-dissolved into the buffer (10 μl, 20 mM Tris-HCl, pH 7.5). Different microbial surface components (1 μl) were incubated with the 45% ammonium sulfate fraction of hemolymph at room temperature for 15 min. Half of the reaction mixtures were separated by 10% SDS-PAGE and immunoblot analysis was performed using serpin-8 antibody as the primary antibody (diluted 1: 2000), and goat anti-rabbit IgG-alkaline phosphatase conjugate (BioRad, diluted 1: 1000) as the secondary antibody.

Purified serpin-8-ΔN (150 ng/μl, 1 μl) was incubated with *Anopheles gambiae* HP14 catalytic domain (AgHP14cat) (100 ng/μl, 2 μl) in the buffer (7 μl, 20 mM Tris-HCl, pH 7.5, 50 mM NaCl) at room temperature for 30 min. AgHP14cat was purified by Wang Yang in the laboratory. The reaction mixture (10 μl) was subjected to 10% SDS-PAGE and immunoblot analysis for detection of the serpin-proteinase complex using His5 antibody (BioRad) as the primary antibody (diluted 1: 2000), and goat anti-mouse IgG-alkaline phosphatase conjugate (BioRad, diluted 1: 1000) as the secondary antibody.

Results

cDNA sequence of *M. sexta* serpin-8

The serpin-8 cDNA, isolated by my labmate Subrahmanyam Rayaprolu, contains 2673 nucleotides, with a 121-bp 5'-noncoding region, a 1458-bp open reading frame, and a 1094-bp 3'-noncoding region, including a 9-bp poly (A) tail (Fig. 3). The 3'-noncoding region contains five putative polyadenylation signals (AATAAA or ATTAAA). The open reading frame encodes a protein of 485 amino acid residues, with a predicted 18-residue signal peptide for secretion. The

open reading frame of serpin-8 is longer than other *M. sexta* serpins, because it has a 95 residue N-terminal extension. There are two potential *N*-linked glycosylation sites at Asn^{275} and Asn^{451}. There are seven putative *O*-linked glycosylation sites at Thr^{74}, Thr^{78}, Thr^{81}, Thr^{92}, Thr^{93}, Ser^{85} and Ser^{87}, all of which are located in the N-terminal extension region. The calculated molecular mass of mature serpin-8 is 51,487Da and its calculated isoelectric point is 8.51.

Sequence comparison of *M. sexta* serpin-8 with other insect serpins

BLAST search and sequence alignment indicated that *M. sexta* serpin-8 is most similar in amino acid sequence to *B. mori* serpin-12 (NP_001036857), with 55% identity and 77% similarity. They have a similar reactive center loop sequence, as 6 out 10 residues are the same from P5 to P5' region (Fig. 4). Among the nine serpins, *M. sexta* serpin-8, *B. mori* serpin-12 and *Drosophila* Nec have two distinctive features. First, they have a Leu residue at the predicted P1 site, indicating that they are inhibitors of elastase- and chymotrypsin-like proteases, and second, they have an N-terminal extension. Necrotic was reported to negatively regulate the extracellular activation of the *Drosophila* Toll-mediated antifungal signaling pathway (Levashina et al., 1999; Ligoxygakis et al., 2002; Robertson et al., 2002). *B. mori* serpin-12 has not been characterized further than genome sequencing.

Expression and purification of *M. sexta* serpin-8-ΔN

To explore the biochemical function of *M. sexta* serpin-8, we expressed the serpin-8 core region (serpin-8-ΔN) using the baculovirus system, because it is reported that both full-length and the core serpin (serpin-ΔN) are active inhibitors (Pelte et al., 2006). The fragment of the serpin-8-ΔN was inserted into the *Eco*RI-*Xho*I restriction site of the expression vector, $pMFH_6$ which has a honeybee mellitin signal peptide and C-terminal $(His)_6$-affinity tag (Lu et al., 2008). The recombinant serpin-8-ΔN was soluble and secreted into the cell culture medium. After removing cells from the culture, the protein was first enriched by ion exchange chromatography and eluted

from the dextran sulfate (DS) column with a linear gradient of NaCl. The fractions containing serpin-8-ΔN were pooled and loaded onto the nickel-affinity column. The protein was eluted with a linear gradient of imidazole. Serpin-8-ΔN migrated as a 41 kDa single band on 10% SDS-PAGE under reducing condition (Fig. 5). The molecular mass of serpin domain (serpin-ΔN) in which N-terminal extension is not included is 40,919Da and its calculated isoelectric point is 8.55.

M. sexta serpin-8 mRNA and protein levels after bacterial challenge

In order to examine the transcriptional regulation of serpin-8 gene in response to bacterial challenge, the serpin-8 mRNA level was analyzed by RT-PCR. Serpin-8 mRNA was constitutively expressed at a low level in hemocytes and increased dramatically 24 h after bacteria challenge. The amount of mRNA in fat body slightly increased after immune challenge (Fig. 6A).

The induction pattern of serpin-8 protein in hemolymph was also examined by immunoblot analysis using serpin-8 antibody. A low level of serpin-8 was present in naïve hemolymph. After injecting the larvae with killed *E.coli*, a small decrease of the 50 kDa band protein was detected at 12 h. Serpin-8 protein level increased continuously and significantly around 24 h after the immune challenge and remained high up to 32 h (Fig. 6B). The increase in serpin-8 concentration at 6 h and decrease at 12 h may reflect the individual variations.

M. sexta serpin-8 mRNA levels in different tissues and developmental stages

The mRNA level of serpin-8 was examined in the following tissues: cuticle, midgut, salivary gland, muscle, nerve, trachea, Malpighian tubules by RT-PCR (Fig. 7A). Serpin-8 gene was not expressed in midgut. A low level of serpin-8 mRNA was detected in salivary gland and muscle. Serpin-8 transcript levels were moderate in cuticle and Malpighian tubules and much higher in nerve and trachea.

We examined the levels of sepin-8 mRNA in fat body of different developmental stages (Fig. 7B). A slight decrease in serpin-8 mRNA level occurred in day 4 and day 5 of 4th instar larval stage. The mRNA slightly increased in 5th instar larval stage, compared to 4th instar larval stage. There was no substantial change in mRNA level during 5th instar larval stage and wandering stage. The serpin-8 mRNA level dramatically decreased during pupal and adult stage.

Inhibitory activity of *M. sexta* serpin-8-ΔN

In order to determine the inhibitory specificity of serpin-8, recombinant serpin-8-ΔN was used to test its inhibition of commercial proteinases (Fig. 8A). Among these proteinases, serpin-8-ΔN showed strong inhibitory activity against chymotrypsin, cathepsin G and elastase, but no inhibitory activity against trypsin or proteinase K. Serpin-8-ΔN inhibited chymotrypsin by 70%, cathepsin G by 94%, and elastase by 85% at the molar ratio (proteinase:serpin-8 = 1:1.3), indicating that serpin-8-ΔN is a potent inhibitor of cathepsin G and elastase and less effective in inhibiting chymotrypsin.

In the inhibition reaction between a serpin and a susceptible proteinase, an SDS-stable inhibitor-enzyme complex formed. Such complexes were detected when we incubated serpin-8-ΔN with chymotrypsin, cathepsin G and elastase (Fig. 8B). The combined apparent molecular mass of serpin-8-ΔN (41 kDa) and the proteinases (~30 kDa) is close to the size of the complex (~70kDa).

To further characterize the serpin-proteinase reaction, the association rate constants (k_a) were determined. The inhibition reactions between serpin-8-ΔN and elastase, and between serpin-8-ΔN and cathepsin G had the similar k_a, which were two times higher than between serpin-8-ΔN and chymotyrpsin (Table 1).

Inhibition of *M. sexta* prophenoloxidase activation by serpin-8-ΔN

To investigate the physiological function of serpin-8, we tested its effect on proPO activation. Different amounts of recombinant serpin-8-ΔN were incubated with plasma for 5 min before adding *M. luteus* into the reaction. The reaction mixture was then incubated for another 10 min at room temperature before measurement of PO activity. Serpin-8-ΔN at 200ng/μl inhibited proPO activation by 50% (Fig. 9). Since PAPs are not supposed to be inhibited by serpin-8 due to inappropriate substrate specificity, serpin-8 must inhibit at least one proteinase upstream of PAPs in the proPO activation cascade.

cDNA sequence and structural features of *M. sexta* HP19

The HP19 cDNA (Jiang et al., 2005) contains 2480 nucleotides, with an 83-bp 5'-noncoding region, a 1647-bp open reading frame, and a 750-bp 3'-noncoding region, including a 26-bp poly (A) tail (Fig. 10). The 3'-noncoding region contains four putative polyadenylation signals (AATAAA or ATTAAA). The open reading frame encodes a protein of 548 amino acid residues, with a predicted 19-residue signal peptide. There are two potential *N*-linked glycosylation sites at Asn^{368} and Asn^{403}. The calculated molecular mass of mature HP19 is 58,938Da and its calculated isoelectric point is 7.66. HP19 has a C-terminal catalytic domain and an N-terminal region with unknown function. The molecular mass of HP19 catalytic domain is 28,499Da and its calculated isoelectric point is 6.64.

The predicted proteolytic cleavage site is located between Leu^{276} and Val^{277} (Jiang et al., 2005). Therefore, the activating enzyme for proHP19 may be a serine proteinase with chymotrypsin-like specificity. The catalytic domain is similar in sequence to serine proteinases with elastase specificity, including the catalytic triad of His^{321}, Asp^{375}, and Ser^{474}. The primary substrate-specificity pocket (Perona et al., 1995) is likely composed of Ser^{468}, Ser^{495}, and Val^{510}, suggesting that HP19 has a specificity for cleavage after the C-terminus of Ala, Val, or Leu. BLAST search and sequence alignment indicated that *M. sexta* HP19 is most similar in amino

acid sequence to *T. castaneum* HP19 (XP_970870.2), with 38% identity and 54% similarity. *T. castaneum* HP19 has not been characterized.

Expression and purification of *M. sexta* HP19 catalytic domain (catHP19)

The fragment of the HP19 catalytic domain was amplified using PCR from HP19 cDNA (Jiang et al., 2005) and cloned into the expression vector, $pMFH_6$ which has a honeybee mellitin signal peptide and C-terminal $(His)_6$-affinity tag (Lu et al., 2008), using *Mfe*I and *Xho*I restriction sites. The N-terminal residues "Val-Val-Asp-Gly" of HP19 catalytic domain was replaced by "Gly-Ile-Gly-Gly" in order to fit into the expression vector and have the least changes in amino acid residues. The recombinant catHP19 was soluble and secreted into the cell culture medium. The cell culture medium was clarified by centrifugation, and the supernatant was applied to ion exchange column and eluted from the column with a linear gradient of NaCl. The elution fractions containing catHP19 were combined and loaded onto the nickel-affinity column. The bound protein was eluted with imidazole. The catHP19 migrated as a 30kDa single band on 10% SDS-PAGE under reducing condition (Fig. 11).

***M. sexta* HP19 mRNA and protein levels after bacterial challenge**

In order to investigate the transcriptional regulation of HP19 gene in response to bacterial challenge, the HP19 mRNA level was analyzed by RT-PCR (Fig. 12A). HP19 mRNA was constitutively expressed at a moderate level in fat body with no significant increase 24 h after bacterial challenge. The HP19 mRNA level was a little higher in hemocytes than in fat body, and the amount of mRNA slightly increased after immune challenge.

The induction pattern of HP19 protein in hemolymph was also examined by immunoblot analysis using HP19 antibody (Fig. 12B). A low level of HP19 was present in naïve larval hemolymph. After injecting the larvae with killed *E.coli*, the protein level remained at low until

24 h of after bacterial injection. The amount of HP19 protein level increased dramatically around 24 h after immune challenge and remained high up to 32 h.

M. sexta catHP19 amidase activity

To investigate whether the recombinant catHP19 had amidase activity, it was incubated with an artificial substrate, AAPL*p*Na and A_{405} was monitored in the kinetic mode. CatHP19 had low AAPLase activity (~0.2U) and correlation coefficient of 0.689. Since catHP19 has an elastase-like specificity which may cleave after the C-terminus of Phe, Val, or Leu, AAPV*p*Na and AAPF*p*Na were also used as substrates to observe amidase activity of catHP19. We did not detect catHP19's activity (results not shown). It is reported that insect proPO can be activated by detergent besides proteolytic cleavage (Hall et al., 1995). Cetylpyridinium chloride (CPC), a cationic detergent, was used to test if it can enhance catHP19 activity. A great increase of AAPLase activity was observed (with the value above 0.6 and correlation coefficient of 0.912) when catHP19 was incubated with CPC prior to activity measurement (Fig. 13).

Role of catHP19 in *M. sexta* proPO activation

To investigate the role of catHP19 in *M. sexta* proPO activation cascade, control hemolymph was incubated with microbial elicitor, *M. luteus* and recombinant catHP19 (Fig. 14). The control hemolymph sample had low basal PO activity and could be activated dramatically by *M. luteus*, which indicated that the proPO activation system was functional in the hemolymph. There was a great increase of PO activity when catHP19 was added to the control hemolymph in the absence of microbial elicitor. When catHP19, *M. luteus*, and control hemolymph were incubated together, a high PO activity was observed, but this PO activity was not higher than the one when hemolymph was incubated with catHP19 only, which implied that there was no additive effect of catHP19 and *M. luteus* on enhancement of PO activity.

Inhibition of HP19 *by M. sexta* serpin-8-ΔN

A characteristic feature of the inhibition of serine proteinases by serpins is the formation of a serpin-proteinase complex that is stable in SDS. Such a complex formed between serpin-8-ΔN and catHP19 as indicated by immunoblot analysis (Fig. 15), when serpin-8-ΔN and catHP19 were incubated at room temperature for 30 min. In the controls of HP19 or serpin-8-ΔN only, HP19 antibody recognized the proteinase, but not serpin-8-ΔN, and serpin-8 antibody recognized the inhibitor, but not the proteinase. A new immunoreactive band was detected by both serpin-8 and HP19 antibodies at 70 kDa, but was absent in the controls. The apparent molecular size of this band is close to that predicted for the complex formed between recombinant serpin-8-ΔN and catHP19. However, there was no complex detected when serpin-8-ΔN was incubated with catHP19 in the presence of CPC (result not shown), indicating that CPC may affect the activity of serpin-8-ΔN.

To further characterize the inhibition reaction, we determined the cleavage site of serpin-8-ΔN upon reaction with catHP19 by MALDI mass spectrometry. A major peak of 5,441 Da was detected in the serpin-8-ΔN and catHP19 mixture and the intensity of this 5,441 Da peak was about 8800, which probably represents the carboxyl-terminal peptide released from proteolytic cleavage of serpin-8-ΔN by catHP19 (Fig. 16C). In the control spectrum of catHP19 only, there was no major mass peak in the range of 2000-7000 Da (Fig. 16A). In the other spectrum of serpin-8-ΔN only, there was no mass peak at 5,441 Da, but a mass peak of 5,442 Da was detected with a low intensity of about 3600 (Fig. 14B). Based on the sequence alignment (Fig. 4), the predicted scissile bond in serpin-8-ΔN was after Leu^{447}. Mass of the resulting serpin-8-ΔN C-terminal peptide (S^{448}YDEPSLYFRANKPFLAILWDNRSSIPLFMARIMDPT-LEHHHHHH) is 5442.1 Da. The one Da difference was within the experimental error and detection of the 5,442 Da peak in the control spectrum of serpin-8-ΔN only may be due to the cleavage of serpin-8-ΔN during purification as shown in Fig. 15. Other small peaks within the mass range of 5000 to 6000 Da represented the peptides released from non-specific cleavage near Leu^{447}: the 5,355 Da peak

for $Y^{449}DE…H_6$ (calculated mass: 5,355.1 Da), the 5,555 Da peak for $L^{447}SY…H_6$ (calculated: 5,555.3 Da), the 5,725 Da peak for $V^{445}AL…H_6$ (calculated: 5,725.5 Da), and the 5,796 Da peak for $A^{444}VA…H_6$ (calculated: 5,796.6 Da), and the 5,867 Da peak for $A^{443}AV…H_6$ (calculated: 5,867.7 Da). Taken together, the mass analysis indicated that the scissile bond of serpin-8 is between Leu^{447} and Ser^{448}, consistent with the substrate specificity of HP19.

Cleavage of *M. sexta* serpin-8 N-terminus upon peptidoglycan stimulus from Gram-positive bacteria

A previous study found that *Drosophila* Nec was cleaved off at the N-terminal end by either fungal or Gram-positive bacterial infection (Pelte et al., 2006). Such cleavage was blocked by mutations in *Persephone* which is required in Toll Pathway activation (Ligoxygakis et al., 2002). It is unclear if Nec is directly cleaved by Persephone or if Persephone activates a downstream proteinase that is responsible for the N-terminal cleavage of Nec (Pelte et al., 2006). In order to test if the N-terminus of *M. sexta* serpin-8 can be cleaved by immune challenge, 45% ammonium sulfate precipitated fraction of induced hemolymph was incubated with various microbial components from Gram-positive and Gram-negative bacteria, and fungi. According to protein size, the serpin-8-ΔN in the hemolymph is about 10 kDa smaller than the intact serpin-8, similar to the size of the recombinant serpin-8-ΔN. The result suggested that only surface components from Gram-positive bacteria induced the N-terminal cleavage of serpin-8 (Fig. 17A). There was a clear band corresponding to serpin-8-ΔN in the reaction mixture containing hemolymph and insoluble PG from *S. aureus* (Fig. 17A, lane 7) and a faint band detected when hemolymph was incubated with *M. luteus* (Fig. 17A, lane 2). No cleavage was observed when Gram-negative surface component (LPS) or fungal PG (laminarin or zymosan) was added into hemolymph. To rule out the possibility of the cross reaction between serpin-8 antibody and insoluble PG from *S. aureus*, the PG was included in Fig. 15B to react with serpin-8 antibody.

The result of Fig. 17B indicated that PG did not react with serpin-8 antibody and the cleavage occurred when hemolymph was stimulated with PG.

Detection of *M. sexta* serpin-8-proteinase complex in hemolymph

While recombinant serpin-8-ΔN formed a complex with HP19 catalytic domain *in vitro* (Fig. 15), is the same complex present in hemolymph also? The 0-45% AS fraction of induced hemolymph was incubated with *S. aureus* insoluble PG. Then the reaction mixtures were separated by 10% SDS-PAGE and immunoblot analysis was performed using serpin-8 antibody. A new band was detected by serpin-8 antibody around 70 kDa (Fig. 18A). This band was absent in the hemolymph alone sample. The apparent molecular size of this band is close to that predicted for the complex formed between serpin-8-ΔN and an unknown proteinase. Surprisingly, when HP19 antibody was used to react with the same sample, no complex band was detected (data not shown). Since the scissile bond of serpin-8 is between Leu^{447} and Ser^{448}, also consistent with the substrate specificity of HP14 (Wang et al., 2006), HP14 antibody was used to test if the complex is formed by HP14 catalytic domain and serpin-8. The result showed that a band was detected by HP14 antibody around 70 kDa, and a band around 30 kDa which corresponded to HP14 catalytic domain, appeared as well (Fig. 18B, lane 2). To test the hypothesis that serpin-8-ΔN can form complex with HP14 in vitro, we made use of the *A. gambiae* HP14 catalytic domain (AgHP14cat), as *M. sexta* HP14 catalytic domain is not available. AgHP14cat was expressed in Baculovirus expression system and used as material for our mosquito project. AgHP14 (AgCP12488) and *M. sexta* HP14 are orthologs (Ji et al., 2004). The result showed that a complex band appeared when serpin-8-ΔN was incubated with AgHP14cat (Fig. 18C). Since serpin-8-ΔN and AgHP14cat are recombinant proteins with His-tag at C-terminus, the antibody against His-tag recognized both proteins and the complex. The His5 antibody did not recognize the cleaved serpin-8-ΔN shown in Fig. 15C suggesting that the cleaved serpin-8-ΔN lost the C-terminus.

These results indicate that it is possible for serpin-8 to inhibit *M. sexta* HP14 besides HP19 under physiological condition.

Discussion

Upon infection or injury, an extracellular serine proteinase cascade is activated leading to the converstion of inactive proPO to active PO which catalyzes melanin formation (Ashida et al., 1997). The proPO activation pathway is regulated by serpins to prevent unnecessary activation and limit melanization as a transcient and local reaction (Kanost et al., 2004).

In this study, I have expressed and purified a new immune responsive serpin, serpin-8 from *M. sexta*. Its mRNA is constitutively expressed at a low level in hemocytes and at a moderate level in fat body. After bacterial injection, serpin-8 mRNA level increased both in hemocytes and fat body (Fig. 6A). Serpin-8 protein is constitutively present in larval plasma at a low concentration, which increased significantly at 24 h after immune challenge (Fig. 6B).

M. sexta serpin-8 is most similar in amino acid sequence to *B. mori* serpin-12 of unknown function including very similar reactive center loop sequences (Fig. 4). According to sequence alignment, *M. sexta* serpin-8, *B. mori* serpin-12 and Nec have a Leu at their predicted P1 site (Fig. 4), indicating that they are inhibitors of elastase- and chymotrypsin-like proteinases. Furthermore, the three serpins have an N-terminal extension which is unusual among other serpins. Although the function of the extension is unclear, Nec extension contains stretches of glutamines and prolines, including a 9-residue polyglutamine repeat (Pelte et al., 2006). However, *M. sexta* serpin-8 and *B. mori* serpin-12 do not have any structural features or repeats within the N-terminal extension. A previous study found that the expression of full-length Nec was not successful in *E. coli*, resulting in a shortened protein that contained only the common serpin core (serpin-ΔN) and they showed that the N terminus is not required for inhibitory activity (Robertson et al., 2003). Another study also found that both full-length Nec and the core serpin

are active inibitors of a range of serine proteinases (Pelte et al., 2006). Furthernore, *M. sexta* serpin-8 has seven putative *O*-linked glycosylation sites in the N-terminal extension, which may affect protein expression. Therefore, we expressed the serpin-8 core domain (serpin-8-ΔN) using the baculovirus/insect cell system.

RT-PCR analysis showed that serpin-8 mRNA level is high in larvae, and low in pupae and adults in unchallenged tobacco hornworm (Fig. 7B). Serpin-8 transcript was not present in midgut, but in cuticle and Malpighian tubules. The amount of transcript was most abundant in nerve and trachea (Fig. 7A). These results are not consistent with Nec expression pattern. Soukup et al. (2009) found that Nec mRNA level is moderate in larvae and adults, and higher in pupal stages. They also reported that *nec* transcript was detected in mid- and hind-gut, but not in Malpighian tubules or brain tissue. The comparison may suggest that the spatial distribution of specific serpins is important to their function in the immune response and also in other processes such as insect development.

To examine the inhibitory profile of serpin-8, a panel of proteinases was chosen by virtue of each being an easily available, well characterized proteinase. Results from this study showed that serpin-8-ΔN has a specificity being able to inhibit elastase- and chymotrypsin-like enzymes (Fig. 8A and Table 1). We have shown that serpin-8-ΔN successfully forms inhibitory complexes with chymotrypsin, Cathepsin G, and elastase (Fig. 8B). Therefore, serpin-8 may act *in vivo* on a number of serine proteinases with certain specificity, performing a role as a broad-spectrum proteinase inhibitor.

Addition of recombinant serpin-8-ΔN to plasma suppressed proPO activation (Fig 9). According to their specificity, PAPs, HP6, HP8 and HP21 are not supposed to be inhibited by serpin-8, serpin-8 inhibits at least one upstream proteinase in the proPO activation cascade. *M. sexta* HP19 is an immune responsive serine proteinase with elastase specificity, suggesting that HP19 has the specificity for cleavage after the C-terminus of Ala, Val, or Leu. The mRNA and protein levels of HP19 increased after immune challenge (Fig. 12). It is difficult to purify active

proteinases from hemolymph, because they are present in plasma at low concentration and regulated tightly by serpins. We thus tried to express the catalytic domain of HP19 (catHP19). Although the amidase activity of catHP19 was low (Fig. 13), addition of catHP19 increased PO activity in plasma (Fig. 14), and catHP19 formed inhibitory complexes with serpin-8-ΔN (Fig. 15), suggesting HP19 may be a physiological target proteinase of serpin-8 in *M. sexta*. The cleavage site of serpin-8-ΔN upon reacting with catHP19 was determined by mass spectrometry (Fig. 16). The result indicates that the scissile bond of serpin-8 is between Leu^{447} and Ser^{448}, consistent with the substrate specificity of HP19.

Serpin-8 N-terminal extension was cleaved upon encountering peptidoglycan from Gram-positive bacteria (Fig. 17). N-terminal cleavage of Nec was induced by either fungal or Gram-positive bacterial infection (Pelte et al., 2006) and they found *Drosophila* Persephone, required for fungal response in Toll pathway (Ligoxygakis et al., 2002) is related to this cleavage, but they are not sure if the interaction is direct or indirect. So far, no specific proteinase was identified to be responsive for the cleavage of the N-terminal extension of serpin-8. However, it is supposed to function in the immune pathway mediated by Gram-positive bacteria.

Serpin-8 complex was detected in hemolymph by serpin-8 antibody and HP14 antibody, but not by HP19 antibody (Fig 19A and B), which may be due to the low reactivity of HP19 antibody. HP14 is a chymotrypsin-like serine proteinase preferring to cleave after Leu, which matches the P1 site of serpin-8 (Wang et al., 2006). Upon peptidoglycan challenge, the complex band was detected around 70 kDa by serpin-8 antibody and HP14 antibody, and the catalytic domain of HP14 was detected as well, which is consistent with the previous study (Wang et al., 2006). It suggests a possible regulatory mechanism for the pathway initiation. AgHP14cat was made use to test if serpin-8-ΔN forms complex with HP14 *in vitro*. Similar assay was applied to *A. gambiae* serpin-6 which formed complex with *M. sexta* PAP-1, PAP-3 and HP6 (An et al., 2012). These results suggest that serpin-8 may regulate more than one serine proteinases in *M. sexta*

proPO activation cascade. Similar cases can be found in *M. sexta* serpin-3, serpin-4, serpin-5 and serpin-6 (Christen et al., 2012; Tong et al., 2005; Zou et al., 2005).

Several considerations should be taken in understanding the results of this study. First, it is possible that serpin-8-ΔN may lack some of the specificity-determining regions that could be present in the N-terminal extension. Alternatively, the N-terminal extension may change the rate of serpin-8 association of inhibition with its target proteinase by influencing the stability of the native serpin. To further study the function of the full-length protein could be useful to solve this problem. In addition, the data of the association rate constant between serpin-8-ΔN and catHP19 is unavailable, due to the low activity of catHP19. CPC may affect the ability of serpin-8-ΔN to form complex with proteinaes, as no complex was detected when serpin-8-ΔN was incubated with catHP19 in the presence of CPC (data not shown). More assays to test if CPC affects the inhibitory activity of serpin-8-ΔN are useful to address the problem. The availability of *M. sexta* active HP14 will allow us to further confirm that *M. sexta* HP14 is a physiological target of serpin-8.

Overall, this study has shown conclusively that serpin-8-ΔN is a serine proteinase inhibitor, with the specificity to inhibit elastase- and chymotrypsin-like proteinases. Prediction of physiological targets of serpin-8 is based on analysis of the specificity pocket architecture of *M. sexta* proteinases. Our data supports that HP19 and HP14 are possible physiological targets of serpin-8.

Figure 3. Nucleotide and deduced amino acid sequence of *M. sexta* serpin-8. The one-letter code for amino acid residue is shown below the nucleotide sequence and aligned with the second nucleotide of the corresponding codon. Numbers on the left are assigned to nucleotide residues and amino acid residues, including negative numbers for residues in the secretion signal peptide which is underlined. Two putative *N*-linked glycosylation sites are marked with # after the Asn residues. Seven putative *O*-linked glycosylation sites are marked with & after the Thr and Ser residues. The predicted P1 and P1’ sites are shaded and marked. The putative polyadenylation signals (AATAAA or ATTAAA) near the 3’-terminal of cDNA are double-underlined.

```
Ms serpin-8        -----MKILISIFFCYFSLGVHSQLNVIPLNNDADPNSIYFADNMRPFVRSSGFNQNMQT
Bm serpin-12       -----MKVFISLTVCCFVLSADSQSSFRTQNQYPKYDSTINSDQIYFDDNRPSGSINIQK
Ms serpin-4        ------MKCVLVIVLCIVSCYCDDLPAKVRNGLTEKIGNFSIELLYHTSKSQPENQ----
Ms serpin-5        -----MMMKCAIFVLFFGACYCDVD-------FYERPRNFSIELLYHTQLQTGG------
Ms serpin-1J       ---------MKIIMCIFGLAALAMAGETDLQKILRESNDQFTAQMFSEVVKANPGQ----
Dm Necrotic        -----MASKVSILLLLTVHLLAAQTFAQELIAWQRQQQQQQQQQLQLQQQLLLQQQQHQR
Ms serpin-6        ------MLKSAALVLLVATCVSSQCFSKDDSSKKLDPGARTSLYSGQLAFTLNLFQTINS
Ms serpin-3        -----MTSTIYFAFFVAPLLLCSLADDVDPNTLRAVFGYSALDQAALVGAESNKQAATVT
Dm serpin-27A      MTKMGGNLAVMLLSLFLSALATGNGNSIPTTTTPQGVFETRTDKLPGGAASVPSGAGIYD


Ms serpin-8        NTRGPFESQFDIQASLQTTKSQREQQPQING------GVHSPTRSPTQDTPFKSLSPMIP
Bm serpin-12       ELSNLNGLTIGTKIPIINPNFGAPQYSPYANNVIIQPSIQTYNQETTKIVPQKSGTPAKK
Ms serpin-4        ------------------------------------------------------------
Ms serpin-5        ------------------------------------------------------------
Ms serpin-1J       ------------------------------------------------------------
Dm Necrotic        NPRPELGLRSLPGNPWTQNNQEAISDVVAVDLTKREPVTPPPNRPPPVFSYMDRFSSELF
Ms serpin-6        AVPDD---------------------------------------------------------
Ms serpin-3        PDNGTLVDPDYWDTEEFQPSTADYDIFDWVLTKR--------------------------
Dm serpin-27A      DIDTFVPFRSDSHDPFSWHLLKTVLQN---------------------------------


Ms serpin-8        TTSSFHSGPAS-----------TSFGVNVFKQMATEQSGNLAASPFSITILLAMLQQGAA
Bm serpin-12       MTDTFFQAQATRPEIDSIDYPITHFGINIFKQITSSQSGNMVVSPFSITTLLALLQQGAT
Ms serpin-4        ----------------------------------------NLVLSPITVWTALAVISEGAT
Ms serpin-5        ----------------------------------------HVVISPFGIWTLMTGIALGAT
Ms serpin-1J       ---------------------------------------NVVLSAFSVLPPLGQLALASV
Dm Necrotic        KEIIKSQSQQ-----------------------------NVVFSPFSVHALLALIYGASD
Ms serpin-6        ----------------------------------------NIFFSPFSVYQSLLLAYFSTG
Ms serpin-3        --------------------------------VASTSNANFLLSPLGLKLALAILTEAAT
Dm serpin-27A      ---------------------------------ETADKNVIISPFSVKLVLALLAEAAG
                                                   :.  *.: :   :     .:

Ms serpin-8        G--NTLDEITRALQMTPEK---SAEIFKKVNEEIQKRNSRNILKTANNVFLSENFNLNPQ
Bm serpin-12       G--STLDQISAALHLAPLK---TSEVFRNVMENVQKRQSQNILKTLNNIFVAETFNLNRD
Ms serpin-4        G--NTRREINHALRITNRNKNVTRANYREISNWLVVKTKTVELAKINAIFVDQQRLPQED
Ms serpin-5        G--NSYKQLSRAFILPKNPDTLTEGYKSLTNVVLDPSSNAVALTSKNFVFLDNDFNVYPD
Ms serpin-1J       G--ESHDELLRALALPNDN--VTKDVFADLNRGVRAVKG-VDLKMASKIYVAKGLELNDD
Dm Necrotic        G--KTFRELQKAGEFSKNAMAVAQDFESVIKYKKHLEGADLTLATKVYYNRELG-GVNHS
Ms serpin-6        G--RTEESLKKSLEIEDNMDKMNLMTAYKVDKRSRMTNNNSDSYEFTTANKLFVANELQV
Ms serpin-3        G--STRSELASALGFGLDR-TEVRRKFSTIIESLKRESPDYILNLGSRIYMGEGVQPRQR
Dm serpin-27A      AGTQTQVELANTQTDIRSQNNVREFYRKTLNSFKKENQLHETLSVRTKLFTDSFIETQQK
                   .   :  .:  :

Ms serpin-8        FKRIAVNNFDSDLTPTYFGKPALAAQNINSWIASKTNDKIDKLVSPDDLSGNTQMVMVNA
Bm serpin-12       FERIAKSGFGSGVTLMNFGRPDVAIQRINNWVGAMTNGKIENLLSQDAISQSSQLVLVNV
Ms serpin-4        FIAIAKEIYDTNMVPLKFEESDVAADVINRQISNVTHGRIKNIVNSESFKE-SKMILTSA
Ms serpin-5        FRLRLQKDFSAAIKVLDFGDPNSAR--IANTYIEKSGGRVSNVLQSDDFQE-SRMLLTNV
Ms serpin-1J       FAAVSRDVFGSEVQNVDFVKSVEAAGAINKWVEDQTNNRIKNLVDPDALDETTRSVLVNA
Dm Necrotic        YDEYAKFYFSAGTEAVDMQNAKDTAAKINAWVMDTTRNKIRDLVTPTDVDPQTQALLVNA
Ms serpin-6        RQCMFDLFGEEIEALNFRENPEVSREYINNWVERITKNHIKKLLPADGVSEFTKLVLANA
Ms serpin-3        FAAIAQEFYKTELKTTNFFKPEVAAREINNWVSNATQGKIPNLVEADDVADVILLILN-T
Dm serpin-27A      FTATLKHFYDSEVEALDFTNPEAAADAINAWAANITQGRLQQLVAPDNVRS-SVMLLTNL
                                 .  :   *       : .:: .::    .      ::

Ms serpin-8        VYFKGLWEIPFREQATQKRNFTLNGGEKK-VASFMQTRRYFKAGTHKPAMAKVVVLPFE-
Bm serpin-12       VYFKGLWQIPFRTESTVPQPFLLKGGIQK-TAPFMRTRRYFRTGLDPITNAKVISLPFE-
Ms serpin-4        LYFKAQWTVPFNASSTTKMPFHDSHGKKIGEVNMMYNRQTYPFANMRQLQARVIELPYGS
Ms serpin-5        ISFKGLWATPFNKSDTVLEPFYNENKEVIGSVNMMYQKAQIPFSNIRDLKAFAIELPYGD
Ms serpin-1J       IYFKGSWKDKFVKERTMDRDFHVS-KDKTIKVPTMIGKKDVRYADVPELDAKMIEMSYE-
Dm Necrotic        VYFQGRWEHEFATMDTSPYDFQHTNGRIS-KVAMMFNDDVYGLAELPELGATALELAYK-
Ms serpin-6        AYFKGVWASKFSPERTKKEPFFVSETRQT-LVPFMKQKGTFHYGVSEELGAQVLELPYK-
Ms serpin-3        LYFKGTWRHQFAPNATKPGPFYVSPQLQK-TVPFMNVKDNFYYVDSSRFDAKILRLPYR-
```

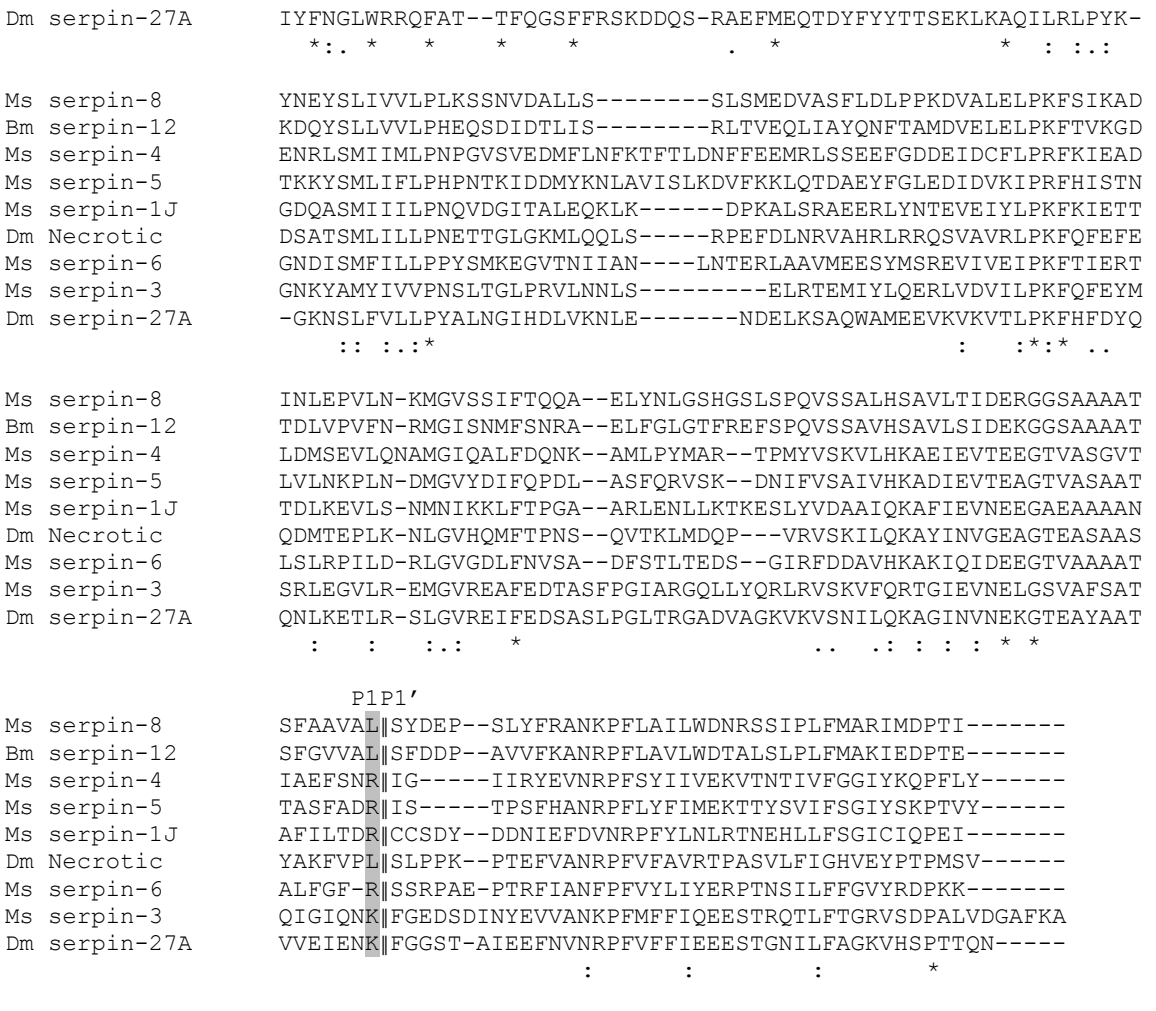

Figure 4. Sequence alignment of nine insect serpins. The amino acid sequences of *M. sexta* serpin-1J, serpin3-6, serpin-8, *D. melanogaster* serpin-27A, *D. melanogaster* Necrotic and *B. mori* serpin-12 are aligned. The secretion signal peptide sequences are underlined. The predicted scissile bonds are indicated by "‖" between P1 (shaded) and P1' residues. "*" indicates positions which have an identical residue. ":" indicates positions which have strongly conserved residues. "." indicates positions which have weakly conserved residues.

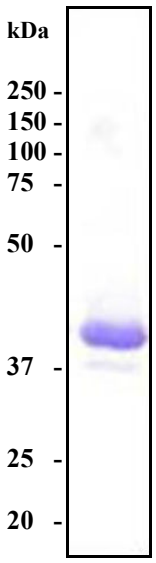

Figure 5. Purification of *M. sexta* serpin-8-ΔN from the baculovirus-infected insect cells. Purified serpin-8-ΔN (50 ng/μl, 10 μl) was analyzed by 10% SDS-PAGE and Coomassie blue staining. Positions and sizes of marker proteins are indicated on the left.

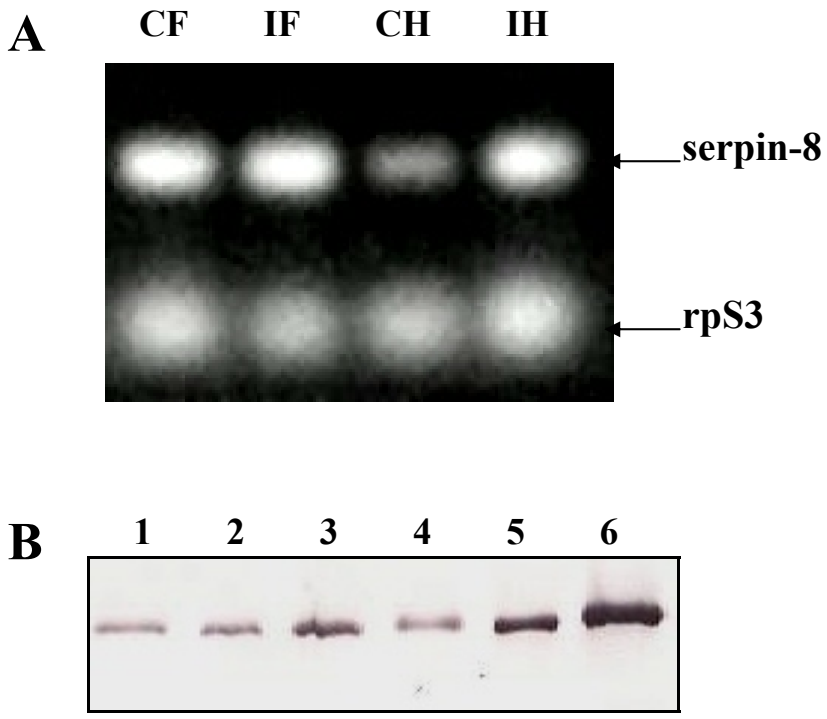

Figure 6. Changes in *M. sexta* serpin-8 mRNA and protein levels upon bacterial challenge. A, Total RNA samples from control (C) and induced (I) larvae fat body (F) and hemocyes (H) were analyzed by RT-PCR using gene specific primers. The *M. sexta* ribosomal protein S3 mRNA was used as an internal standard. CF and CH: fat body and hemocytes from the naïve larvae; IF and IH: hemocytes and fat body from the larvae after 24 h after injection of a mixure of *M. luteus* and *E. coli*. B, cell-free hemolymph samples (2 μl) collected at 0, 1, 6, 12, 24, and 32 h (Lane 1-6) after fifth instar day 2 larvae had been injected with 1×10^8 killed *E.coli* cells were subjected to 10% SDS-PAGE analysis under reducing condition. Immunoblotting was performed using 1: 2000 diluted serpin-8 antiserum as the primary antibody.

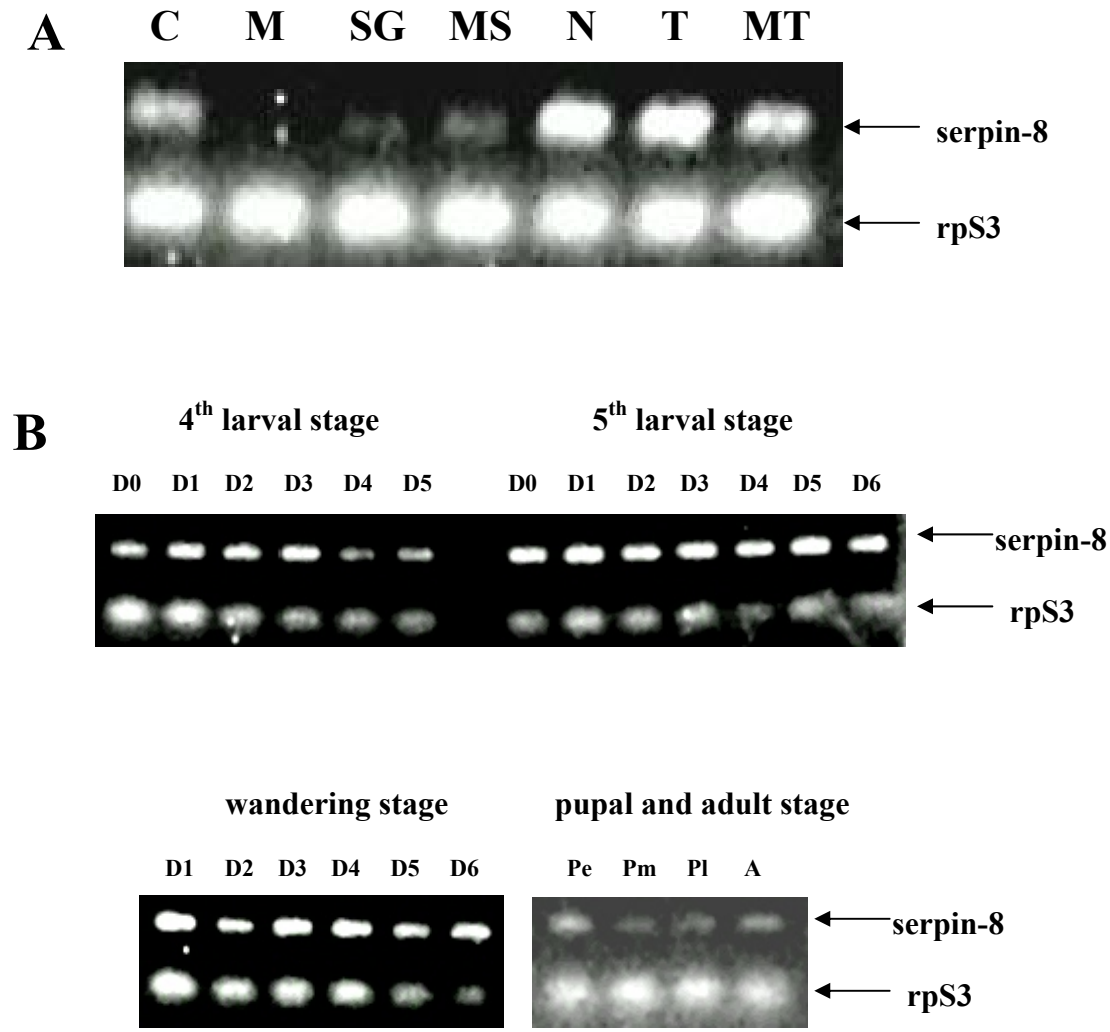

Figure 7. *M. sexta* serpin-8 mRNA levels in different tissues and different developmental stages. A, Total RNA samples of various tissues collected from day 3, 5th instar naïve larvae were analyzed. C: cuticle; M: midgut; SG: salivary gland; MS: muscle; N: nerve; T: trachea; MT: Malpighian tubules. B, Total RNA samples were collected from fat body of day 0-6 of 4th instar naïve larvae, day 1-6 of 5th instar naïve larvae, day1-6 of wandering larvae, and early, middle, late stage from pupae, and adult moth. The *M. sexta* ribosomal protein S3 mRNA was used as an internal standard.

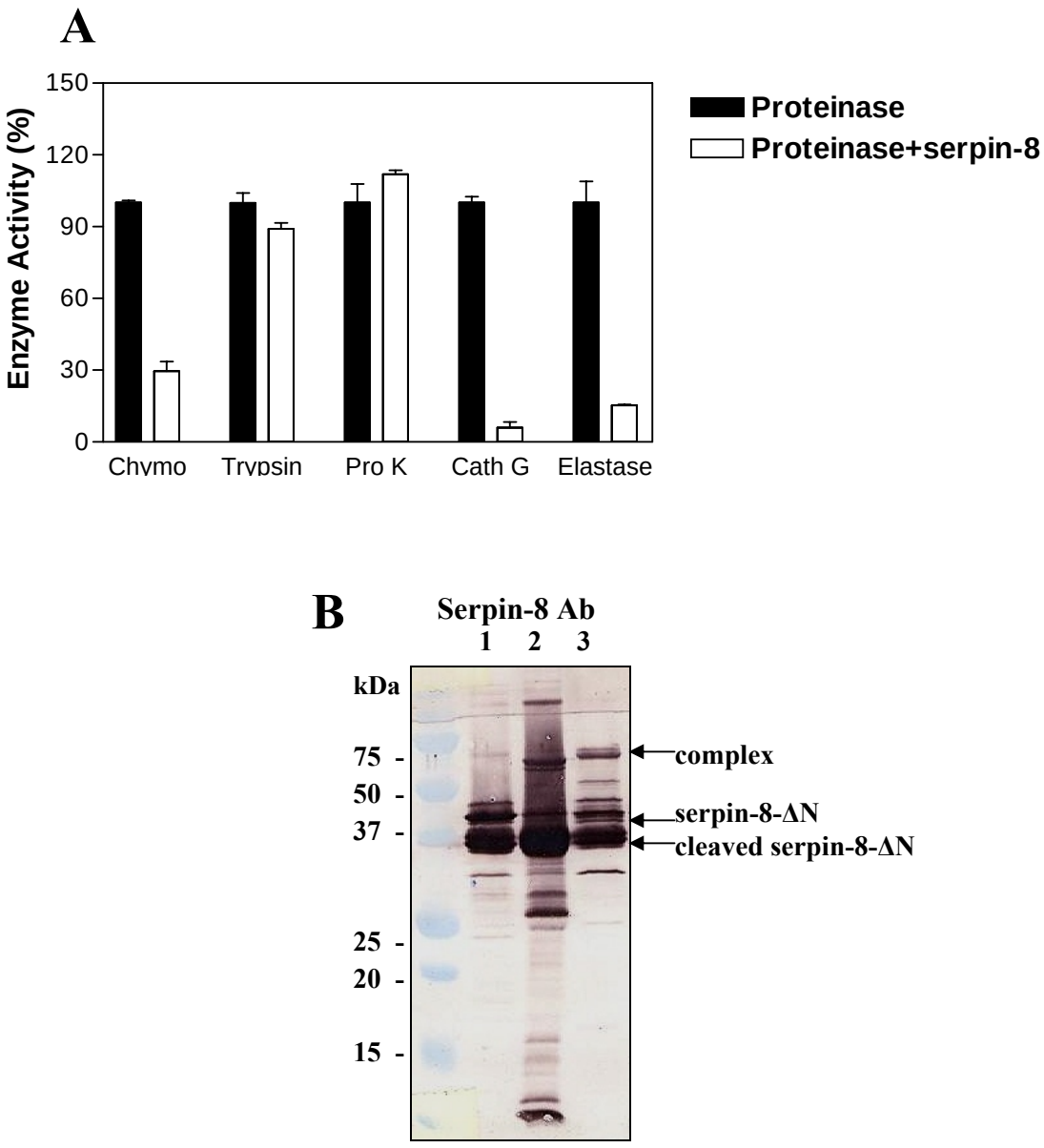

Figure 8. Inhibitory activity of *M. sexta* serpin-8-ΔN. A, Inhibition of enzymatic activity of various proteinases by *M. sexta* serpin-8-ΔN. Purified recombinant serpin-8-ΔN (200 ng/μl, 1 μl) was incubated with various proteinases (100 ng/μl, 1 μl) in the buffer (8 μl, 20mM Tris-HCl, pH 8.0) at room temperature for 10 min. The residual amidase activity (mean ± S.D., n = 3) was then measured using 150 μl different artificial substrates. Chymo: bovine α ─ chymotrypsin, AAPF*p*Na (100 μM) was used as its substrate; Trypsin: bovine pancreatic trypsin, IEAR*p*Na (50 μM) was used as its substrate; Pro K: proteinase K, AAPF*p*Na (100 μM) was used as its substrate; Cath G: human neutrophil Cathepsin G, AAPF*p*Na (100 μM) was used as its substrate; Elastase: porcine pancreatic elastase, AAPL*p*Na (100 μM) was used as its substrate. B, Detection of SDS-stable serpin-proteinase complexes by immunoblot analysis. Tracks contain a mixture of

serpin-8-ΔN (200 ng/μl, 1 μl) and three proteinases (100 ng/μl, 1 μl). Tested proteinases are bovine α－chymotrypsin (Lane 1), porcine pancreatic elastase (Lane 2), and human neutrophil Cathepsin G (Lane 3). Sizes and positions of molecular mass marker are indicated on the left. Ab: antibody.

Table 2. Association rate constants (k_a) for inhibition of three proteinases by *M. sexta* serpin-8-ΔN

Serpin/proteinase molar ratio	Concentration of proteinases	Concentration of serpin-8-ΔN	k_a ($M^{-1}s^{-1}$)
20:1	chymotrypsin 2 μM	40 μM	1.1×10^4
20:1	porcine pancreatic elastase 6 μM	120 μM	2.3×10^4
20:1	human neutrophil Cathepsin G 50 μM	1 mM	2.5×10^4

Bovine α-chymotrypsin (2 μM, 1 μl), porcine pancreatic elastase (6 μM, 1 μl), and human neutrophil Cathepsin G (50 μM, 1 μl) were incubated for varying time at room temperature with excessive moles of serpin-8-ΔN (1 μl) in the buffer (8 μl, 20 mM Tris-HCl, pH 7.5). The residual amidase activities of three proteinaes were measured using sustrates as described in Materials and Methods. Half-life time ($t_{0.5}$) was calculated by linear regression curves plotting ln(residue amidase activity) vs. incubation time (t). Association rate constants (k_a) were calculated using equation $k_a=0.693/(t_{0.5}*I^0)$, I^0 is the initial concentration of the serpin (Beatty et al., 1979).

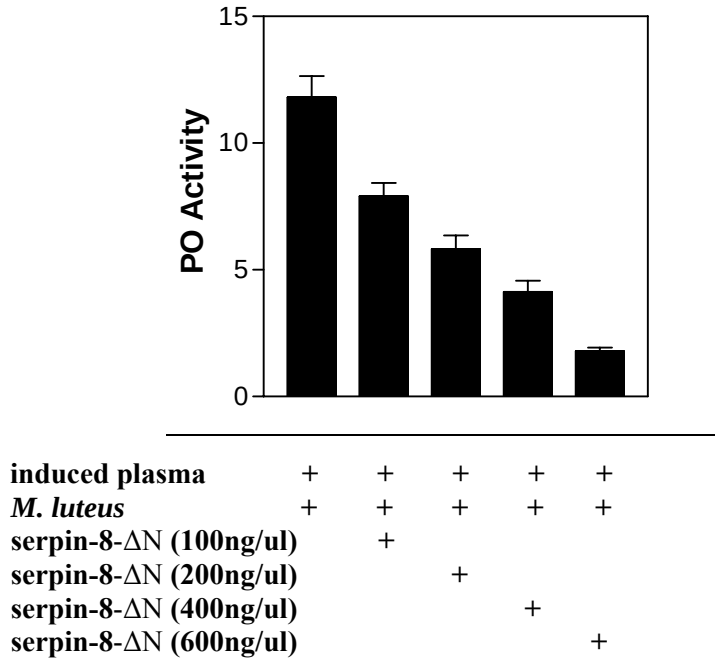

Figure 9. Inhibition of *M. sexta* proPO activation by serpin-8-ΔN. Induce plasma sample (1 µl) was incubated for 5 min at room temperature with different concentrations of recombinant serpin-8-ΔN (1 µl) in the buffer (7 µl, 20 mM Tris-HCl pH 8.0, 1 mM $CaCl_2$, 0.001% Tween-20). Then 1 µl of *M. luteus* (1 µg/µl) was added and incubated at room temperature for 10 min prior to PO activity (mean ± S.D., n = 3) measurement.

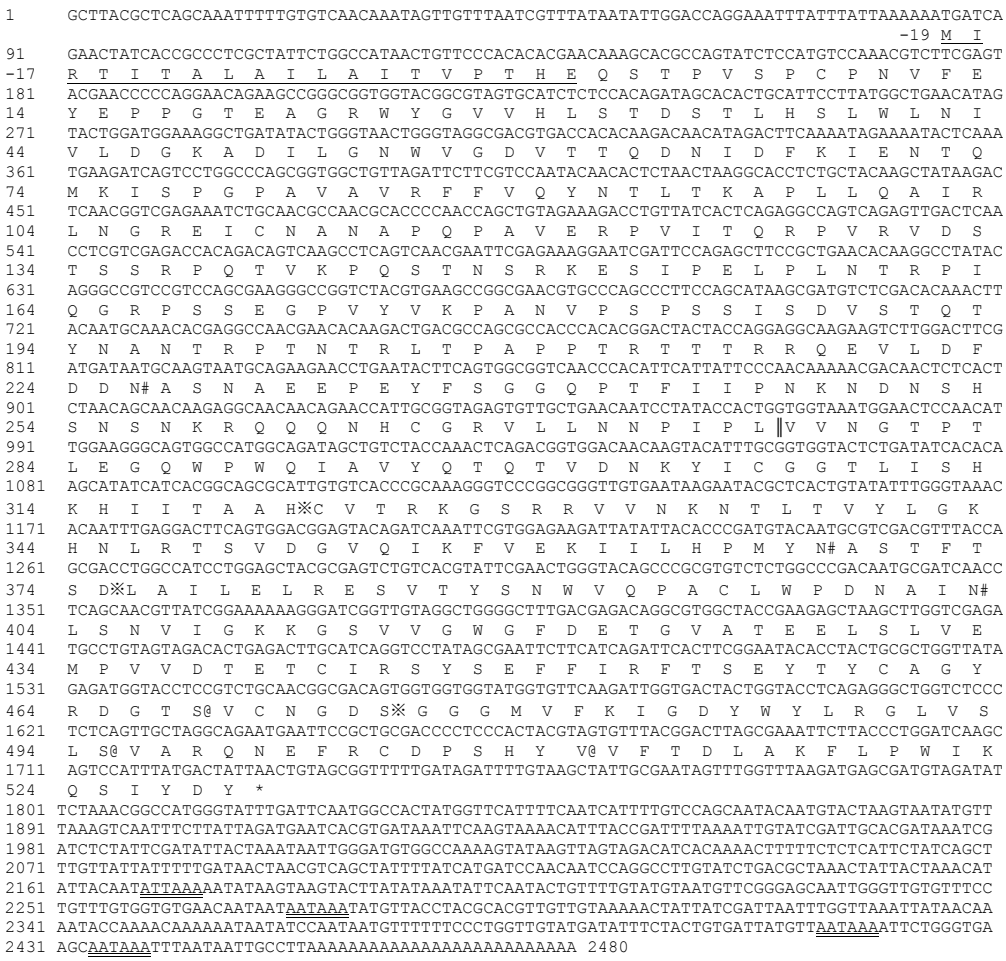

Figure 10. Nucleotide and deduced amino acid sequence of *M. sexta* HP19. The one-letter code for amino acid residue is shown below the nucleotide sequence and aligned with the second nucleotide of the corresponding codon. Numbers on the left are assigned to nucleotide residues and amino acid residues, including negative numbers for residues in the secretion signal peptides which are underlined. Putative *N*-linked glycosylation sites are marked with # after the Asn residues. The predicted proteolytic cleavage site is marked by ‖. The catalytic triad residues are marked by ※. The residues that make the primary substrate-specificity pocket are marked by @. The putative polyadenylation signals (AATAAA or ATTAAA) near the 3'-terminus of cDNA are double-underlined.

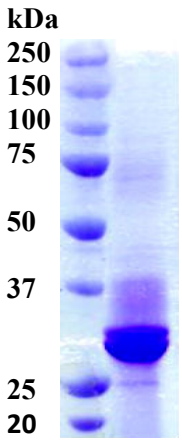

Figure 11. Purification of *M. sexta* catHP19 from the baculovirus-infected insect cells. Purified catHP19 (50 ng/μl, 10 μl) were analyzed on 10% SDS-PAGE and Coomassie blue staining. Positions and sizes of marker proteins are indicated on the left.

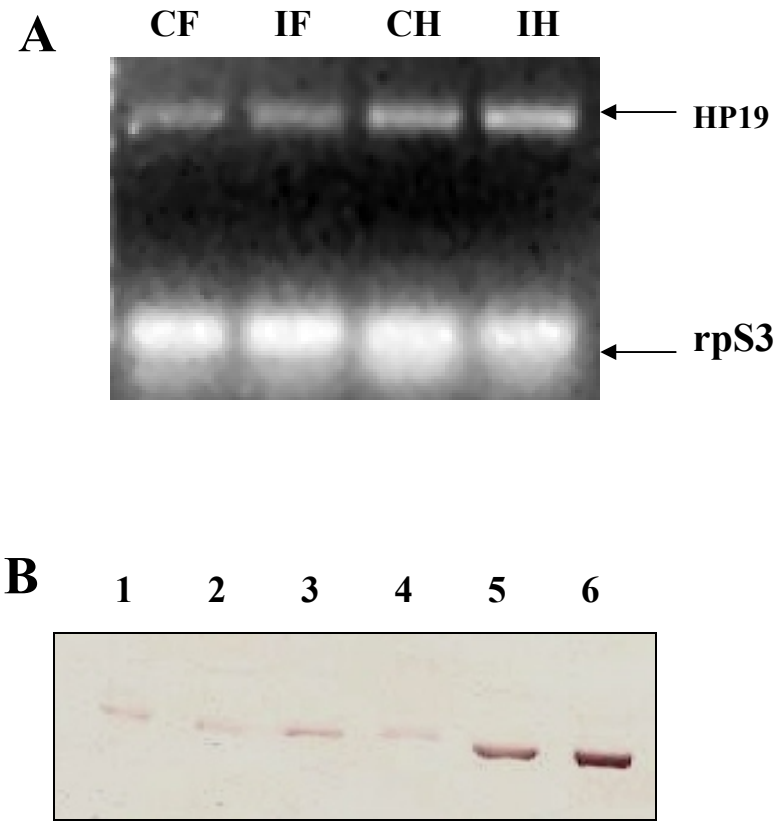

Figure 12. Changes in *M. sexta* HP19 mRNA and protein levels upon bacterial challenge. A, Total RNA samples from fat body (F) and hemocyes (H) of control and induced larvae were analyzed by RT-PCR using gene specific primers. The *M. sexta* ribosomal protein S3 mRNA was used as an internal standard. CF and CH: fat body and hemocytes from the naïve larvae; IF and IH: hemocytes and fat body from the larvae after 24h after injection of a mixure of *M. luteus* and *E. coli*. B, cell-free hemolymph samples (2 µl) collected at 0, 1, 6, 12, 24, and 32 h (Lane1-6) after fifth instar day 2 larvae had been injected with 1×10^8 killed *E.coli* cells were subjected to 10% SDS-PAGE analysis under reducing condition. Immunoblotting was performed using 1: 2000 diluted HP19 antiserum as the primary antibody.

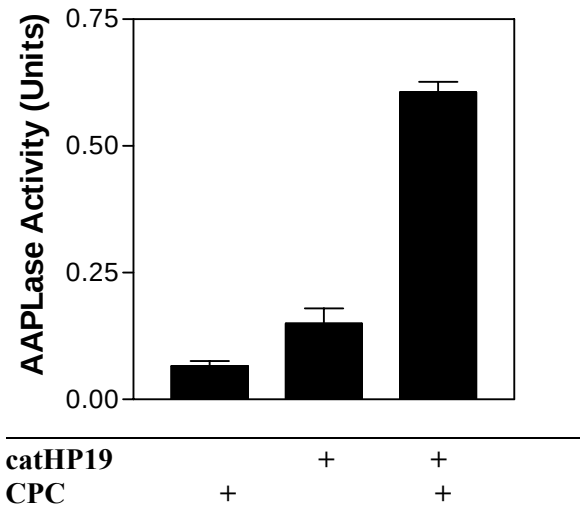

Figure 13. CPC-induced *M. sexta* catHP19 activity using substrate AAPL*p*Na. Purified recombinant catHP19 (150 ng/µl, 2 µl) was incubated with 6 mM CPC (1 µl) in the buffer (7 µl, 20 mM Tris-HCl, pH 7.5, 50 mM NaCl) at room temperature for 5 min. The residual amidase activity (mean ± S.D., n = 3) was then measured using an artificial substrate, AAPL*p*Na (100 µM, 150 µl). CPC or catHP19 alone was used as negative control.

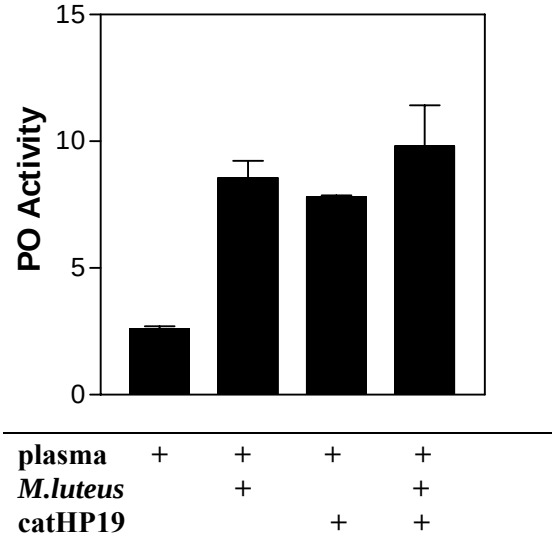

Figure 14. Role of catHP19 in *M. sexta* proPO activation. Naïve hemolymph (1 µl), *M. luteus* (1 µg/µl, 1 µl), and catHP19 (100 ng/µl, 1 µl) were incubated in the buffer (7 µl, 20 mM Tris-HCl pH 8.0, 1 mM $CaCl_2$, 0.001% Tween-20) at room temperature for 30 min. PO activity (mean ± S.D., n = 3) was measured using dopamine as a substrate. Controls reactions were plasma only and plasma with *M. luteus*.

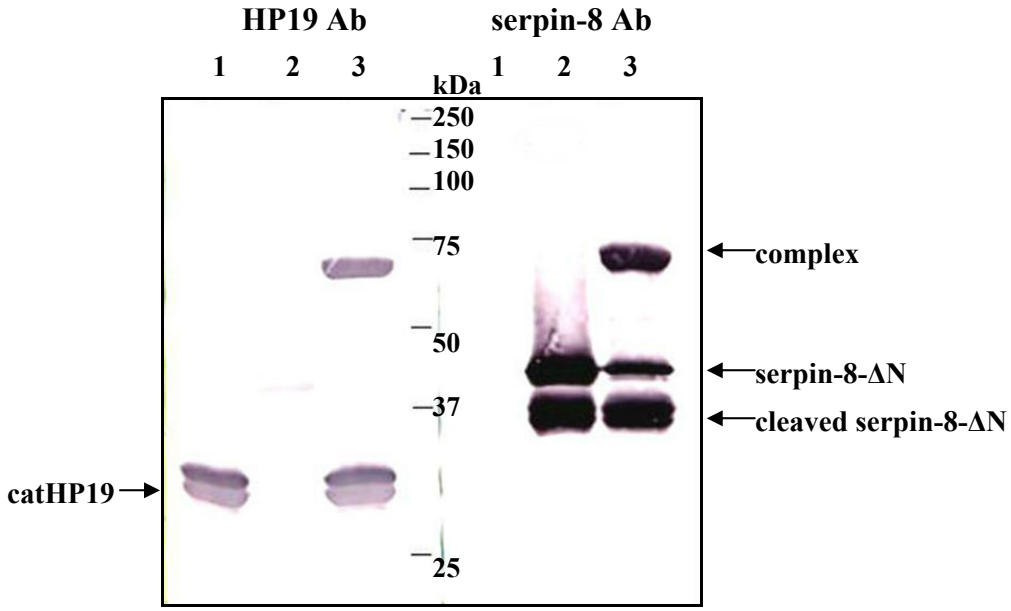

Figure 15. Detection of SDS-stable *M. sexta* serpin-8-ΔN-catHP19 complex by immunoblot analysis. Purified serpin-8-ΔN (150 ng/µl, 1 µl) was incubated with catHP19 (100 ng/µl, 1 µl) in the buffer (13 µl, 20 mM Tris-HCl, pH 7.5, 50 mM NaCl) at room temperature for 30 min. The reaction mixture (15µl) was subjected to immunoblot analysis for detection of the complex. Lane 1: catHP19 only; Lane 2: serpin-8-ΔN only; Lane 3: serpin-8-ΔN and catHP19. Sizes and positions of molecular mass markers are indicated in the middle. Ab: antibody.

A

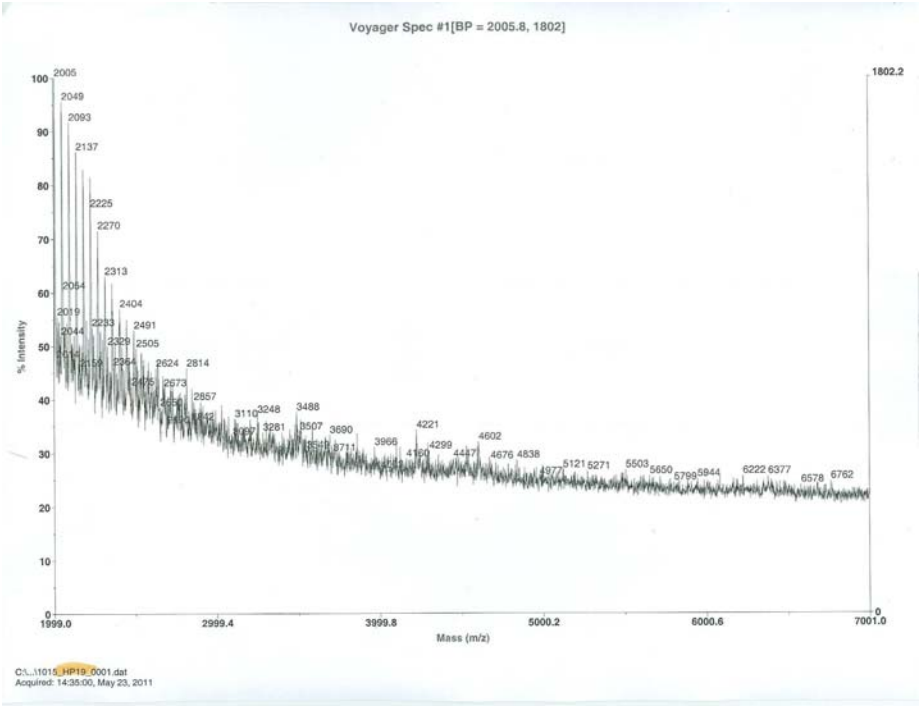
Voyager Spec #1[BP = 2005.8, 1802]
% Intensity
Mass (m/z)
1999.0
2999.4
3999.8
5000.2
6000.6
7001.0
1802.2
2005
2049
2093
2137
2225
2270
2313
2404
2491
2505
2624
2814
2857
3110
3248
3281
3488
3507
3690
3966
4221
4299
4602
4676
4838
5121
5271
5503
5650
5799
5944
6222
6377
6578
6762
C:\...\1015_HP19_0001.dat
Acquired: 14:35:00, May 23, 2011

B

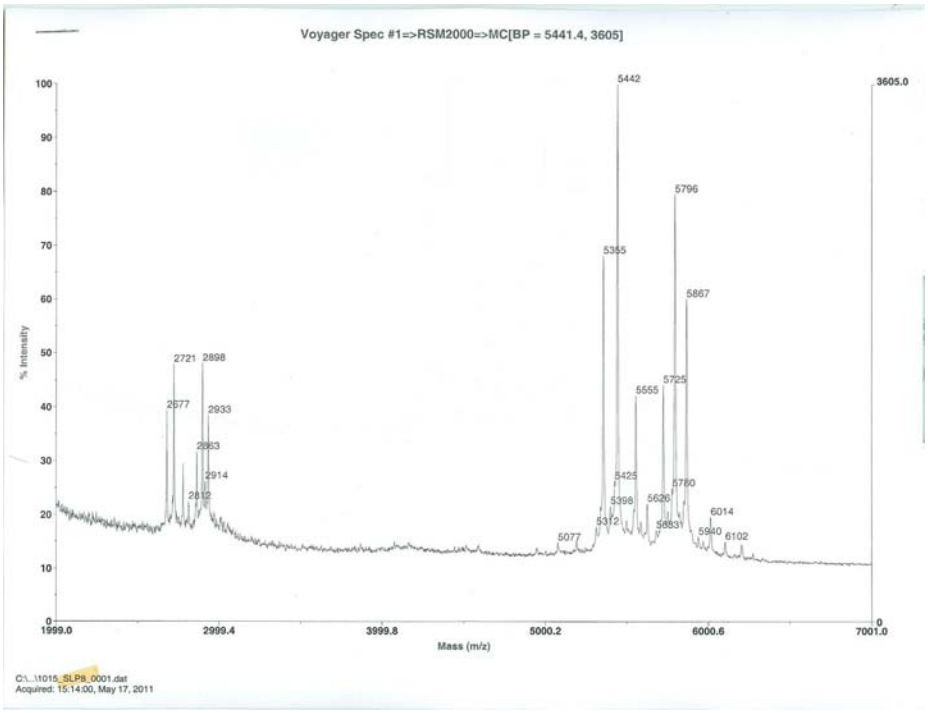
Voyager Spec #1=>RSM2000=>MC[BP = 5441.4, 3605]
% Intensity
Mass (m/z)
1999.0
2999.4
3999.8
5000.2
6000.6
7001.0
3605.0
5442
5796
5355
5867
5725
5555
2721
2898
2577
2933
2863
2914
2812
5425
5398
5626
5760
5312
5883
6014
5077
5940
6102
C:\...\1015_SLP8_0001.dat
Acquired: 15:14:00, May 17, 2011

C

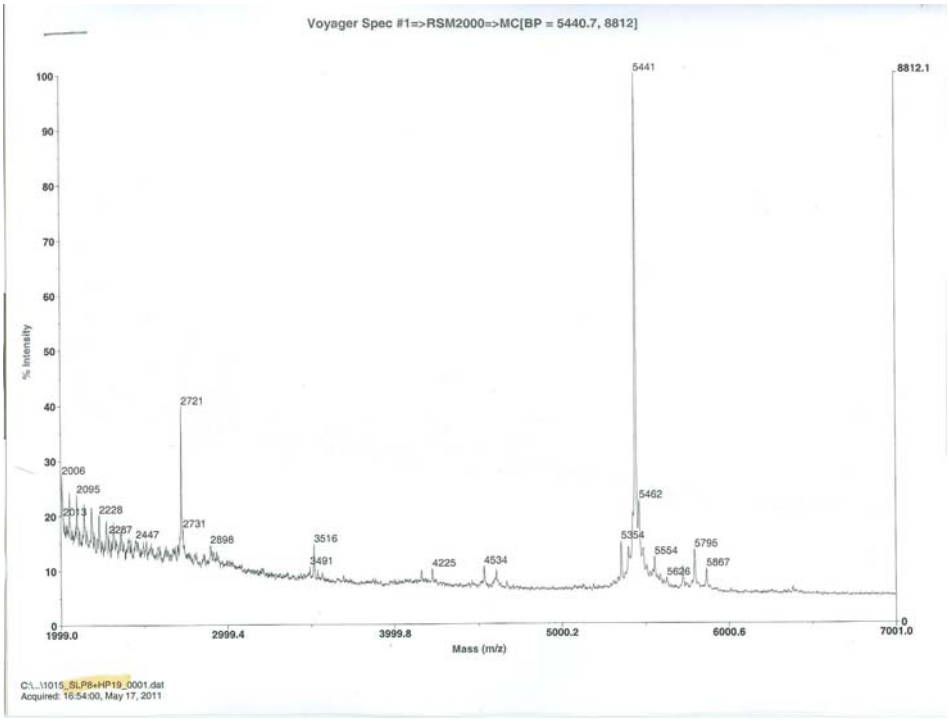

Figure 16. Cleavage site determination of *M. sexta* serpin-8. Purified serpin-8-ΔN (150 ng/µl, 1 µl) was incubated with catHP19 (100 ng/µl, 1 µl) in the buffer (13 µl, 20 mM Tris-HCl, pH 7.5, 50 mM NaCl) at room temperature for 30 min. The reaction mixture was directly analyzed by MALDI-TOF mass spectrometry. Representative strong spectra were presented with the mass value on top of the peaks. The spectrum was subjected to noise removal and calibrated with an external standard of horse apomyoglobulin. A, the control spectrum of catHP19. B, the control spectrum of serpin-8-ΔN. C, the spectrum of mixture of serpin-8-ΔN and catHP19.

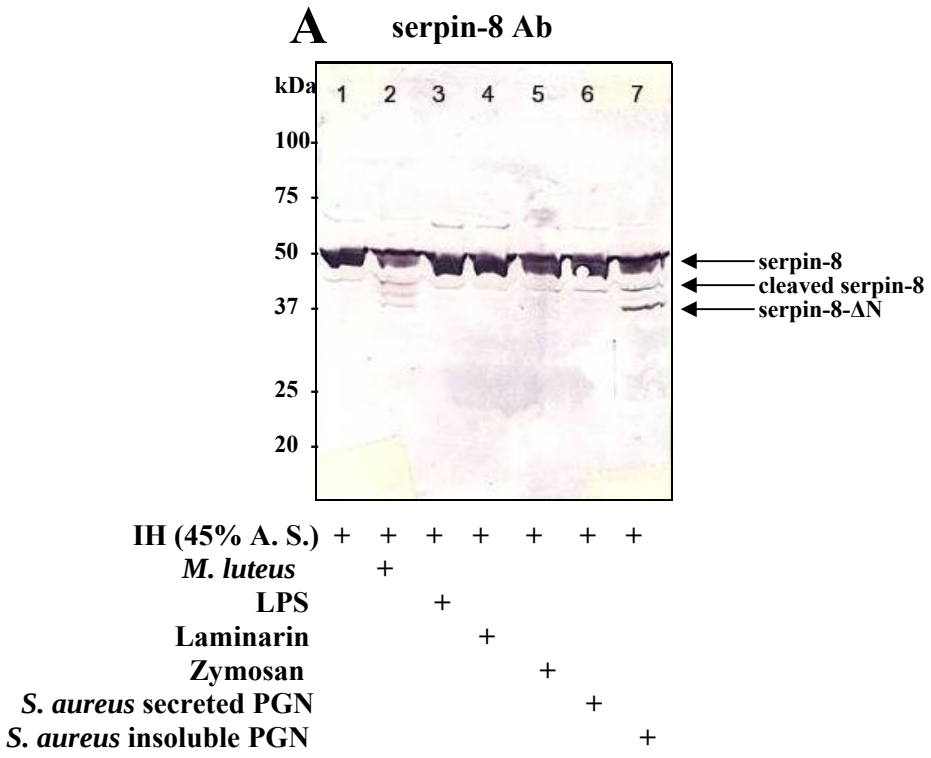
A
serpin-8 Ab
kDa
1 2 3 4 5 6 7
100
75
50
37
25
20
serpin-8
cleaved serpin-8
serpin-8-ΔN
IH (45% A. S.) + + + + + + +
M. luteus +
LPS +
Laminarin +
Zymosan +
S. aureus secreted PGN +
S. aureus insoluble PGN +

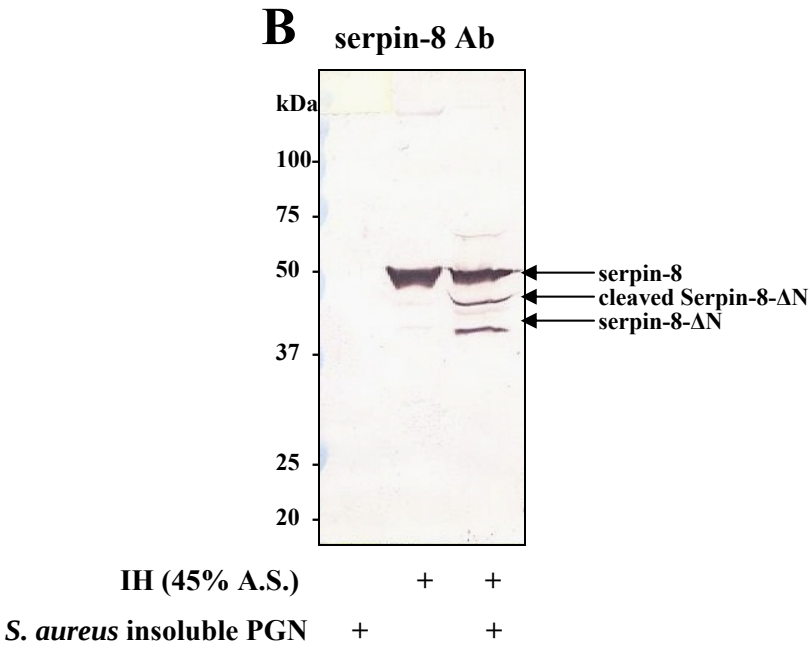
B
serpin-8 Ab
kDa
100
75
50
37
25
20
serpin-8
cleaved Serpin-8-ΔN
serpin-8-ΔN
IH (45% A.S.) + +
S. aureus insoluble PGN + +

Figure 17. Cleavage of *M. sexta* serpin-8 N-terminus upon peptidoglycan stimulus from Gram-positive bacteria. 10 µl of induced hemolymph were mixed with 100% saturated ammonium sulfate (8.2 µl, pH 7.0). The ammonium sulfate (A.S.) was adjusted to 45% saturation, and centrifuged to separate precipitate from the supernatant. The pellet was saved and re-dissolved into the buffer (10 µl, 20 mM Tris-HCl, pH 7.5). Various microbial surface components (1 µg/µl, 1 µl) were incubated with the 45% ammonium sulfate fraction of hemolymph at room temperature for 15 min. *M. luteus* (Sigma); LPS (Invitrogen); Laminarin (Sigma); Zymosan (Sigma); *S. aureus* secreted PGN (Sigma): *Staphylococcus aureus* secreted peptidoglycan; *S. aureus* insoluble PGN (Sigma): *Staphylococcus aureus* insoluble peptidoglycan. The reaction mixtures were separated by 10% SDS-PAGE and immunoblot analysis was performed using serpin-8 antibody. The sizes and positions of molecular weight standards are indicated on the left. Bands representing serpin-8, serpin-8 cleaved products and serpin-8-ΔN are marked by arrows. Ab: antibody.

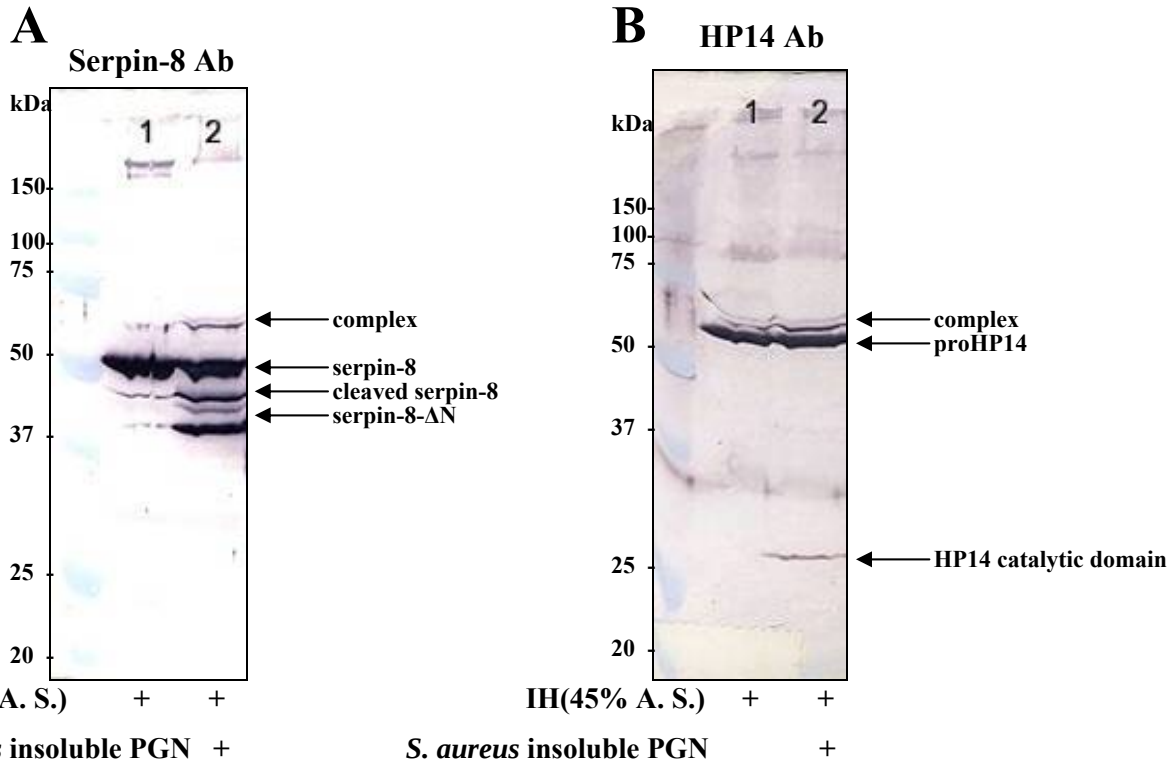

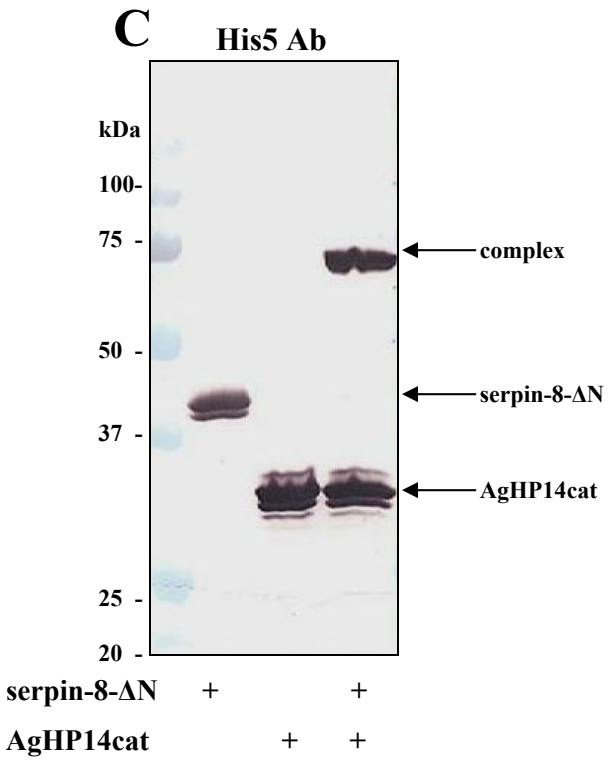

Figure 18. Detection of *M. sexta* serpin-8-proteinase complex in hemolymph. 10 μl of induced hemolumph were mixed with 100% saturated ammonium sulfate (8.2 μl, pH 7.0) to 45% saturation. The suspension was centrifuged to separate precipitate from the supernatant. The pellet was saved and re-dissolved into the buffer (20 μl, 20 mM Tris-HCl, pH 7.5). *S. aureus* insoluble PGN (1 μg/μl, 1 μl) was incubated with the 0-45% AS fraction of induced hemolymph at room temperature for 30 min. Half of the reaction mixtures (10.5 μl) were separated by 10% SDS-PAGE and immunoblot analysis was performed using serpin-8 antibody (A) and the other half of the reaction mixtures (10.5 μl) were treated the same way except for using HP14 antibody (Wang et al., 2006) (B). C, Detection of SDS-stable *M. sexta* serpin-8-ΔN-AgHP14cat complex by immunoblot analysis. Purified serpin-8-ΔN (150 ng/μl, 1 μl) was incubated with AgHP14cat (100 ng/μl, 2 μl) in the buffer (7 μl, 20 mM Tris-HCl, pH 7.5, 50 mM NaCl) at room temperature for 30 min. The reaction mixture (10 μl) was subjected to 10% SDS-PAGE and immunoblot analysis using His5 antibody. The sizes and positions of molecular weight standards are indicated on the left. Bands representing serpin-8, cleaved serpin-8, serpin-8-ΔN, complex, proHP14, HP14 catalytic domain, AgHP14cat are marked by arrows. Ab: antibody.

CHAPTER IV

EXPRESSION, PURIFICATION AND FUNCTIONAL STUDY OF *MANDUCA SEXTA* CLIP-DOMAIN HEMOLYMPH PROTEINASE-1

Introduction

Extracellular serine proteinase cascades are involved in some biological processes in vertebrates and invertebrates, such as blood coagulation and complement system in mammals, development and immune responses in invertebrates (Ashida, et al., 1997). Melanization, an insect defense response to wounding and infection, involves such a serine proteinase network. Insect PO is synthesized as inactive zymogen proPO. The proteolytic cleavage of proPO occurs as the final step in a serine proteinase cascade activated by tissue damage or microorganism invasion (Cerenius et al., 2008). The final step of proPO activation has been well studied in many insects. Three *M. sexta* PAPs effectively activate proPO to PO in the presence of cofactors, serine proteinase homologs (SPHs) (Yu et al., 2003). Three *T. molitor* PPAFs have been identified and two of them have been crystallized providing insights into the activation mechanism (Kan et al., 2008; Park et al., 2007; Lee et al., 2004).

To elucidate the complex pathway components, cDNA cloning and functional study of HPs are essential. HP1-HP4 were the first four serine proteinases isolated in *M. sexta* by designing degenerate primers coding for the conserved sequences around the catalytic residues (Jiang et al., 1999). After successfully isolated the four HP cDNAs, 20 additional HP cDNAs have been cloned (Jiang et al., 2005). It is reported that mRNA and protein levels of many HPs increase after the immune challenge. Polyclonal antibodies were generated against recombinant

HPs, which allows us to detect proteolytic cleavages occurred in plasma after bacterial injection.

The initiation of *M. sexta* proPO activation is via HP14 autoactivation upon recognition of fungal surface components, which sequentially activate HP21, PAP-2 and -3, and eventually convert proPO to PO (Wang et al., 2007). Another clip-domain serine proteinase of *M. sexta*, HP6 was identified. It was shown to occupy a position as the penultimate proteinase in two different immune pathways, one led to activation of proPO and the melanization response and the other triggered the activation of spätzle and synthesis of AMPs (An et al., 2009). *Drosophia* serine proteinase, Persephone, an ortholog to *M. sexta* HP6 is found to be involved in a fungal-specific branch of Toll receptor activation (Levashina et al., 1999; Ligoxygakis et al., 2002). Persephone can be activated either by the secreted fungal virulence factor PR1 or by endogenous proteolytic activity in hemolymph downstream of GNBP3 (Gottar et al., 2006). However, the activators of both *M. sexta* HP6 and *Drosophila* Persephone are not yet identified.

As mentioned above, HP1 is one of the first four serine proteinases isolated in *M. sexta*. Based on sequence alignment, the proteolytic activation site of HP1 is predicted between residues Arg^{140} and Val^{141}, which indicates that HP1 has trypsin-like specificity (Jiang et al., 1999). HP1 is most similar in sequence to the proclotting enzyme from horseshoe crab, *T. tridentatus*. HP1 mRNA is expressed highly in hemocytes, but not in fat body. The amount of HP1 mRNA does not change significantly after *E. coli* injection (Jiang et al., 1999). No further study has been reported to investigate the biological functions of HP1. Recently, we found one HP1 clone whose sequence is slightly different from the one published. To distinguish them, we designate the published HP1 as HP1a and the new one as HP1b. Most of serine proteinases including HP1 are synthesized as zymogens in plasma. Their active forms are difficult to purify from hemolymph due to low concentrations and regulation by serpins. Expression catalytic domains of serine proteinase may provide a good way to obtain active proteinases and study their functions. Availability of recombinant zymogens and active forms of HPs may facilitate us to use them as substrates in pathway perturbation assays.

Here we report the expression and functional characterization of *M. sexta*, HP1. HP1 zymogen forms, proHP1a and proHP1b, and the catalytic domains catHP1a and catHP1b were produced. These purified proteins were used as reagents to examine their proteolytic activity *in vitro* and *in vivo*. The role of HP1 in *M. sexta* proPO activation pathway was examined. We also analyzed the complex formed by HP1 and serpins in plasma.

Materials and Methods

Insects and hemolymph collection

M. sexta eggs were originally purchased from Carolina Biological Supply, and the larvae were reared as described by Dunn and Drake. Control hemolymph was collected from cut prolegs of day 2, 5th instar larvae. Day 2, 5th instar larvae were injected with a mixture of formaldehyde-killed *E. coli* (1×10^8 cells/larvae) and 100 μg of *Micrococcus luteus* (Sigma) suspended in 100 μl of saline (0.9% w/v of NaCl). Induce hemolymph was collected 24 h after injection. A few crystals of diethyldithiocarbamate and phenylthiourea were added to the tubes before collection to prevent melanization of hemolymph. Hemolymph from the naïve and induced insects were aliquoted and stored at -80°C.

Expression and purification of *M. sexta* proHP1a, proHP1b, and catalytic domains of HP1, catHP1a and catHP1b

ProHP1a was amplified by PCR using forward primer j1351 (5'-GAA TTC GAG ATT ACT CCG AAC TGC A-3', *Eco*RI site underlined) and reverse primer j587 (5'-CTC GAG CCG TGC ATT CTC CAT G-3', *Xho*I site underlined) from HP1a cDNA clone. ProHP1b was amplified by PCR using the same pair of primers (forward primer j1351 and reverse primer j587) from HP1b cDNA clone. CatHP1a was amplified by PCR using forward primer j586 (5'-CAA TTG GCG GCC GCC CAG CAA-3', *Mfe*I site underlined) and reverse primer j587 (5'-CTC

GAG CCG TGC ATT CTC CAT G-3', *Xho*I site underlined) from HP1a cDNA clone. CatHP1b was amplified by PCR using the same pair of primers (forward primer j586 and reverse primer j587) from HP1b cDNA clone.

The amplified fragment was purified with Wizard PCR Preps DNA Purification System (Promega) and ligated into pGEM-T vector (Promega). From the resulting plasmid, the *Eco*RI-*Xho*I fragment for proHP1a/b and *Mfe*I-*Xho*I fragment for catHP1/b were retrieved by restriction digestion and directionally inserted to the same sites of $pMFH_6$ (Lu et al., 2008) a plasmid vector modified from pFastBac1, to generate recombinant baculovirus according to the manufacture's instruction. The recombinant plasmid, $pMFH_6$-proHP1a/b or $pMFH_6$-catHP1a/b was transformed into *E. coli* strain DH10Bac, which contains a bacmid and a helper plasmid. The recombinant bacmid obtained by transposition of $pMFH_6$-proHP1a/b or $pMFH_6$-catHP1a/b donor plasmid was isolated. The insertion of proHP1a/b or catHP1a/b sequence in the recombinant bacmid was confirmed by PCR using a proHP1a/b or catHP1a/b gene-specific forward primer and a reverse primer located downstream of the transposition site on the bacmid.

For protein expression, the initial viral stock (V_0) was obtained by transfected *Spodoptera frugiperda* Sf9 cells with a bacmid-cellFECTIN mixture, and its titer was improved through serial infections. Sf9 cells (at 2.0×10^6 cells/ml) in 100 ml of Sf-900 II serum-free medium (Invitrogen) were infected with the baculovirus stocks at a multiplicity of infection of 10 and grown at 27°C for 96 h with gentle agitation (100 rpm).

ProHP1a and proHP1b purifications were carried out using 500 ml of the cell culture medium. The cells were removed by centrifugation at 5,000×*g* for 15 min. The supernatant was mixed with an equal volume of distilled water (500 ml) with 1mM benzamidine at 4°C for 30 min. After centrifugation at 12,000×*g* for 30 min, the cleared supernatant (1000 ml) was applied to a dextran sulfate (DS)-Sepharose column (40 ml) (Nakamura et al., 1985) equilibrated with

buffer A (10 mM potassium phosphate, pH 6.4, 1 mM benzamidine) and washed with 200 ml of buffer A, bound proteins were eluted with a linear gradient of 0-1.0 M NaCl in buffer A (100 ml).

The fractions (4 ml/tube) were collected and aliquots of the fraction (7 μl) were subjected to SDS-PAGE and immunoblot analysis using HP1 antibody (Jiang et al., 1999). Fractions containing *M. sexta* proHP1a/b were pooled and applied onto nickel-nitrilotriacetic-acid-agarose column (2 ml), equilibrated with buffer B (50 mM potassium phosphate, pH 8.0, 300 mM NaCl, 10 mM imidazole, 0.005% Tween-20) and washed with 10 ml of buffer B, bound proteins were eluted from the column with a linear gradient of 10-100 mM imidazole in buffer B (10 ml). Finally, tightly bound proteins were eluted with 5 ml of buffer B containing 250 mM imidazole. The fractions (1 ml/tube) were collected and subjected to SDS-PAGE and immunoblot analysis using HP1 antibody. Fractions containing proHP1a/b were pooled and concentrated using Amicon ultracentrifugal 30K MWCO filter device (Millipore). Buffer of the concentrated protein was exchanged with 20 mM Tris-HCl, pH 7.5, 50 mM NaCl using the same filter and stored at -80°C in aliquots. CatHP1a/b was purified from the conditioned medium (1 liter) by the same protocol except for using Amicon ultracentrifugal 10K MWCO filter device (Millipore) to concentrate proteins.

ProPO activation assay

One μl of hemolymph was incubated for 30 min at room temperature with *M. luteus* (1 μg/μl in saline, 1 μl) in the buffer (8 μl, 20 mM Tris-HCl pH 8.0, 1 mM $CaCl_2$, 0.001% Tween-20). PO activity was measured by adding 150μl of 2 mM dopamine (in 100 mM sodium phosphate buffer, pH 7.5) as a substrate and monitoring A_{470} for 10 min on a microplate reader (Jiang et al., 2003a). Hemolymph samples which have low basal PO activity were selected for the assay.

To dertermine the role of proHP1a/b or catHP1a/b in proPO activation, naïve hemolymph (1 μl), *M. luteus* (1 μg/μl, 1 μl), and proHP1a/b (100 ng/μl, 1 μl) or catHP1a/b (50 ng/μl, 1 μl)

were incubated in the buffer (7 µl, 20 mM Tris-HCl pH 8.0, 1 mM $CaCl_2$, 0.001% Tween-20) at room temperature for 30 min. PO activity was measured using dopamine as described above. An average activity data were plotted as mean ± S.D. (n = 3) in the bar graph. Control reactions were plasma only and *M. luteus* with plasma.

To test possible additive effect of proHP1- or catHP1-elicitor interaction on proPO activation, four samples were used as decribed above: naïve plama (1 µl in 9 µl buffer) (#1), elicitor (1 µg/µl, 1 µl) + plasma (1 µl in 8 µl buffer) (#2), enzyme (1 µl) + plasma (1 µl in 8 µl buffer) (#3) and elicitor (1 µg/µl, 1 µl) + enzyme (1 µl) + plasma (1 µl in 7 µl buffer) (#4). PO activities of #4 and (#2 + #3 - #1) were directly compared using unpaired t-test (Wang et al., 2011).

Immunoblot analysis

Cell-free hemolymph samples were collected as described above, and these plasma samples or purified proteins were separated by 10% SDS-PAGE. Immunoblot analysis was performed using rabbit polyclonal antiserum against HP6 as the primary antibody (diluted 1: 2000) and goat anti-rabbit IgG-alkaline phosphatase conjugate (BioRad, diluted 1: 1000) as the secondary antibody. Amounts of hemolymph and each protein for a particular experiment are provided in the legends to Fig. 24, 27-29.

Cleavage of *M. sexta* proHP6 by HP1 in the presence of CPC

Purified recombinant proHP6 (An et al., 2009) was incubated with proHP1a in the presence of CPC, or various types of detergents in the buffer (20 mM Tris-HCl pH 7.0, 20 mM NaCl) at 37°C for 4 h. Amounts of each protein for a particular experiment are provided in the legends to Fig. 24, 26-29.

Determination of amino-terminal sequences

Purified recombinant proHP6 (150 ng/μl, 2 μl) (An et al., 2009) was incubated with proHP1a (300 ng/μl, 2 μl) and 6 mM CPC (1 μl) in the buffer (10 μl, 20 mM Tris-HCl pH 7.0, 20 mM NaCl) at 37°C for 4 h. The reaction mixture was treated with SDS-loading buffer containing DTT and separated on 10% SDS-PAGE. The protein was then transferred to a polyvinylidene difluoride (PVDF) membrane and stained with Coomassie Blue. The 30 kDa polypeptide corresponding to the cleaved HP6 was cut out and subjected to automated Edman degradation in Nevada Proteomics Center.

Assay of amidase activity

Purified recombinant proHP1a (250 ng/μl, 2 μl) or catHP1a (150 ng/μl, 2 μl) was incubated with various concentrations of cetylpyridinium chloride (CPC, 1 μl) in the buffer (7 μl, 20 mM Tris-HCl pH 7.0, 20 mM NaCl) at room temperature for 5 min. The residual amidase activity was then measured using the artificial substrates, N-acetyl-Ile-Glu-Ala-Arg-*p*-nitroanilide (IEAR*p*Na, 50 μM, 150 μl, Sigma) or N-acetyl-Leu-Asn-Leu-His-*p*-nitroanilide (LDLH*p*Na, 100μM, 150 μl, KSU) by monitoring A_{405} in the kinetic mode on a plate-reader (Molecular Device). One unit activity is defined as ΔA_{405}/min=0.001. Activity data were plotted as mean ± S.D. (n = 3) in the bar graph.

Immuno-affinity purification of *M. sexta* HP1-serpin complex

HP1 antibody-coupled Protein-A Sepharose CL-4B beads were prepared (Harlowet al., 1988). Briefly, Protein-A Sepharose CL-4B beads (Sigma) were hydrated in PBS and washed three times with PBS. About 2 ml of the beads were resuspended in 10 ml of PBS and mixed by rotation for 2 h at room temperature with 2 ml of HP1 rabbit antiserum. Then the beads were washed three times with 10 volumes of PBS and twice with 10 volumes of 0.2 M sodium borate, pH 9.0. Solid dimethylpimelimidate was added to a final concentration of 20 mM to the beads resuspended in 10 volumes of 0.2 M sodium borate, pH 9.0 and mixed overnight at room

temperature. The coupling was terminated by washing the beads with 0.2 M ethanolamine-HCl, pH 8.0 and reacted with it for 2 h at room temperature. Finally, the beads were washed with PBS and stored in PBS at 4°C.

To purify HP1-serpin complex from hemolymph, 15-20 ml of naïve hemolymph was collected from day 3 fifth instar larvae. The plasma was mixed with a protease inhibitor cocktail (Sigma, P-8849, 1 ml to 20 ml of plasma) and incubated for 10 min to inactivate proteases. The plasma was centrifuged at 5000×g for 15 min at 4°C to remove any precipitate. The supernatant was mixed overnight at 4°C with 2 ml of HP1-antibody-coupled Protein-A Sepharose CL-4B beads, and the mixture was packed into a column. The column (2 ml of bed volume) was washed with 20 volumes of 1 M NaCl and then 10 volumes of 10 mM sodium phosphate buffer, pH 6.5. Finally the column was eluted with 10 volumes of 100 mM glycine-HCl, pH 2.5, 10% ethylene glycol. Fractions (1 ml each) were collected into 0.1 ml of 1 M sodium phosphate, pH 8.0. The fractions were analyzed by 10%SDS-PAGE and immunoblotting analysis.

Orbitrap MS analysis of *M. sexta* HP1-serpin complexes

To identify HP1-serpin complexes after separation by SDS-PAGE, the complex bands were cut out, and Orbitrap mass spectrometry (MS) of tryptic fragments was performed by the Recombinant DNA/Protein Core Facility at Oklahoma State University. The protein bands were reduced with DTT and alkylated with iodoacetamide, and then subjected to in-gel trypsin digestion. The peptide masses were compared with the predicted masses of tryptic peptides derived from *M. sexta* hemolymph proteases in *M. sexta* database which includes the protein sequences from NCBI, and contig sequences from the pyrosequencing project (Zhang et al., 2011). Mascot was used as search engine, and the results were displayed by Scaffold.

Results

cDNA sequence and structural features of *M. sexta* HP1b

The cDNA sequence of HP1 was published previously (Jiang et al., 1999). The open reading frame encodes a protein of 388 amino acid residues, with a predicted 14-residue secreted signal peptide. The calculated molecular mass of mature HP1 is 41,934Da and its calculated isoelectric point is 5.67. Recently we found one HP1 clone whose sequence is slightly different from the reported one. Thus, we designate the published one as HP1a and the new one as HP1b.

The HP1b cDNA contains 1349 nucleotides, with a 10-bp 5'-noncoding region, a 1167-bp open reading frame, and a 172-bp 3'-noncoding region, including a 18-bp poly (A) tail. The 3'-noncoding region contains one putative polyadenylation signals (AATAAA) (Fig. 19). The open reading frame encodes a protein of 388 amino acid residues, with a predicted 14-residue secreted signal peptide. There are two potential *N*-linked glycosylation sites at Asn^{205} and Asn^{261}. The calculated molecular mass of mature HP1b is 41,843Da and its calculated isoelectric point is 5.38.

Based on sequence alignment, HP1a and HP1b are 89% identical and 95% similar in amino acid sequence (Fig. 20). The predicted proteolytic cleavage sites of HP1a and HP1b are located between Arg^{140} and Val^{141} indicating that the activating enzyme for proHP1 may be a serine proteinase with trypsin-like specificity. Both proHP1a and proHP1b are clip domain serine proteinases composing of an amino-terminal clip domain connected by a linker region to a carboxyl-terminal serine proteinase domain. Their catalytic domains include a catalytic triad of His^{182}, Asp^{231}, and Ser^{324}. Their primary substrate-specificity pocket is likely composed of Asp^{318}, Gly^{346}, and Gly^{356}, suggesting that HP1a and HP1b have the specificity for cleavage after positively charged amino acid residues, Lys or Arg. A new BLAST search indicated that *M. sexta* HP1 is most similar in amino acid sequence to *B. mori* hemocyte proteinase-1 (BAG70409.1), with 67% identity and 83% similarity. *B. mori* hemocyte proteinase-1 has not been characterized.

Expression and purification of *M. sexta* proHP1a, proHP1b, and catalytic domains catHP1a and catHP1b

The fragment of proHP1a/b was inserted into the *Eco*RI-*Xho*I restriction site of the expression vector, $pMFH_6$ which has a honeybee mellitin signal peptide and C-terminal $(His)_6$-affinity tag (Lu et al., 2008), and the fragment of catHP1a/b was inserted into the *Mfe*I-*Xho*I restriction site of the same vector. The N-terminal residues "Val-Phe-Gly-Ser" of HP1a catalytic domain and the N-terminal residues "Val-Phe-Asp-Ser" of HP1b catalytic domain were replaced by "Gly-Ile-Gly-Gly" in order to fit into the expression vector and have the least changes in amino acid residues. All the recombinant proteins were soluble and secreted into the cell culture medium. After removing the cells from the culture, the protein was purified by ion exchange column and eluted from the dextran sulfate (DS) column with a linear gradient of NaCl. The elution fractions which contained the target proteins were pooled and loaded onto the nickel-affinity column. The protein was eluted with a linear gradient of imidazole. The proHP1a and proHP1b migrated as a 50kDa single band (Fig. 21A and C) on 10% SDS-PAGE under reducing condition. The apparent molecular masses of proHP1a and proHP1b were greater than the predicted masses for the mature proenzyme. This may indicate that proHP1 is post-translationally modified by glycosylation. CatHP1a and catHP1b migrated as a 30kDa band (Fig. 21B and D) on 10% SDS-PAGE under reducing condition.

Roles of proHP1a and proHP1b in *M. sexta* proPO activation

To study the roles of proHP1a and proHP1b in *M. sexta* proPO activation cascade, control hemolymph was incubated with microbial elicitor, *M. luteus* and recombinant proHP1a and proHP1b. The control hemolymph sample had low basal PO activity and could be activated substantially by *M. luteus*, which indicated that the proPO activation system was functional in the hemolymph. As shown in Fig. 22, there was an increase of PO activity when proHP1a or proHP1b was added to the control hemolymph in the absence of microbial elicitor. When

proHP1a or proHP1b, *M. luteus*, and control hemolymph were incubated together, a greater enhancement of PO activity was observed than the one when hemolymph was incubated with proHP1a or proHP1b only. But the statistical analysis indicated that there was no additive effect of proHP1a and *M. luteus* , or proHP1b and *M. luteus* on increase of PO activity.

Roles of catHP1a and catHP1b in *M. sexta* proPO activation

The roles of catHP1a and catHP1b in *M. sexta* proPO activation cascade were also investigated (Fig. 23). The control hemolymph with low basal PO activity and high sensitiviry to *M. luteus* was incubated with microbial elicitor and catHP1a or catHP1b prior to PO activity measurement. A dramatic increase of PO activity was observed when catHP1a alone was added into hemolymph, and a moderate increase of PO activity when catHP1b alone was incubated with hemolymph. When catHP1a or catHP1b, *M. luteus*, and control hemolymph were incubated together, PO activity was as high as catHP1a or catHP1b alone was incubated with hemolymph, indicating that there was no additive effect of either catHP1a or catHP1b and *M. luteus* on enhancement of PO activity.

***M. sexta* proHP6 cleavage in plasma by catHP1a and catHP1b**

We used immunoblot analysis to investigate which endogenous serine proteinase(s) can be activated by catHP1a in *M. sexta* plasma with various antibodies against hemolymph serine proteinases (Jiang et al., 2005). There was no major difference in HP2, HP5, HP9, HP12-19, HP21, HP22, HP25, PAP-2 and PAP-3 precursor levels (data not shown). On the other hand, the cleavage of proHP6, proHP8 and proPAP-1 were observed (Fig. 24A). Proteolytic activation of proHP6 is predicted to resulting in decrease intensity of a band corresponding to HP6 zymogen and the appearance of a band corresponding to the HP6 carboxyl-terminal catalytic chain (our antisera to HP6 does not react well with the light chain). ProHP6 zymogen band was detected in plasma, and the intensity of this band decreased while a new band corresponding to the carboxyl-

terminal catalytic chain appeared after catHP1a was added into the plasma. After catHP1a treatment, the intensity of proHP8 zymogen band detected in plasma decreased, but no clip domain band or catalytic domain band was detected. ProPAP-1 zymogen band and clip domain band were observed in plasma before catHP1a addition (our antisera to PAP-1 did not react well with its catalytic heavy chain, Wang et al., 2008). The zymogen band disappeared and the intensity of the clip domain band increased after catHP1a was added into plasma. According to the previous study (An et al., 2009), HP6 activates proHP8 and proPAP-1. Therefore, the proteolytic cleavages of proHP8 and proPAP-1 may be caused by the activation of proHP6 after catHP1a was added into hemolymph. We propose the hypothesis that the activation of proHP6 may be related to HP1.

To further observe the cleavage of proHP6 in plasma, naïve and induced hemolymph samples were used, and catHP1a or catHP1b were added into plasma. The 37 kDa proHP6 zymogen band was detected in both naïve and induced plasma, and this band disappeared after plasma was treated with bacteria as was reported previously (An et al., 2009), or after catHP1a or catHP1b was added into plasma (Fig 24B and C). The disappearance of the proHP6 zymogen correlated with the appearance of a higher molecular weight band not detected in the hemolymph alone sample. This band is likely a covalent complex of HP6 catalytic chain with a serpin present in plasma. The appearance of serpin-proteinase complexes is a strong evidence that HP6 was indeed activated. The addition of recombinant proHP6 to plasma to increase it concentration led to increase in intensity of the zymogen band detected by immunoblot analysis. After treating proHP6-supplemented plasma with bacteria or catHP1a/b, a putative HP6-serpin complex appeared as well as an additional band at 30 kDa, representing the HP6 catalytic domain. Under non-reducing condition (SDS loading buffer without DTT or beta-mercaptoethonal), the active HP6 bands migrated as a series of bands around 37 kDa, indicating that the clip domain chain and catalytic chain remain attached by an interchain disulfide bond after cleavage.

In order to see if catHP1a or catHP1b was able to cleave proHP6 directly *in vitro*, catHP1a or catHP1b was incubated with proHP6 in the absence of plasma at 37°C for 2 h. Then the reaction mixture was subjected to immunoblotting using HP6 antibody. No cleavage of proHP6 was observed (result not shown). We further measured the amidase activity of catHP1a using artificial substrate, LDLH*p*Na. The activity was low (Fig. 25B), which might be the reason that catHP1a or catHP1b could not cleave proHP6 directly.

CPC-induced *M. sexta* proHP1a, catHP1a, proHP1b and catHP1b amidase activities

Insect proPO was reported to be activated by a cationic detergent, cetylpyridinium chloride (CPC) besides proteolytic cleavage (Hall et al., 1995). CPC was used to test if it can enhance the amidase activities of proHP1a. CPC concentration was optimized for proHP1a activation. The greatest enhancement occurred when proHP1a was incubated with 6 mM CPC in the reaction mixture (Fig. 25A). The result showed that proHP1a activation did not act in a CPC-concentration-dependent manner, suggesting that the concentration of CPC is critical to enzyme activation and denaturation. ProHP1a had low activity when CPC concentrations were below 6 mM, and the activity did not increase when CPC concentrations were higher than 6 mM, suggesting that CPC worked best at 6 mM for proHP1a activation. The activation caused by CPC occurred well below its critical micellar concentration (0.8 M) (Hall et al., 1995).

Optimal amount of CPC (6 mM) was used to test if it can enhance the amidase activities of the four enzymes using another colorimetric substrate, LDLH*p*Na which mimicked the cleavage site of proHP6. ProHP1a, catHP1a and catHP1b had a greater increase in activity after CPC treatment, whereas proHP1b had a small increase in activity after incubation with CPC (Fig. 25B and C).

***M. sexta* proHP6 alternative cleavage by proHP1a in the presence of detergents**

In Fig. 26A, immunoblot analysis using HP6 antibody showed that HP6 zymogen (proHP6) migrated at a molecular mass of 37 kDa. No cleaved band was detected when proHP6 was incubated with proHP1a or CPC alone. A new 30 kDa band was observed when proHP6 was incubated with proHP1a and CPC, while the HP6 zymogen band disappeared. ProHP1a, proHP6, and proHP1a with CPC were used as negative controls. The positive control using plasma incubated with microbial elicitor was included as well. As described previously, in the positive control, the disappearance of the proHP6 zymogen correlated with the appearance of a faint 30 kDa band and a higher molecular weight band not detected in the hemolymph alone sample. The novel cleaved band in Lane 6 migrated at the similar position as the one in Lane 8. Edman degradation showed that the sequence of the 30 kDa band in Lane 6 matches sequence at the N-terminus of HP6 zymogen (proHP6-ΔC) (Table. 2), indicating that the hydrolysis did not occur at the activation site but within the catalytic domain. This was confirmed by immunoblot analysis under reducing and non-reducing conditions (Fig. 26B). If the hydrolysis occurs at the activation site, under non-reducing condition, the active HP6 migrated as a series of bands around 37 kDa (Fig. 25B and C), indicating that the clip domain chain and catalytic chain remain attached by an interchain disulfide bond after cleavage. However, we detected two bands in Lane 2 of Fig. 8B under non-reducing condition, suggesting that the cleavage site was in the catalytic domain.

Various detergents were tested to see if it would help the cleavage of proHP6 by proHP1a. Different types of detergents were tested. CPC and CTAB are cationic detergents, SDS is anionic detergent, Triton-X114, Tween-20 and NP-40 are non-ionic detergent. Of all these various types of detergents, only cationic detergents, CPC and CTAB helped proHP1a to process proHP6 at the non-activation site (Fig. 26C), as the 30 kDa was not able to jump to the 37 kDa band under non-reducing condition.

M. sexta proHP6 alternative cleavage by proHP1a, proHP1b, catHP1a and catHP1b in the presence of CPC

We showed that in the presence of detergent CPC, proHP1a was able to process proHP6 in an alternative way (Fig. 26). In order to investigate if other forms of HP1 could react with proHP6 in the same way, recombinant HP6 zymogen was incubated with proHP1a, proHP1b, catHP1a and catHP1b respectively in the presence of CPC. The cleavage of hemolymph proHP6 in the presence of microbial elicitor was used as the control. The results showed that after HP6 zymogen was incubated with proHP1a and CPC for 4 h, the HP6 zymogen was completed cleaved into the alternative cleavage band (proHP6-ΔC) (Fig. 27). The similar cleavage occured when proHP6 was incubated with catHP1b and CPC except that proHP6 was incompletely cleaved. Two bands appeared when HP6 zymogen was incubated with proHP1b and CPC, or with catHP1a and CPC. One cleaved band was corresponding to the band proHP6-ΔC (data not shown under non-reducing condition). But the other band was not identified.

***M. sexta* hemolymph corrects HP6 activation by catHP1b**

We previously found that proHP6 can be activated in hemolymph by catHP1a or catHP1b in the absence of microbial elicitors (Fig. 24). However, when HP6 zymogen was incubated with catHP1a or catHP1b alone without hemolymph, the activation did not occur. When HP6 zymogen was incubated with catHP1a or catHP1b in the presence detergent CPC, proHP6 was processed in a different way. These results indicated that some hemolymph factor(s) in the hemolymph was important to correct HP6 activation. We reduced the amount of naïve plasma from one micro liter to one tenth micro liter in the reaction mixture of plasma, recombinant proHP6 and catHP1b. The activation of HP6 occurred when one half or one fourth micro liter was present, but the amount of active HP6 decreased as the amount of plasma reduced (Fig. 28). Under non-reducing condition, the active HP6 bands migrated to 37 kDa, indicating that the cleavage occurred between the clip domain and the catalytic domain. When the amount of plasma reduced to one tenth micro liter, no cleavage was detected.

Effects of *M. sexta* hemolymph and CPC on the activation of HP6

In order to study the addictive effects of hemolymph and CPC on the activation of proHP6, a series of diluted hemolymph were combined with proHP6 and catHP1b in the presence of three different concentrations of CPC. Results suggested that CPC at the concentration of 0.6 mM works best for processing of HP6 in all dilutions of naïve or induced hemolymph (Fig. 29A and B). This CPC concentration (0.6 mM) is ten times lower than that used when proHP6 was incubated with catHP1b in the absence of hemolymph. However, since the reaction mixtures were not subjected to SDS-PAGE under non-reducing condition, it is not known whether the cleavage is between the clip domain and the catalytic domain. After the optimal CPC concentration (0.6 mM) was determined, we combined proHP6, catHP1b, and CPC (0.6 mM) with a series of diluted hemolymph and separated the reaction mixtures under reducing and non-reducing conditions. The amount of active HP6 did not decrease significantly as the amount of plasma reduced (Fig. 29C), when compared to the results showed in Fig. 28, which might be due to the addition of CPC. When the amount of hemolymph reduced to one eighth micro liter, a significant amount of cleaved HP6 was not able to migrate back to 37 kDa (Fig. 29C, lane 6, -DTT), which means this cleavage site is different from other reaction samples in which the cleavage was between the clip domain and the catalytic domain. Only a very little of cleaved HP6 was not able to migrate back to 37 kDa (Fig. 29C, lane 5, -DTT), indicating that the HP6 cleaved band in lane 5 (+DTT) consisted of different cleavage products which coincidently migrated at the same position. These results suggested that hemolymph factor(s) is important for correct cleavage of proHP6 and CPC helps catHP1b process more HP6 zymogens.

Inhibition of *M. sexta* HP1 activation

To investigate the regulation of HP1, we tested if activation of proHP1 could be inhibited by some serpin(s) in *M. sexta* hemolymph. Previous study showed that HP1 was detected in the *M. sexta* serpin-4 and serpin-5 complex (Tong et al., 2005). However, the size of the HP1-serpin-

4/5 complexes they purified was around 90 kDa which was larger than the predicted size of the complex consisting of the catalytic domain of HP1 and serpin-4/5. Therefore, we want to further characterize the 90 kDa complex of HP1. First, we tried to detect HP1-serpin complex in hemolymph. 0-35% AS fraction of hemolymph was incubated with microbial elicitor or recombinant serpin-4. No cleavage products were detected for HP1 after incubation of plasma with microbial elicitor, but a more intense band possibly representing HP1-serpin complex was detected by both HP1 and serpin-4 antibodies, when additional recombinant serpin-4 was added into plasma (Fig. 30), suggesting that active HP1 was inhibited by serpin-4. Less intense bands were observed in plasma alone, which indicated that HP1 possibly has been active without bacterial stimulation.

Purification and identification of *M. sexta* HP1-serpin complex

In Tong's paper, he used immunoaffinity chromatography with serpin antibodies to isolate serpin-protease complexes and detected that HP1 was contained in both serpin-4-protease and serpin-5-protease complexes (Tong et al., 2005). In this study, we used immunoaffinity chromatography with HP1 antibody to isolate HP1-serpin complex and to further characterize the complex. According to the results shown in Fig. 30, microbial elicitor had little effect on complex formation. Thus, naïve hemolymph was not challenged by bacteria before purification. The 90 kDa complex band was showed in Coomassie Blue stained gel and recognized by HP1, serpin-4 and serpin-5 antibodies (Fig. 31), which was consistent with the previous results (Tong et al., 2005). Other plasma proteins that co-purified with the complex were not recognized by HP1 antibody. One band around 75kDa was recognized by serpin-4 antibody, but not HP1 or serpin-5 antibodies. This band probably was the complex formed by serpin-4 with other protease that co-purified with serpin-4.

Identification of HP1 and serpins in *M. sexta* HP1-serpin complex

To identify the components in the complex, peptide mass fingerprint analysis was used. Masses of tryptic peptides derived from the 90kDa band matched well with those of the predicted tryptic peptides of serpin-4 and serpin-5. The experimental peptide masses of the 90kDa complex covered 34% of the sequence of serpin-4 (Fig. 34) and 31% of the sequence of serpin-5 (Fig. 35).

Masses of tryptic peptides derived from the 90 kDa complex band matched well with those of the predicted tryptic peptides of HP1 as well, including peptides present only in isoform a or b (Fig. 32 and 33), indicating that both forms of HP1 are present in plasma and can form HP1-serpin complex. The experimental peptide masses of the complex covered 21% of the sequence of HP1a (Fig. 32) and 12% of the sequence of HP1b (Fig. 33). Surprisingly, peptides of HP1a (INQAQNR) and HP1b (ISQAQNR and GCGLSTRPQGR) in the linker region which is located between clip domain and catalytic domain were detected by mass fingerprint analysis. In SDS-PAGE of a protease-serpin complex, it is expected that the catalytic domain of the proteinase will remain connected to the serpin through a covalent bond, and the clip domain is released under reducing condition due to reduction of the disulfide bond that links the clip and protease domains. According to Tong's results, only the tryptic peptides in the catalytic domain of HP1 were detected. Amino-terminal sequencing of the complex containing HP1 and serpin-4 or serpin-5 yielded the N-terminal sequences of serpin-4 and serpin-5, but failed to detect sequence of HP1, perhaps due to blocking of the amino terminus of HP1 (Tong et al., 2005). The detection of the peptides in the linker region of a proteinase formed in a proteinase-serpin complex is uncommon. Since such peptides were observed in both isoform a and b of HP1, the results were meaningful.

Discussion

During the last decade, an increasing number of studies have investigated the serine proteinase cascade involved in immune responses in invertebrates, such as the proPO activation pathway and Toll immune pathway. The genetic studies of the *Drosophila* immune response have

elucidated the role of several serine proteinases in the activation of the Toll receptor. In *M. sexta*, the large moth, more than 20 serine proteinases cDNAs have been isolated from fat body and hemocytes (Jiang et al., 2005). Only a few of these hemolymph proteinases have been studied functionally. *M. sexta* HP6, an ortholog of *Drosophila* Persephone, functions in proPO activation leading to melaniztion, and spätzle activation leading to antimicrobial peptides synthesis (An et al., 2009). HP6 was found to be activated in hemolymph in the absence of microbial elicitor, indicating the existence of an endogenous activating proteinase. However, such proteinase has not yet been identified.

HP1b cDNA sequence was recently found. HP1a and HP1b are highly similar in amino acid sequence (Fig. 20). We produced recombinant HP1 zymogen forms, proHP1a and proHP1b, and the catalytic domains of HP1, catHP1a and catHP1b. These purified proteins were used as reagents for in vitro experiments to examine their proteolytic activity and for in vivo experiments in the complex protein mixture present in hemolymph.

Addition of proHP1a or proHP1b to plasma resulted in activation of proPO, but no addictive effect of proenzymes and *M. luteus* on increase of PO activity (Fig. 22). A dramatic increase of PO activity was observed when catHP1a alone was added into naïve hemolymph, suggesting that catHP1s are active or partially active enzymes that can directly or indirectly cleave unknown proteinase(s) in hemolymph to trigger proPO activation without microbial elicitors. All available antibodies against hemolymph proteinases were used to investigate which endogenous proteinase(s) can be activated by catHP1a in *M. sexta* plasma. The cleavages of proHP6, proHP8 and proPAP-1 were observed after catHP1a alone was incubated with plasma (Fig. 24A). ProHP8 and proPAP-1 were reported to be activated by HP6 (An et al., 2009). Therefore, our results indicate that such proteolytic cleavage of proHP6 is related to HP1 and is physiologically functional.

No cleavage of proHP6 occurred when proHP6 was incubated directly with catHP1a or catHP1b in vitro, which is possibly due to low amidase activity of catHP1s. Insect proPO was

reported to be activated by CPC besides proteolytic cleavage (Hall et al., 1995). An increase of proHP1a amidase activity was observed after addition of CPC (Fig. 25), which may due to the exposure of the active site of proHP1a in the presence of the detergent. Surprisingly, the cleavage of proHP6 by proHP1a in the presence of CPC did not occur at the activation site but within the catalytic domain (Fig. 26), which is confirmed by N-terminal sequencing (Table. 2). This also happened in *Drosophila* serine proteinase Grass (Kellenberger et al., 2011). Since the endogenous activator of Grass in *Drosophila* is unknown, Grass zymogen was submitted to proteolysis by bovine and porcine pancreatic trypsin. Their result showed that the cleavag specifically occurred within catalytic domain, not at the activation site

Results showed that when proHP6 was incubated with catHP1a or catHP1b in the presence of very low amount of hemolymph and absence of CPC, proHP6 was cleaved at its activation site (Fig. 28), indicating that some hemolymph factor(s) is contributed to the cleavage of proHP6 at its correct activation site. *M. sexta* proPO activation requires both PAP-1 and SPHs (Yu et al., 2003). In order to identify such factor(s), we tried to add SPHs into the reaction mixture including proHP6, proHP1a and CPC. The cleavage site was not corrected (data not shown). Then a few recognition proteins, such as GNBP, PGRP1 or βGRP2 were tried. They did not work either (data not shown). So far, such hemolymph factors have not been identified. An alternative cleavage was observed in *Drosophila* Persephone, the ortholog of *M. sexta* HP6. They incubated immunoprecipitated Persephone collected from the hemolymph of unchallenged wide-type flies with purified preparations of fungal virulence factor 1 (PR1), a fungal protease. This digestion produced a 33 kDa and a 28 kDa band (Gottar et al., 2006). The 28 kDa band has the similar molecular weight to the predicted Persephone catalytic domain and may correspond to the active form of Persephone, and the 33 kDa was unidentified. The over-expression of Persephone can also lead to the appearance of the 33 kDa band. Interestingly, the *B. mori* clip-domain protease BAEEase is processed first into a 33 kDa band, and second, into a 29.5 kDa band, the latter processing event being essential for activation (Jane et al., 2006). They found that the

cleavage site of the 33 kDa band is located in the linkage region before the activation site. It is not known that if all such alternative cleavages occurred in *M. sexta* HP6, *Drosophila* Persephone and *B. mori* BAEEase have physiological function.

Kellenberger et al. (2011) has established a modified classification of the clip-SPs into three classes based on the phylogenetic analysis by Jiang and Kanost (2000). Members of Group 1 are predicted to have one helix between Cys^3 and Cys^4 in the clip domain and one helix centered on a cysteine of the linker. Group 2 contains two helices between Cys^3 and Cys^4. The Group 1 clip domains contain 8-16 residues between Cys^3 and Cys^4, whereas Group 2 clip domains have a longer sequence of 22-26 residues in this region. The clip domains that are devoid of any helical secondary structure form Group 3. According to their analysis, Group 3 contains only inactive clip-SPHs (Kellenberger et al., 2011). Members of Group 1 are in penultimate position, suggesting that they are enzymes upstream in the pathways having terminal proteinases as their substrates. Group 2 are terminal clip-SPs known to activate spätzle or proPO. The terminal proteinases all have a basic residue, Arg or Lys, at their activation site, whereas the penultimate proteinases instead have Leu (*M. sexta* HP21, *Drosophila* snake), His (*M. sexta* HP6, *Drosophila* Persephone), or Ser (*Drosophila* Spirit) at this position, indicating that proteinases of quite different specificity are required as activating enzymes for Group1 and 2. Both *M. sexta* HP6 and HP1 fall into Group 1 displaying the classical clip-SP cysteine organization consisting of Clip (6 Cys) + linker (1 Cys) + SP (7 Cys). According to the classification analysis of the clip domains and our results, it is possible that HP1 activates HP6 with the help of other factor(s) in *M. sexta* hemolymph.

The HP1-serpin complex was isolated using immunoaffinity chromatography with HP1 antibody. Three peptides in the linker region of HP1a (INQAQNR) and HP1b (ISQAQNR and GCGLSTRPQGR) were detected by MS. The three peptides were not detected (Tong et al., 2005). Furthermore, we found that catHP1a or catHP1b failed to form complex with either serpin-4 or

serpin-5 in vitro (data not shown). According to these results, we propose that HP1 may form complex with serpin-4 or serpin-5 in an uncommon way.

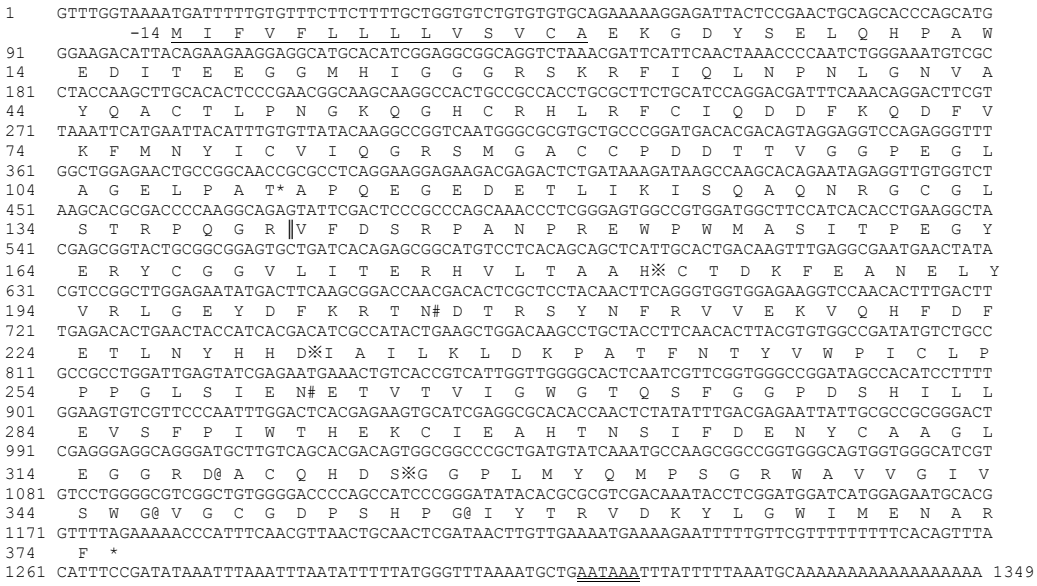

Figure 19. Nucleotide and deduced amino acid sequence of *M. sexta* HP1b. The one-letter code for amino acid residue is shown below the nucleotide sequence and aligned with the second nucleotide of the corresponding codon. Numbers on the left are assigned to nucleotide residues and amino acid residues, including negative numbers for residues in the signal peptides which are underlined. Putative *N*-linked glycosylation sites are marked with # after the Asn residues. Putative *O*-linked glycosylation sites are marked with * after the Thr residues. The predicted proteolytic cleavage site is marked by ‖. The catalytic triad residues are marked by ※. The residues that make the primary substrate-specificity pocket are marked by @. The putative polyadenylation signals (AATAAA) near the 3'-terminus of cDNA are double-underlined.

Figure 20. Sequence alignment of *M. sexta* HP1a with HP1b. The amino acid sequences of *M. sexta* HP1a and HP1b are aligned. The signal peptide sequences are underlined. The predicted proteolytic cleavage sites are indicated by "‖". "*" indicates positions which have an identical residue. ":" indicates positions which have strong conserved residues. "." indicates positions which have weak conserved residues.

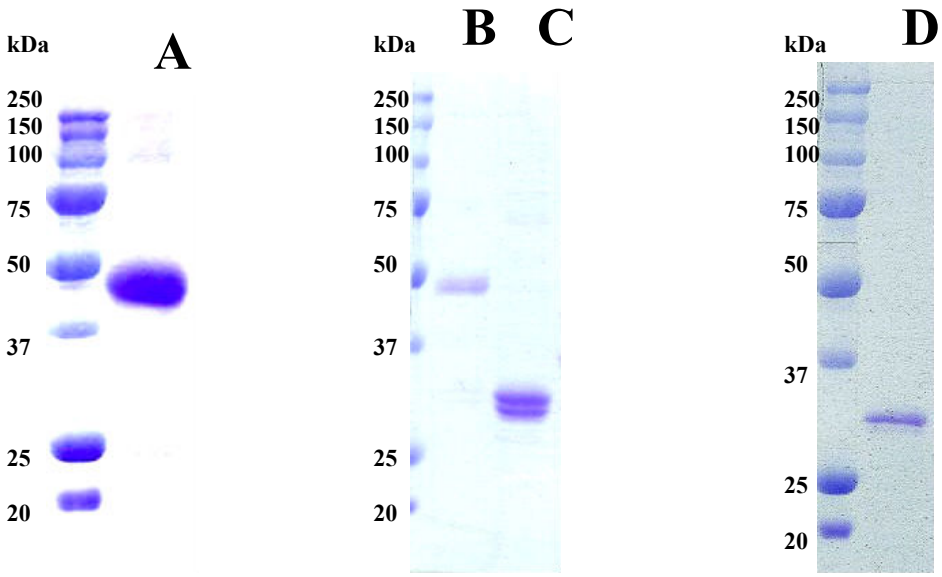

Figure 21. Purification of *M. sexta* proHP1a, proHP1b, catHP1a and catHP1b from the baculovirus-infected insect cells. Purified proteins were analyzed on 10% SDS-PAGE and Coomassie Blue staining. A, proHP1a (200 ng/µl, 6 µl); B, proHP1b (100 ng/µl, 2 µl); C, catHP1a (100 ng/µl, 5 µl); D, catHP1b (100 ng/µl, 3 µl). Positions and sizes of marker proteins are indicated on the left.

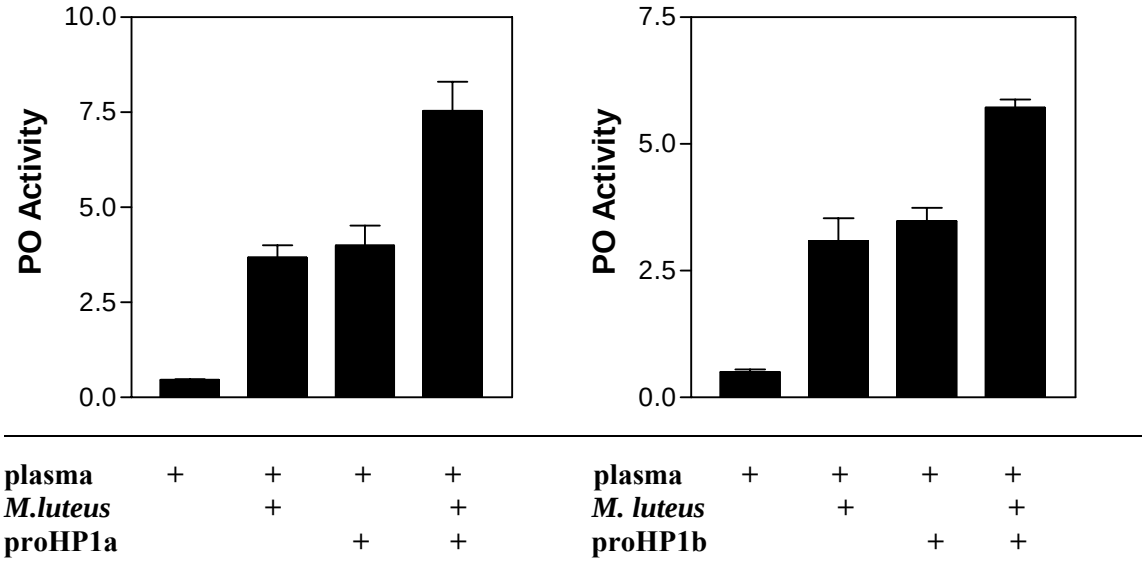

Figure 22. Roles of proHP1a and proHP1b in *M. sexta* proPO activation. Naïve hemolymph (1 µl), *M. luteus* (1 µg/µl, 1 µl), and proHP1a/b (100 ng/µl, 1 µl) were incubated in the buffer (8 µl, 20 mM Tris-HCl pH 8.0, 1 mM $CaCl_2$, 0.001% Tween-20) at room temperature for 30 min. PO activity (mean ± S.D., n = 3) was measured using dopamine as a substrate. Control reactions were plasma only and plasma with *M. luteus*.

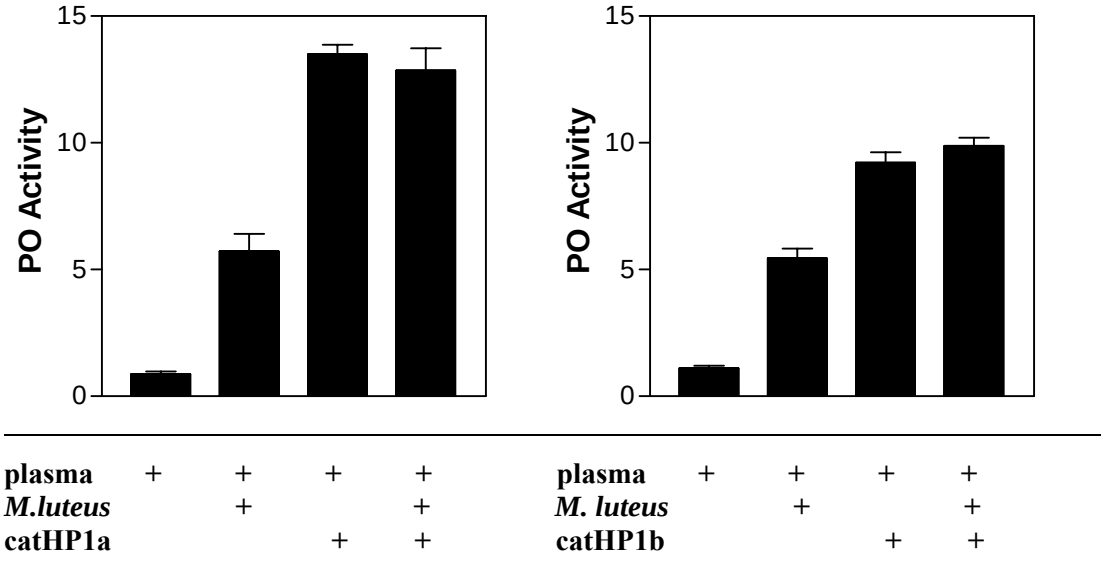

Figure 23. Roles of catHP1a and catHP1b in *M. sexta* proPO activation. Naïve hemolymph (1 µl), *M. luteus* (1 µg/µl, 1 µl), and catHP1a/b (50 ng/µl, 1 µl) were incubated in the buffer (8 µl, 20 mM Tris-HCl pH 8.0, 1 mM $CaCl_2$, 0.001% Tween-20) at room temperature for 30 min. PO

activity (mean ± S.D., n = 3) was measured using dopamine as a substrate. Control reactions were plasma only and plasma with *M. luteus*.

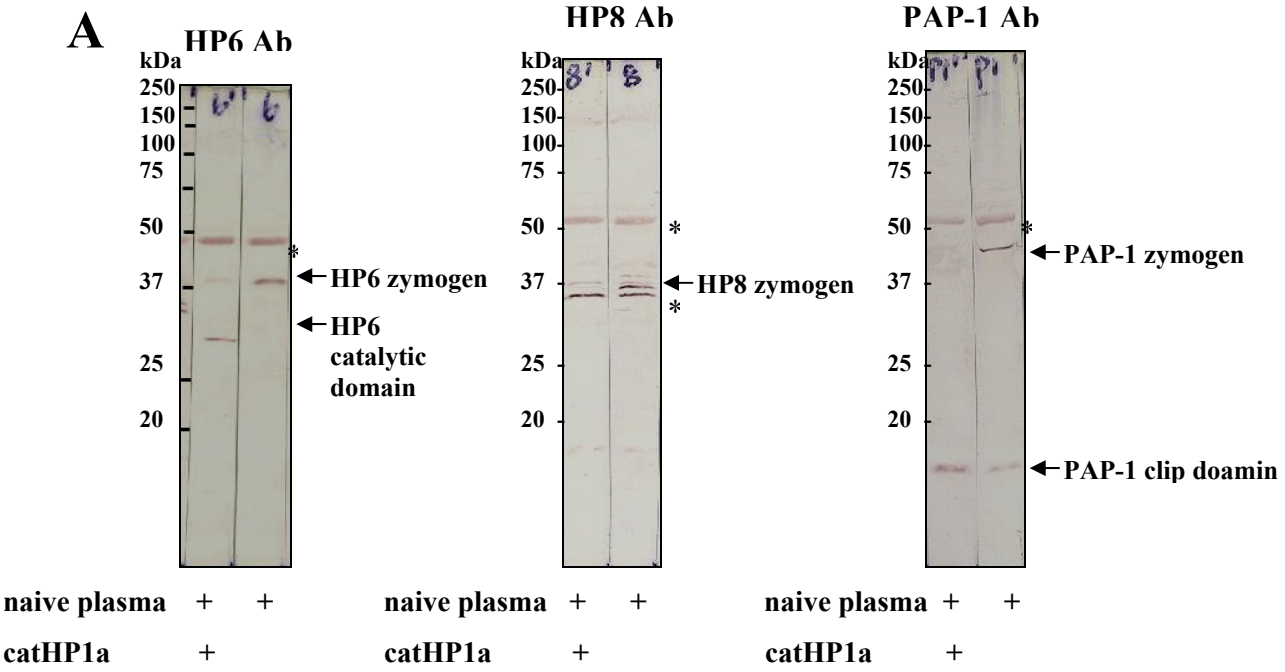

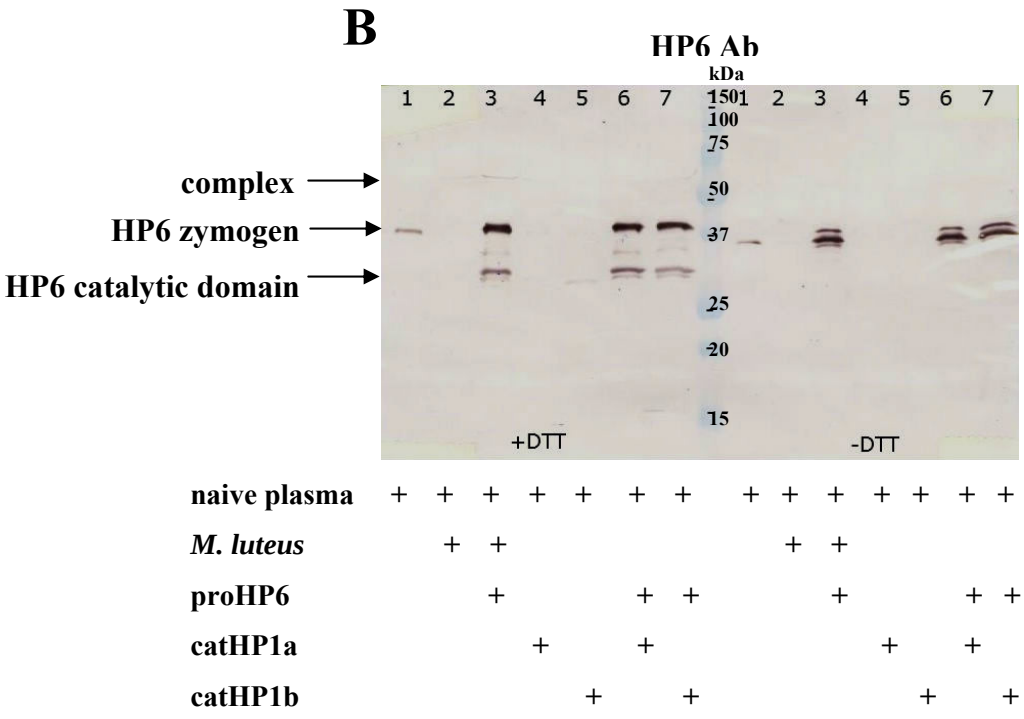

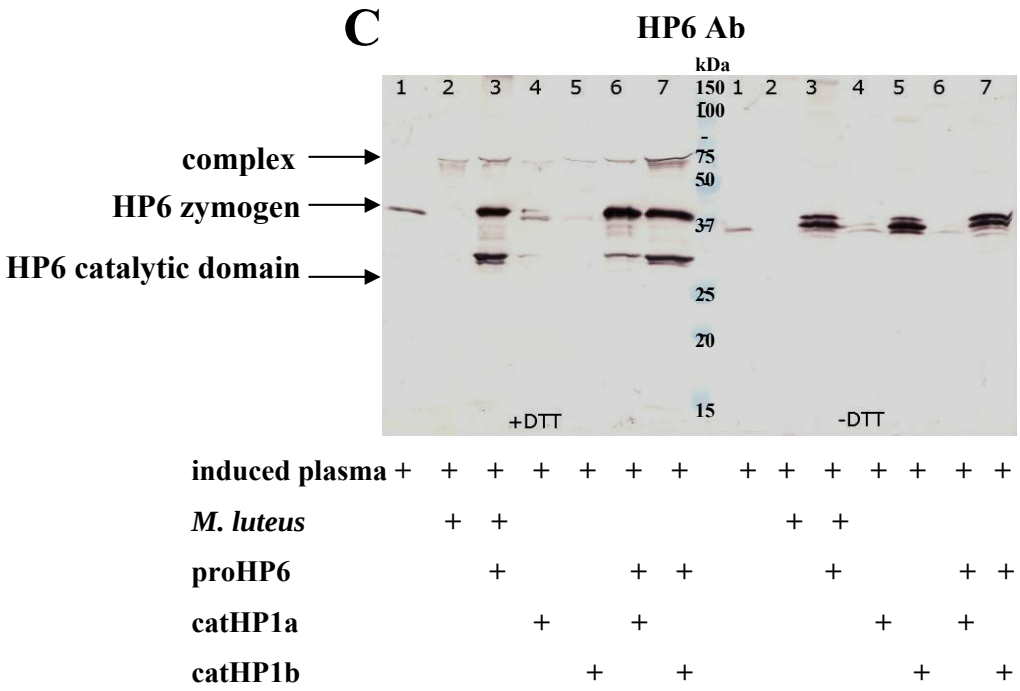

Figure 24. Cleavage of *M. sexta* proHP6 in plasma by catHP1a and catHP1b. A, Naive plasma (1 µl) was incubated with catHP1a (50 ng/µl, 1 µl) in the buffer (8 µl, 20 mM Tris-HCl pH 7.0, 20 mM NaCl) at room temperature for 30 min; B, Purified proHP6 (100 ng/µl, 1 µl) was incubated in the buffer (7 µl, 20 mM Tris-HCl pH 7.0, 20 mM NaCl) at room temperature for 30 min with purified catHP1a (50 ng/µl, 1 µl) or catHP1b (50 ng/µl, 1 µl) and naive plasma (1 µl) (B) or induced plasma (1 µl) (C) in the presence of microbial elicitor, *M. luteus* (1 µg/µl, 1 µl). The reaction mixture were subjected to 10% SDS-PAGE followed by immunoblot analysis using HP6, HP8 and PAP-1 antiserum. The sizes and positions of molecular weight standards are indicated on the left (A) or in the middle (B and C). Bands representing HP6 zymogen, a cleavage product corresponding to its catalytic domain, and a putative HP6-serpin complex are marked by arrows. The nonspecific recognition of hemolymph proteins is marked with "*". Ab: antibody.

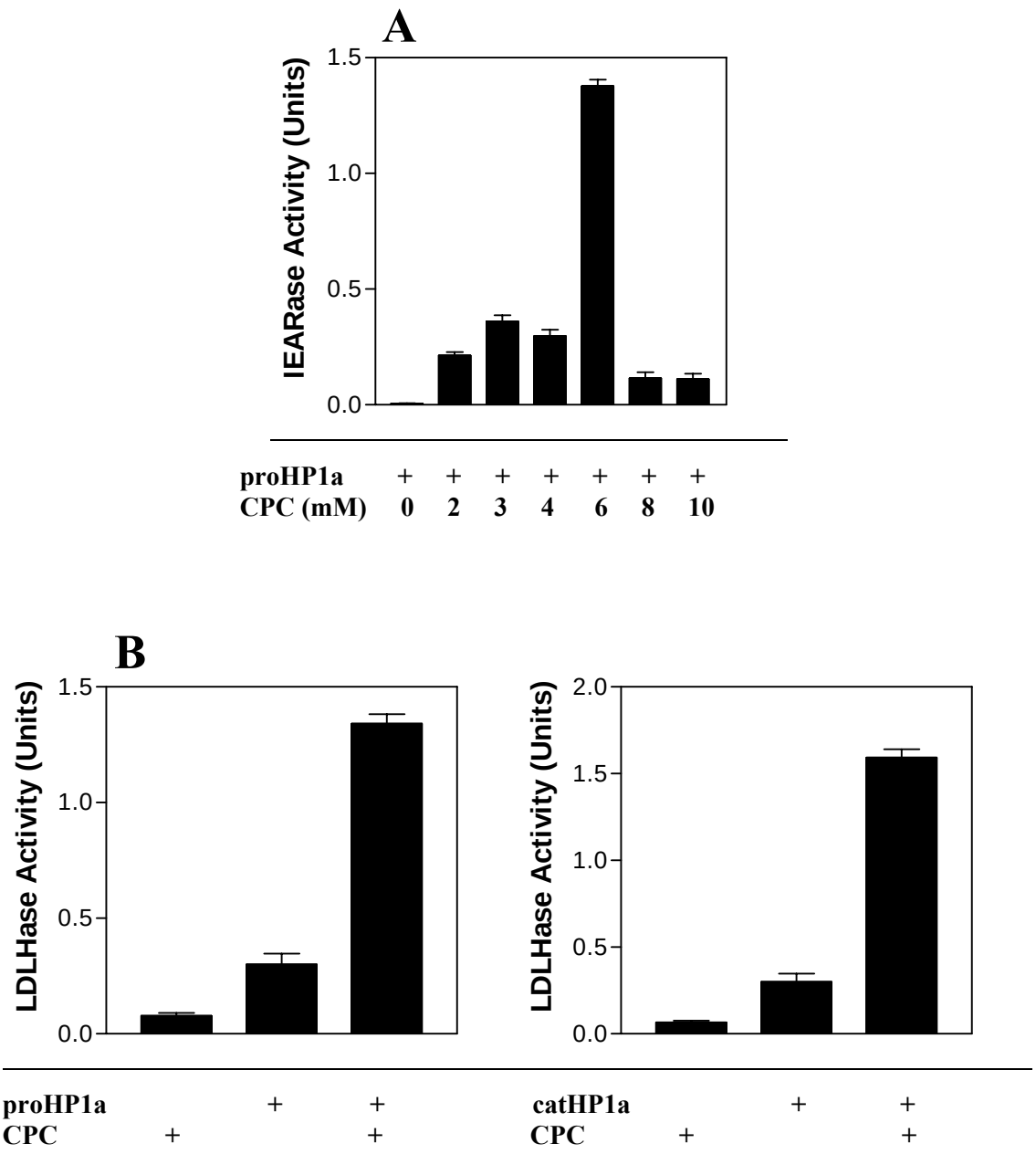
A
IEARase Activity (Units)
1.5
1.0
0.5
0.0
proHP1a + + + + + + +
CPC (mM) 0 2 3 4 6 8 10
B
LDLHase Activity (Units)
1.5
1.0
0.5
0.0
proHP1a + +
CPC + +
LDLHase Activity (Units)
2.0
1.5
1.0
0.5
0.0
catHP1a + +
CPC + +

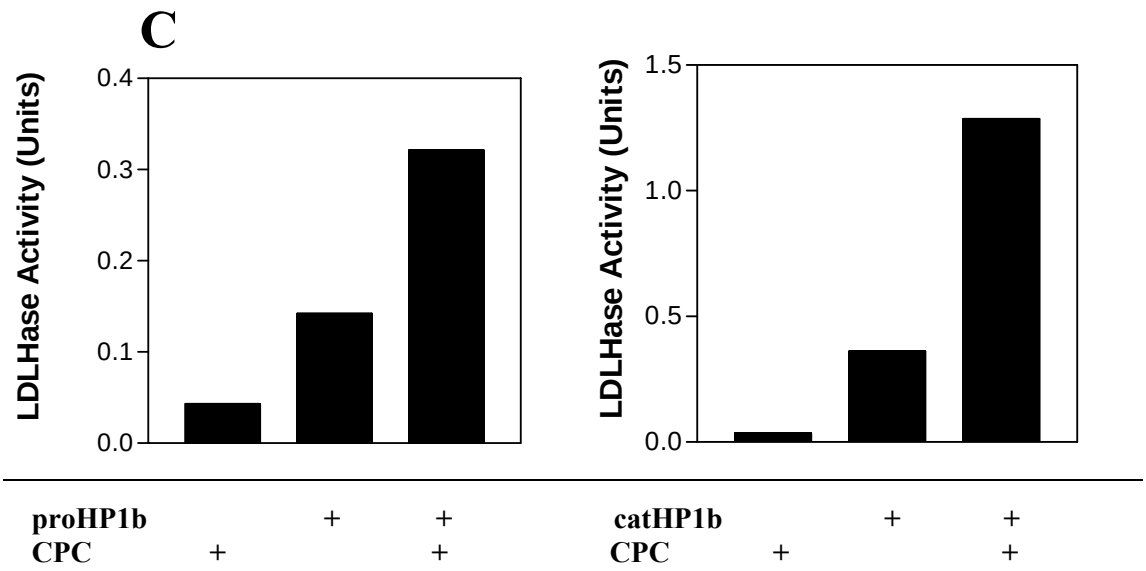

Figure 25. CPC-induced *M. sexta* proHP1a, catHP1a, proHP1b and catHP1b amidase activities. A, Optimization of the CPC concentration in the activation of proHP1a using an artificial substrate, IEAR*p*Na. Purified recombinant proHP1a (250 ng/μl, 2 μl) was incubated with various concentrations of cetylpyridinium chloride (CPC, 1 μl) in the buffer (10 μl, 20 mM Tris-HCl pH 7.0, 20 mM NaCl) at room temperature for 5 min. The residual amidase activity (mean ± S.D., n = 3) was then measured using an artificial substrate, IEAR*p*Na (100 μM, 150 μl); B, CPC-mediated enhancement of proHP1a and catHP1a residual amidase activities using substrate, LDLH*p*Na. C, CPC-mediated enhancement of proHP1b and catHP1b residual amidase activities using substrate, LDLH*p*Na. Purified recombinant proHP1a (250 ng/μl, 2 μl), catHP1a (150 ng/μl, 2 μl), proHP1a (250 ng/μl, 2 μl) or catHP1a (150 ng/μl, 2 μl) was incubated with 6 mM CPC (1 μl) respectively in the buffer (10 μl, 20 mM Tris-HCl pH 7.0, 20 mM NaCl) at room temperature for 5 min. The residual amidase activity (mean ± S.D., n = 3) was then measured using an artificial substrate, LDLH*p*Na (100 μM, 150 μl). CPC, proHP1a, catHP1a, proHP1b or catHP1b alone was used as negative control.

Table 3. Amino-terminal sequencing by automated Edman degradation of cleaved HP6

Cycle #	Amino acids detected (pmoles)
1	E (3.45) G (1.05) A (0.96)
2	N (2.14)
3	V (2.90) P (0.34)
4	G (1.16)
5	D (1.44)

Purified recombinant proHP6 (150 ng/µl, 2 µl) (An et al., 2009) was incubated with proHP1a (300 ng/µl, 2 µl) in the presence of 6 mM CPC (1 µl) in the buffer (10 µl, 20 mM Tris-HCl pH 7.0, 20 mM NaCl) at 37°C for 4 h. The reaction mixture was separated on 10% SDS-PAGE. The protein was then transferred to a polyvinylidene difluoride (PVDF) membrane and stained with Coomassie Blue. The 30 kDa polypeptide corresponding to the cleaved HP6 was subjected to automated Edman degradation in Nevada Proteomics Center.

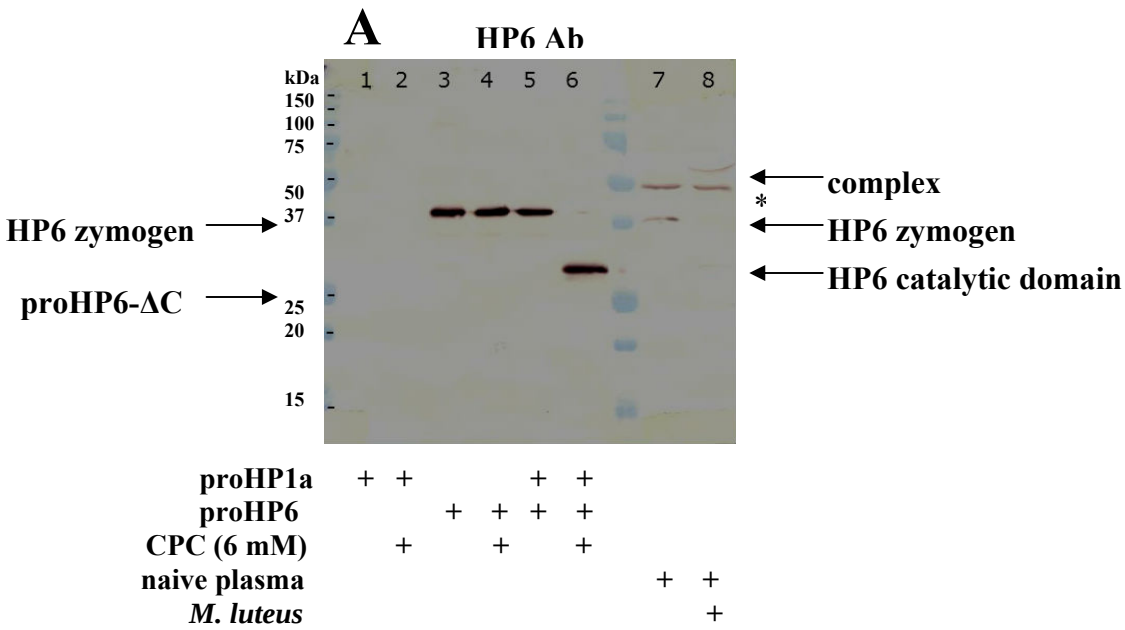
A
HP6 Ab
kDa
150
100
75
50
37
25
20
15
1 2 3 4 5 6 7 8
HP6 zymogen
proHP6-ΔC
complex
*
HP6 zymogen
HP6 catalytic domain
proHP1a + + + +
proHP6 + + + +
CPC (6 mM) + + +
naive plasma + +
M. luteus +

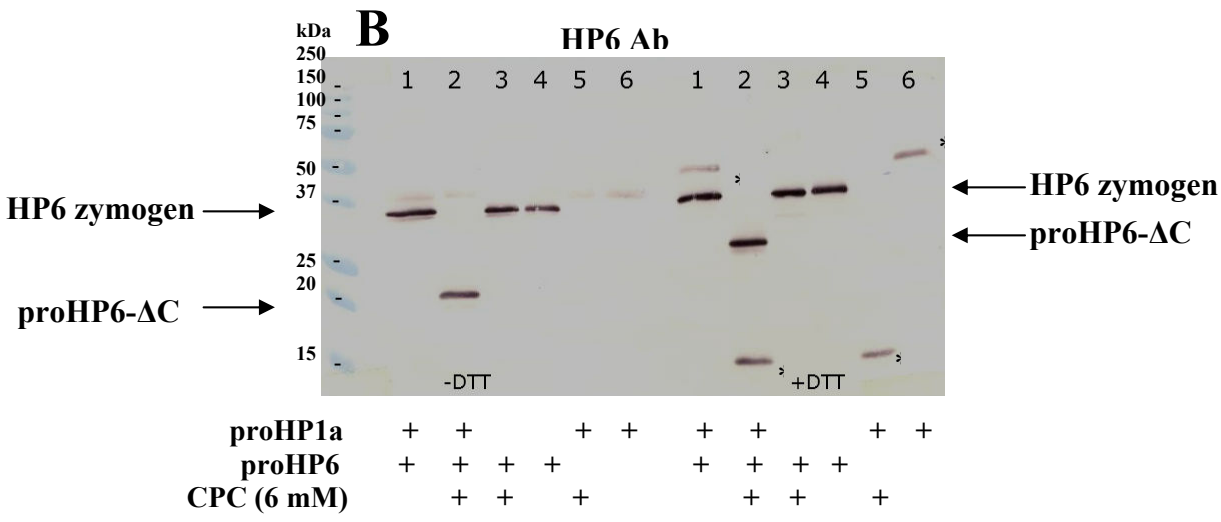
B
HP6 Ab
kDa
250
150
100
75
50
37
25
20
15
1 2 3 4 5 6 1 2 3 4 5 6
-DTT
+DTT
HP6 zymogen
proHP6-ΔC
HP6 zymogen
proHP6-ΔC
proHP1a + + + + + + + + + +
proHP6 + + + + + + + + +
CPC (6 mM) + + + + + + +

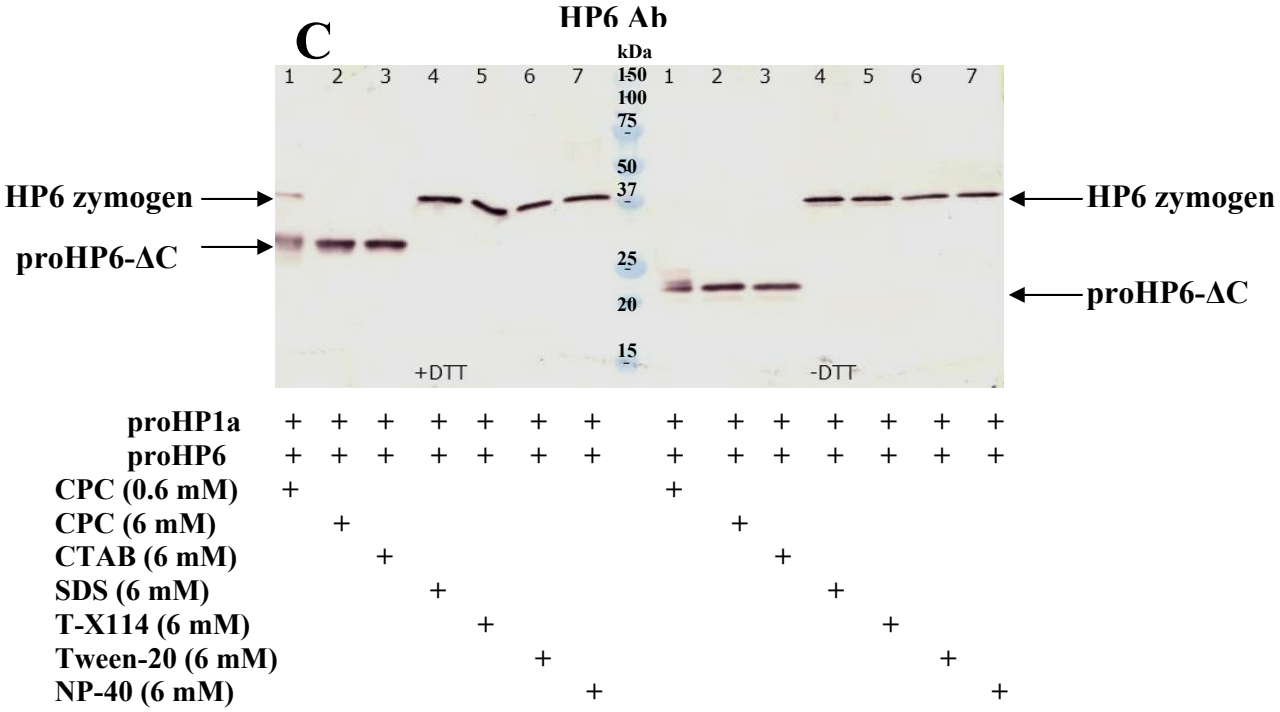

Figure 26. Alternative cleavage of *M. sexta* proHP6 by proHP1a in the presence of detergents. A, Cleavage of proHP6 by proHP1a in the presence of CPC. B, Cleavage of proHP6 by proHP1a in the presence of CPC under reducing (+DTT) and non-reducing (-DTT) conditions. C, Cleavage of proHP6 by proHP1a in the presence of various detergents under reducing (+DTT) and non-reducing (-DTT) conditions. Purified proHP6 (100 ng/µl, 1 µl) was incubated with proHP1a (200 ng/µl, 1 µl) in the presence of detergents (6 mM, 1 µl) in the buffer (7 µl, 20 mM Tris-HCl pH 7.0, 20 mM NaCl) at 37°C for 4 h. Naive plasma (1 µl) was incubated with the microbial elicitor, *M. luteus* (1 µg/µl, 1 µl) in the same buffer (7 µl) at room temperature for 30 min. This reaction was used as the control; CPC: cetylpyridinium chloride; CTAB: cetyltrimethylammonium bromide; SDS: sodium dodecyl sulfate; T-X114: Triton-X114; Tween-20: polysorbate-20; NP-40: nonyl phenoxypolyethoxylethanol. All the reaction mixtures were subjected to 10% SDS-PAGE followed by immunoblot analysis using HP6 antiserum. The sizes and positions of molecular weight standards are indicated on the left (A and B) or in the middle (C). Bands representing HP6 zymogen, HP6 catalytic domain, an alternative cleavage product (proHP6-ΔC), and a putative HP6-serpin complex are marked by arrows. The nonspecific recognition of proteins are marked with "*". Ab: antibody.

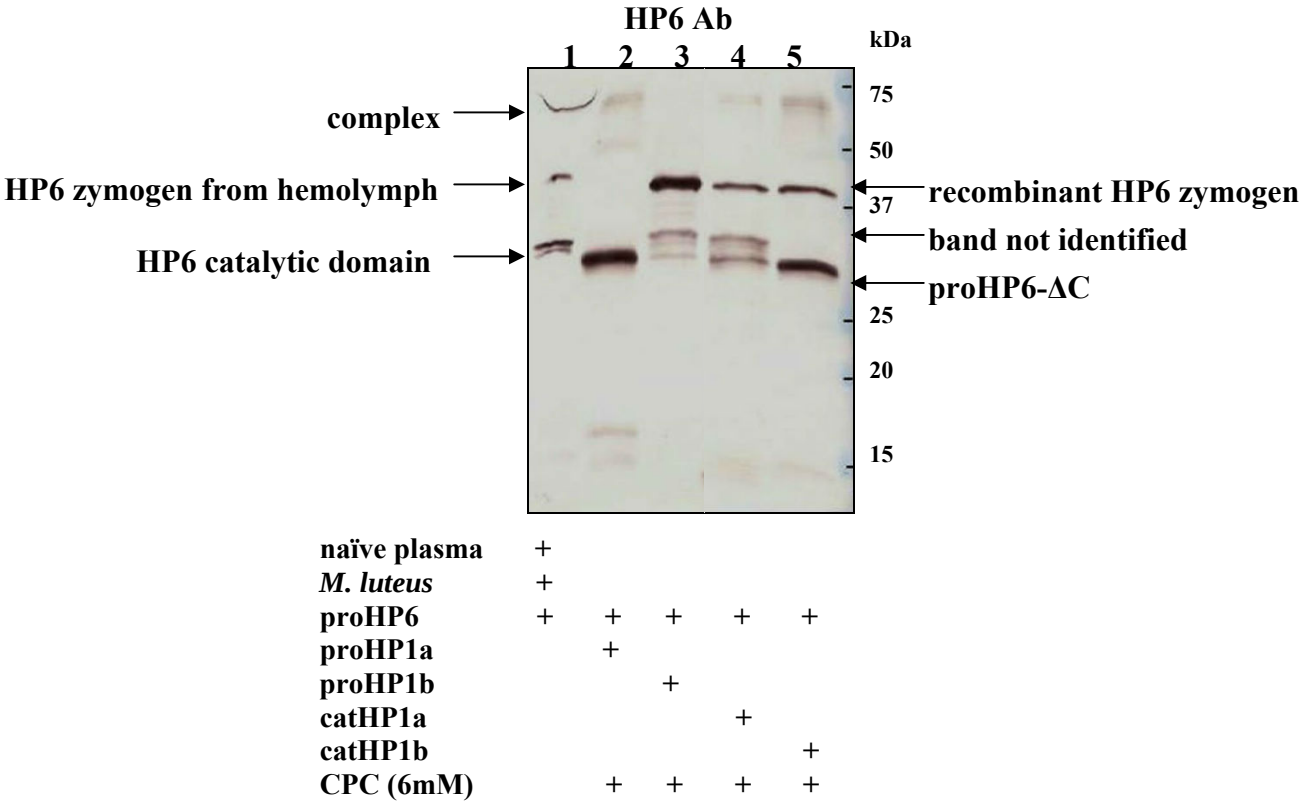

Figure 27. HP6 alternative cleavage by *M. sexta* proHP1a, proHP1b, catHP1a and catHP1b in the presence of CPC. Purified proHP6 (100 ng/µl, 1 µl) was incubated with proHP1a (200 ng/µl, 1 µl), proHP1b (200 ng/µl, 1 µl), catHP1a (100 ng/µl, 1 µl) or catHP1b (100 ng/µl, 1 µl) respectively in the presence of CPC (6 mM, 1 µl) in the buffer (7 µl, 20 mM Tris-HCl pH 7.0, 20 mM NaCl) at 37°C for 4 h (Lane 2-5). Control reaction was naive plasma (2 µl) incubated with proHP6 (100 ng/µl, 1 µl) in the presence of microbial elicitor, *M. luteus* (1 µg/µl, 1 µl) in the same buffer (6 µl) at room temperature for 30 min (Lane 1). All the reaction mixtures were subjected to 10% SDS-PAGE followed by immunoblot analysis using HP6 antiserum. The sizes and positions of molecular weight standards are indicated on the right. Bands representing HP6 zymogen, HP6 catalytic domain, an alternative cleavage product (proHP6-ΔC), an unknown band and a putative HP6-serpin complex are marked by arrows. Ab: antibody.

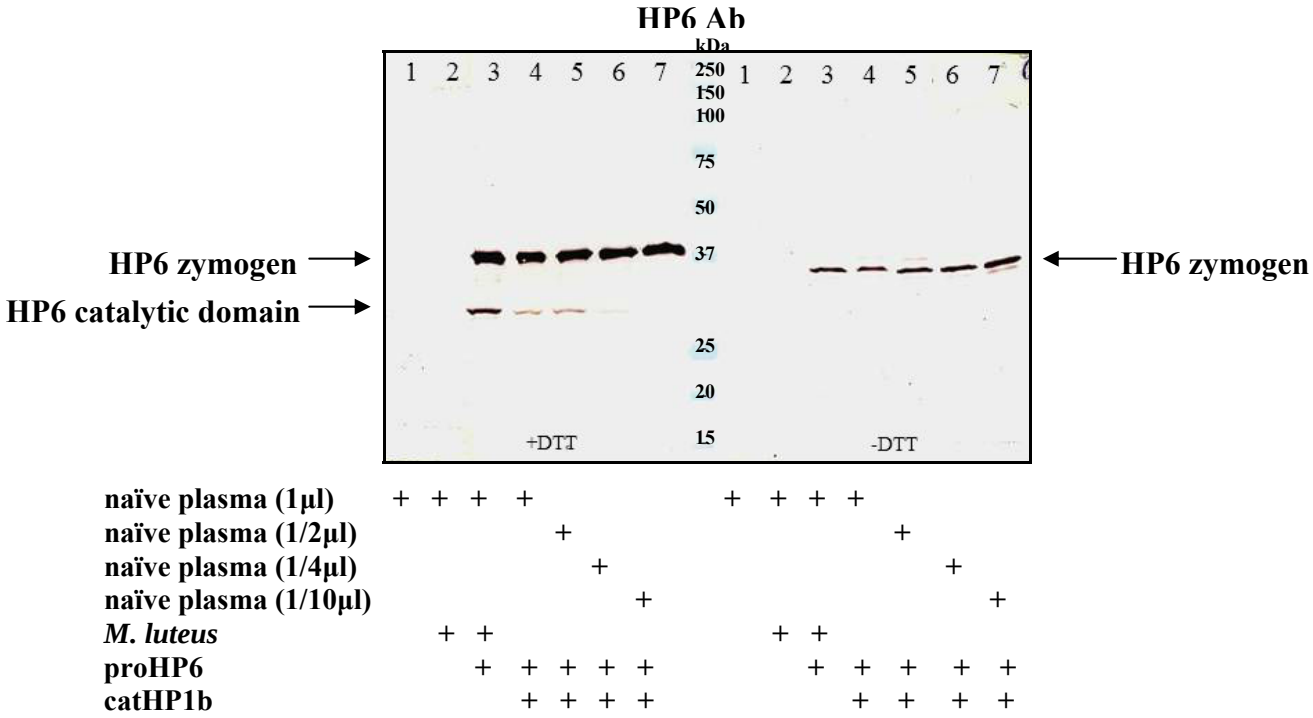

Figure 28. *M. sexta* HP6 activation by catHP1b in the presence of diluted hemolymph. Purified proHP6 (100 ng/µl, 1 µl) was incubated with catHP1b (50 ng/µl, 1 µl) in the presence of a series of diluted plasma in the buffer (7 µl, 20 mM Tris-HCl pH 7.0, 20 mM NaCl) at room temperature for 30 min. Control reactions were plasma alone or naive plasma (1 µl) incubated with the microbial elicitor, *M. luteus* (1 µg/µl, 1 µl) in the same buffer (8 µl) at room temperature for 30 min. All the reaction mixtures were subjected to 10% SDS-PAGE under reducing (+DTT) and non-reducing (-DTT) conditions followed by immunoblot analysis using HP6 antiserum. The sizes and positions of molecular weight standards are indicated in the middle. Bands representing HP6 zymogen and HP6 catalytic domain are marked by arrows. Ab: antibody.

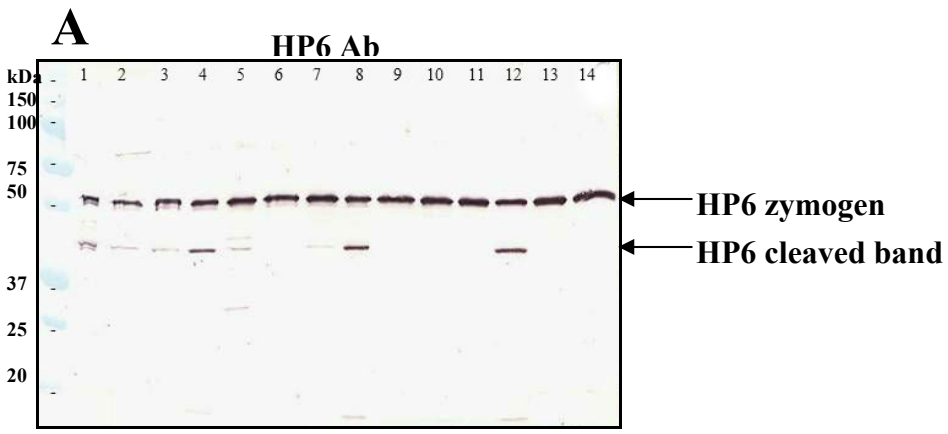

induced plasma (1µl)		+												
M. luteus	+	+												
naïve plasma (1µl)	+													
naïve plasma (1/2µl)			+	+	+	+								
naïve plasma (1/4µl)							+	+	+	+				
naïve plasma (1/8µl)											+	+	+	+
proHP6	+	+	+	+	+	+	+	+	+	+	+	+	+	+
catHP1b			+	+	+	+	+	+	+	+	+	+	+	+
CPC (0.6mM)				+				+				+		
CPC (6mM)					+				+				+	
CPC (60mM)						+				+				+

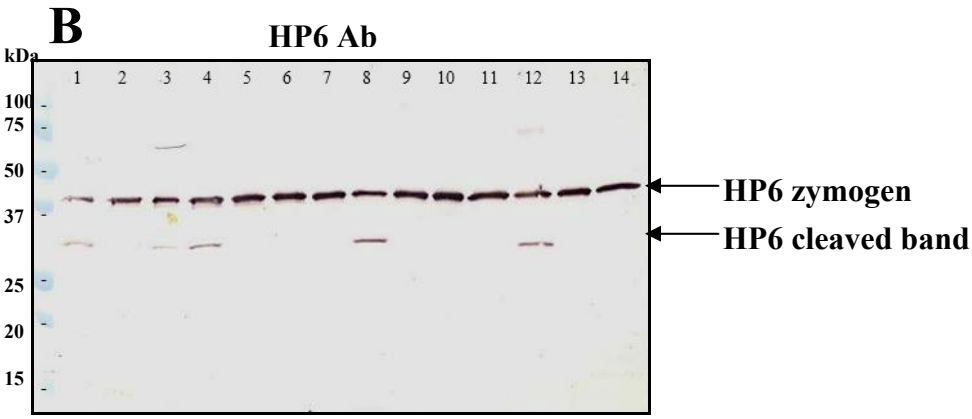

naïve plasma (1µl)	+													
M. luteus	+	+												
induced plasma (1µl)		+												
induced plasma (1/2µl)			+	+	+	+								
induced plasma (1/4µl)							+	+	+	+				
induced plasma (1/8µl)											+	+	+	+
proHP6	+	+	+	+	+	+	+	+	+	+	+	+	+	+
catHP1b			+	+	+	+	+	+	+	+	+	+	+	+
CPC (0.6mM)				+				+				+		
CPC (6mM)					+				+				+	
CPC (60mM)						+				+				+

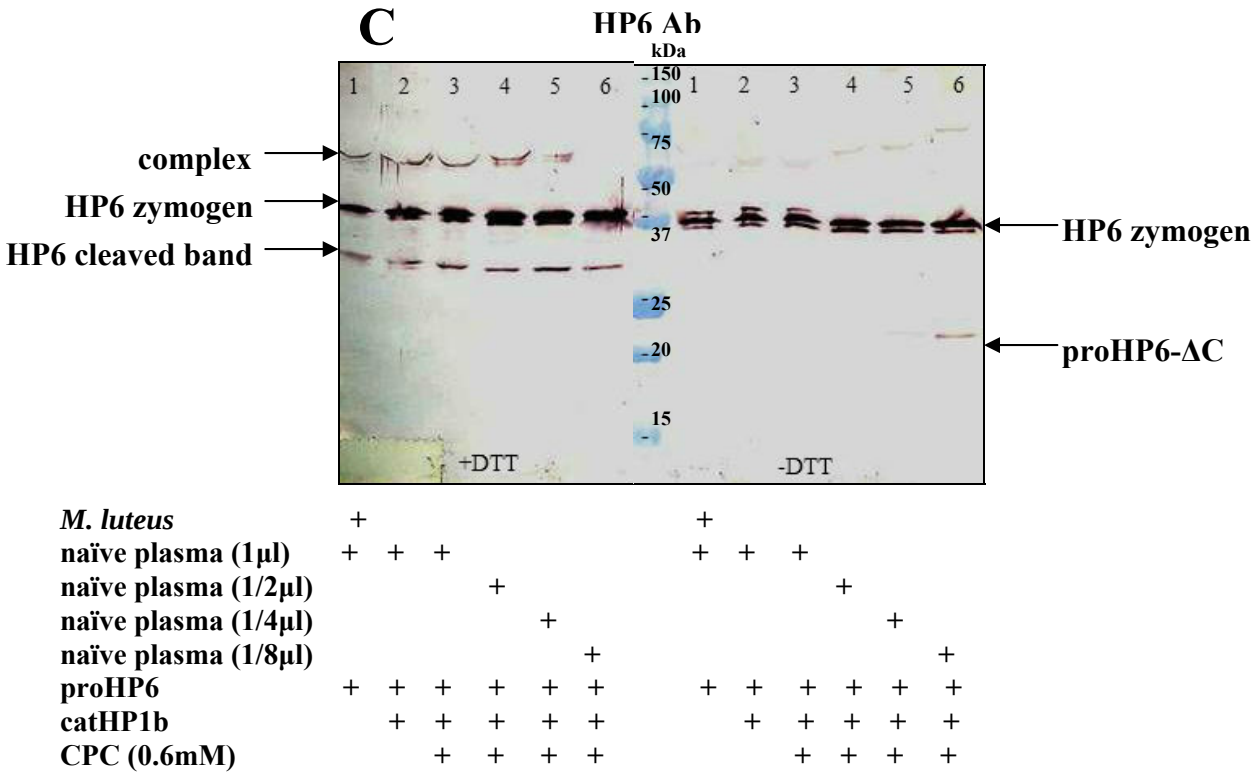

Figure 29. Effects of *M. sexta* hemolymph and CPC on the activation of proHP6. Process of proHP6 by catHP1b in the presence of different conentrations of CPC and a series of diluted naive hemolymph (A) or induced hemolymph (B); Purified proHP6 (100 ng/µl, 1 µl) was incubated with catHP1b (50 ng/µl, 1 µl) in the presence of a series of diluted plasma in the buffer (7 µl, 20 mM Tris-HCl pH 7.0, 20 mM NaCl) at room temperature for 30 min. Control reactions was induced plasma (1 µl) incubated with proHP6 (100 ng/µl, 1 µl) in the presence of microbial elicitor, *M. luteus* (1 µg/µl, 1 µl) in the same buffer (8 µl) at room temperature for 15 min. C, Process of proHP6 by catHP1b in the presence of a series of diluted naive hemolymph and CPC (0.6 mM). Same protocol decribed above except for CPC concentration. All the reaction mixtures were subjected to 10% SDS-PAGE under reducing (+DTT) and non-reducing (-DTT) conditions followed by immunoblot analysis using HP6 antiserum. The sizes and positions of molecular weight standards are indicated in the middle. Bands representing HP6 zymogen, an alternative cleavage product (proHP6-ΔC), HP6 cleaved products and complex are marked by arrows. Ab: antibody.

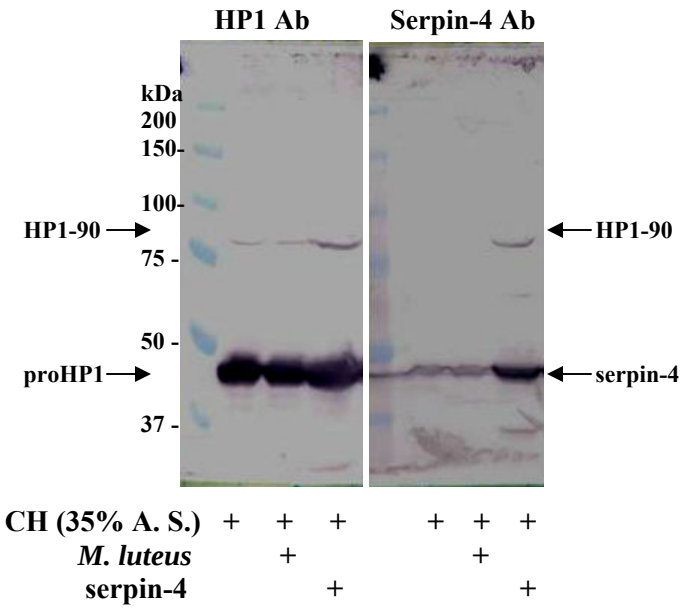

Figure 30. Inhibition of *M. sexta* HP1 activation by serpin-4. 10 µl of induced hemolymph were mixed with 100% saturated ammonium sulfate (5.5 µl, pH 7.0). The ammonium sulfate (A.S.) was adjusted to 35% saturation, and centrifuged to separate precipitate from the supernatant. The pellet was saved and re-dissolved into the buffer (10 µl, 20 mM Tris-HCl, pH 7.5). 35% ammonium sulfate precipitated fraction of control hemolymph was incubated with recombinant serpin-4 (100 ng/µl, 2 µl) (Tong et al., 2005) in the presence of *M. luteus* (1 µg/µl, 1 µl) at room temperature for 30 min. The reaction mixtures were separated by 10% SDS-PAGE and immunoblot analysis was performed using HP1 and serpin-4 antibodies. The sizes and positions of molecular weight standards are indicated on the left. Bands representing proHP1, serpin-4 and complex (HP1-90) are marked by arrows. Ab: antibody.

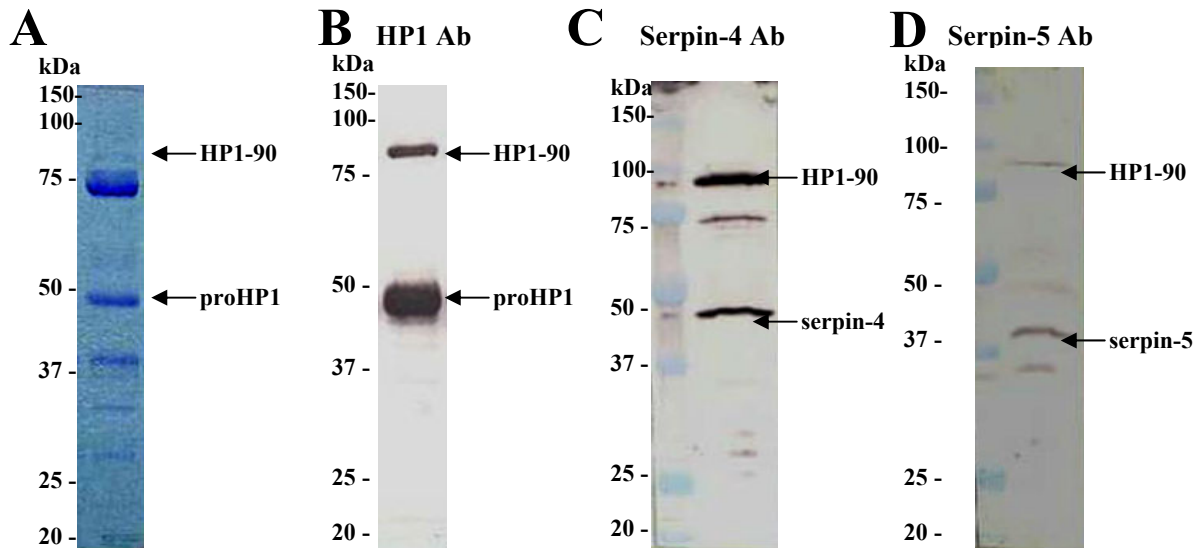

Figure 31. Purification and identification of *M. sexta* HP1-serpin complex from plasma. Elution Franction #2 (12 µl) of immunoaffinity purification was subjected to 10% SDS-PAGE and detected by Coomassie Blue staining or immunoblotting. A, Coomassie Blue stained gel; B, immunoblotting using HP1 antibody; C, immunoblotting using serpin-4 antibody; D, immunoblotting using serpin-5 antibody. . The sizes and positions of molecular weight standards are indicated on the left. Bands representing proHP1, serpin-4, serpin-5 and complex (HP1-90) are marked by arrows. Ab: antibody.

A

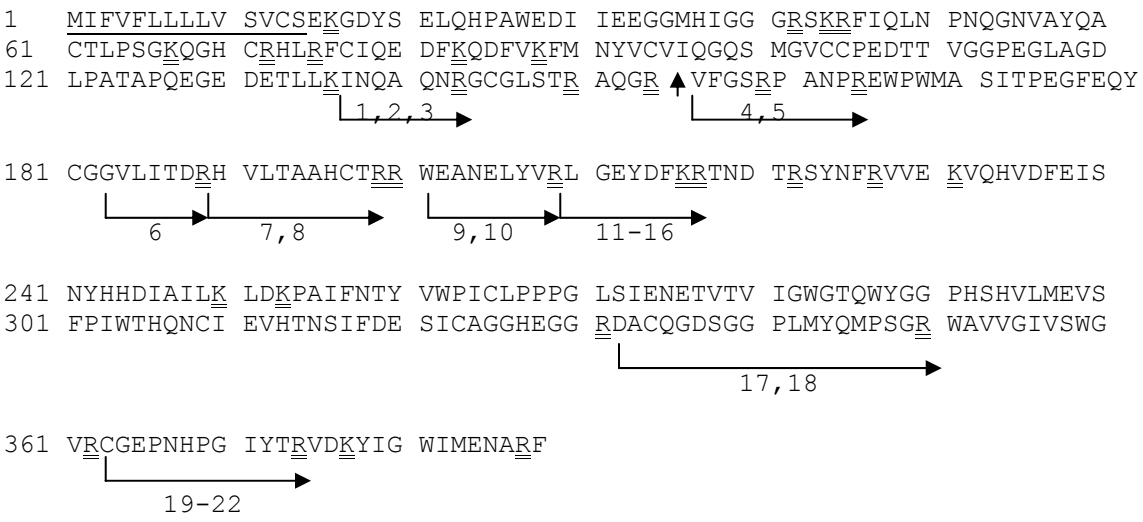

B

Peptide #	Measured Mass (MH^+) from HP1-90	Matched *M. sexta* HP1a Peptide		Putative Residue Modification
		Residues	Computed Mass (MH^+)	
1	842.44	137-143	842.91	
2	842.44	137-143	842.91	
3	842.44	137-143	842.91	
4	1099.59	155-164	1100.25	
5	1099.59	155-164	1100.25	
6	772.45	183-189	772.90	
7	1107.58	190-199	1108.28	①
8	1107.58	190-199	1108.28	①
9	1178.57	201-209	1179.30	
10	1178.57	201-209	1179.30	
11	870.41	210-216	870.96	
12	1026.51	210-217	1027.14	
13	1026.51	210-217	1027.14	
14	1026.51	210-217	1027.14	
15	1026.51	210-217	1027.14	
16	1026.51	210-217	1027.14	
17	1968.83	332-350	1970.18	①, ②, ②
18	1968.83	332-350	1970.18	①, ②, ②
19	1342.63	363-374	1343.48	①
20	1342.63	363-374	1343.48	①
21	1342.63	363-374	1343.48	①
22	1342.63	363-374	1343.48	①

Figure 32. Identification of *M. sexta* HP1a in HP1-serpin complex by MALDI-TOF mass spectrometry. The mass spectral analysis was performed as described in Materials and Methods. A, The amino acid sequence of *M. sexta* HP1a. In the sequence, the signal peptide is underlined. The predicted cleavage site between the clip domain and catalytic domain is indicated by a vertical arrow. Trypsin cleavage sites are double-underlined. The tryptic peptides for which the matching masses were found from mass spectral analysis are indicated with a vertical line (starting point) and an arrow (ending point). The numbers underneath indicate the matching masses listed in B. B, The measured monoisotopic (MH^+) masses from HP1-90 and their corresponding matching peptides from HP1a. The peptides with putative residue modifications are indicated. ①, one cysteine carbamidomethylation; ②, one methionine oxidation.

A

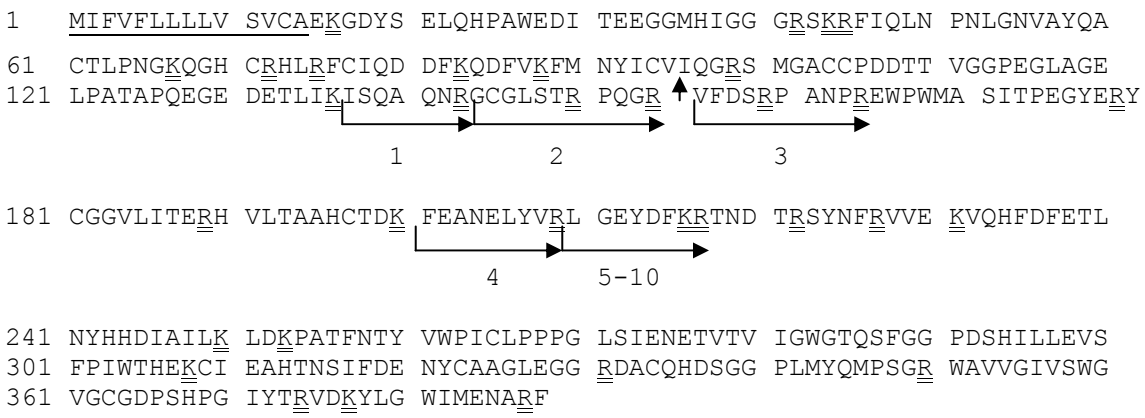

B

Peptide #	Measured Mass (MH^+) from HP1-90	Matched *M. sexta* HP1b Peptide		Putative Residue Modification
		Residues	Computed Mass (MH^+)	
1	815.42	137-143	815.88	
2	1130.58	144-154	1131.27	①
3	1157.59	155-164	1158.28	
4	1139.56	201-209	1140.26	
5	870.41	210-216	870.96	
6	1026.51	210-217	1027.14	

7	1026.51	210-217	1027.14	
8	1026.51	210-217	1027.14	
9	1026.51	210-217	1027.14	
10	1026.51	210-217	1027.14	

Figure 33. Identification of *M. sexta* HP1b in HP1-serpin complex by MALDI-TOF mass spectrometry. The mass spectral analysis was performed as described in Materials and Methods. A, The amino acid sequence of *M. sexta* HP1b. In the sequence, the signal peptide is underlined. The predicted cleavage site between the clip domain and catalytic domain is indicated by a vertical arrow. Trypsin cleavage sites are double-underlined. The tryptic peptides for which the matching masses were found from mass spectral analysis are indicated with a vertical line (starting point) and an arrow (ending point). The numbers underneath indicate the matching masses listed in B. B, The measured monoisotopic (MH^+) masses from HP1-90 and their corresponding matching peptides from HP1b. The peptides with putative residue modifications are indicated. ①, one cysteine carbamidomethylation.

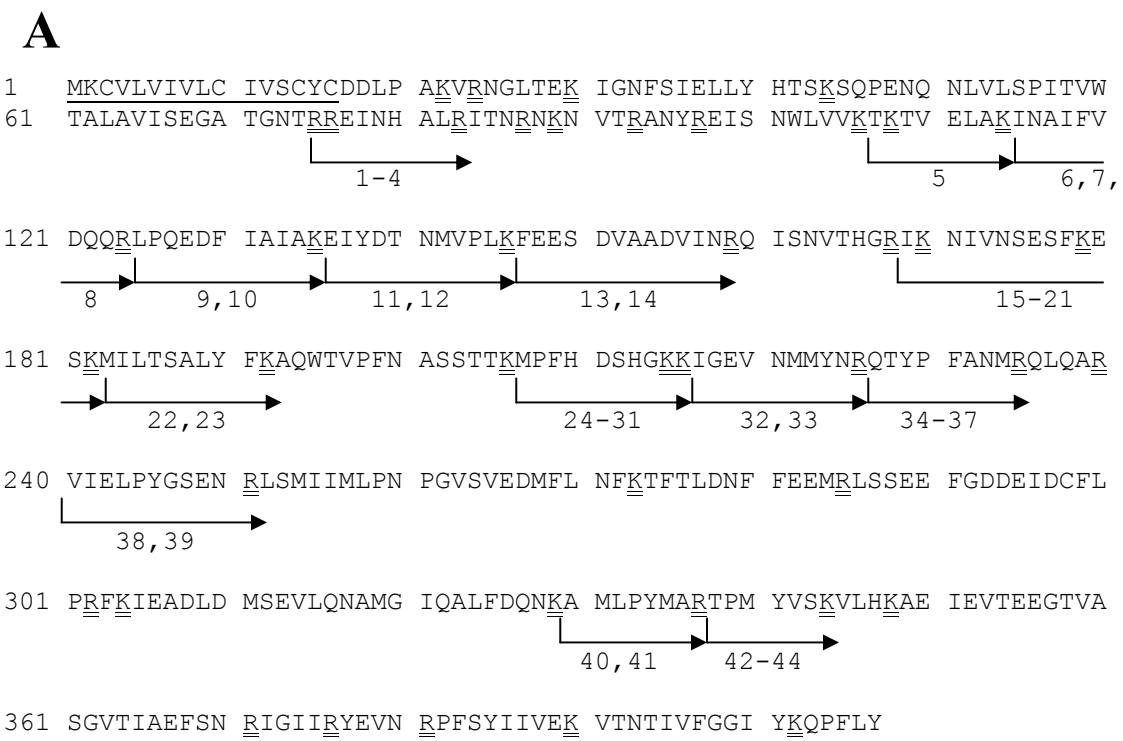

B

Peptide #	Measured Mass (MH^+) from HP1-90	Matched *M. sexta* serpin-4 Peptide		Putative Residue Modification
		Residues	Computed Mass (MH^+)	
1	1007.56	76-83	1008.15	
2	1007.56	76-83	1008.15	
3	851.46	77-83	851.96	
4	851.46	77-83	851.96	
5	888.53	107-114	889.06	
6	1202.64	115-124	1203.36	
7	1202.64	115-124	1203.36	
8	1202.64	115-124	1203.36	
9	1243.68	116-135	1244.45	
10	1243.68	116-135	1244.45	
11	1321.65	136-146	1322.54	②
12	1321.65	136-146	1322.54	②
13	1447.70	147-159	1448.55	
14	1447.70	147-159	1448.55	
15	1277.70	169-179	1278.47	
16	1277.70	169-179	1278.47	
17	1277.70	169-179	1278.47	
18	1621.87	169-182	1622.84	
19	1036.52	171-179	1037.14	
20	1380.69	171-182	1381.51	
21	1380.69	171-182	1381.51	
22	1185.64	183-192	1186.47	②
23	1185.64	183-192	1186.47	②
24	1080.47	207-215	1081.21	②
25	1080.47	207-215	1081.21	②
26	1080.47	207-215	1081.21	②
27	1080.47	207-215	1081.21	②
28	1208.56	207-216	1209.39	②
29	1208.56	207-216	1208.56	②
30	1208.56	207-216	1208.56	②
31	1208.56	207-216	1208.56	②
32	1225.55	217-226	1226.43	②, ②
33	1255.55	217-226	1226.43	②, ②
34	1138.53	227-235	1139.34	②, ③
35	1138.53	227-235	1139.34	②
36	1138.53	227-235	1139.34	②
37	1138.53	227-235	1139.34	②, ③
38	1275.65	241-251	1276.41	
39	1275.65	241-251	1276.41	
40	921.47	330-337	922.11	②

41	921.47	330-337	922.11	②
42	824.41	338-344	824.99	②
43	824.41	338-344	824.99	②
44	824.41	338-344	824.99	②

Figure 34. Identification of *M. sexta* serpin-4 in HP1-serpin complex by MALDI-TOF mass spectrometry. The mass spectral analysis was performed as described in Materials and Methods. A, The amino acid sequence of *M. sexta* serpin-4. In the sequence, the signal peptide is underlined. Trypsin cleavage sites are double-underlined. The tryptic peptides for which the matching masses were found from mass spectral analysis are indicated with a vertical line (starting point) and an arrow (ending point). The numbers underneath indicate the matching masses listed in B. B, The measured monoisotopic (MH^+) masses from HP1-90 and their corresponding matching peptides from serpin-4. The peptides with putative residue modifications are indicated. ②, one methionine oxidation; ③, one glutamine Pyro-cmC.

A

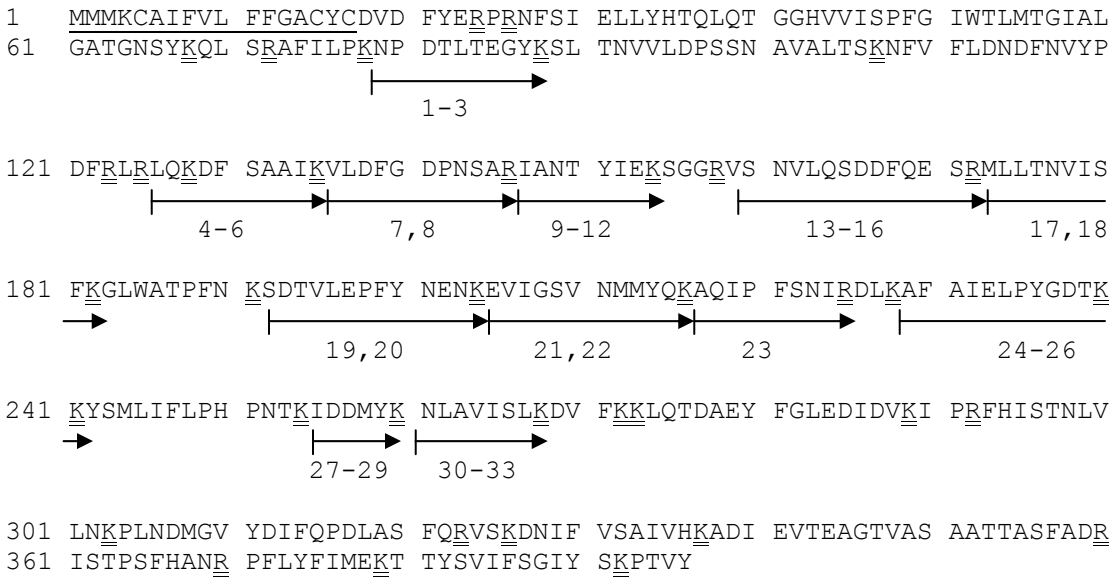

B

Peptide #	Measured Mass (MH^+) from HP1-90	Matched *M. sexta* serpin-5 Peptide		Putative Residue Modification
		Residues	Computed Mass (MH^+)	
1	1136.54	79-88	1137.21	
2	1136.54	79-88	1137.21	
3	1136.54	79-88	1137.21	
4	1119.63	126-135	1120.31	
5	1119.63	126-135	1120.31	
6	750.39	129-135	750.85	
7	1189.57	136-146	1190.28	
8	1189.57	136-146	1190.28	
9	950.51	147-154	951.09	
10	950.51	147-154	951.09	
11	950.51	147-154	951.09	
12	950.51	147-154	951.09	
13	1622.76	159-172	1623.70	
14	1622.76	159-172	1623.70	
15	1622.76	159-172	1623.70	
16	1622.76	159-172	1623.70	
17	1164.65	173-182	1165.46	
18	1164.65	173-182	1165.46	
19	1554.72	192-204	1555.66	
20	1554.72	192-204	1555.66	
21	1397.66	205-216	1398.66	②, ②
22	1397.66	205-216	1398.66	②, ②
23	1044.57	217-225	1045.21	
24	1323.67	229-240	1324.50	
25	1323.67	229-240	1324.50	
26	1451.77	229-241	1452.67	
27	783.34	255-260	783.89	②
28	783.34	255-260	783.89	②
29	783.34	255-260	783.89	②
30	856.54	261-268	857.06	
31	856.54	261-268	857.06	
32	856.54	261-268	857.06	
33	856.54	261-268	857.06	

Figure 35. Identification of *M. sexta* serpin-5 in HP1-serpin complex by MALDI-TOF mass spectrometry. The mass spectral analysis was performed as described in Materials and Methods. A, The amino acid sequence of *M. sexta* serpin-5. In the sequence, the signal peptide is underlined. Trypsin cleavage sites are double-underlined. The tryptic peptides for which the matching masses were found from mass spectral analysis are indicated with a vertical line (starting point) and an arrow (ending point). The numbers underneath indicate the matching

masses listed in B. B, The measured monoisotopic (MH^+) masses from HP1-90 and their corresponding matching peptides from serpin-5. The peptides with putative residue modifications are indicated. ②, one methionine oxidation.

CHAPTER V

CONCLUSIONS

Melanization (prophenoloxidase-activating) is a major innate defense system in many invertebrates. It involves production of highly toxic and reactive compounds around the wounding or infection. The prophenoloxidase-activating pathway includes an extracellular serine proteinase cascade with similarities to blood clotting system and complement system of vertebrates. The recognition of microbial surface components by pattern recognition proteins triggers the activation of the serine proteinase cascade, leading to conversion of inactive prophenoloxidase (proPO) to active phenoloxidase (PO). Inhibitory regulation of the proteinases by serine proteinase inhibitors (serpins) is important for ensuring a localized defense response.

In this study, a new immune responsive serpin from *M. sexta* was investigated. Serpin-8 mRNA and protein levels increased significantly after immune challenge. The amino acid sequence of serpin-8 is similar to *Drosophila* serpin Necrotic. Both of them have an N-terminal extension and a Leu at the predicted P1 site. The serpin-8 core domain (serpin-8-ΔN) was expressed using baculovirus/insect cell system. Serpin-8-ΔN has a specificity being able to inhibit elastase- and chymotrypsin-like proteinases and formed inhibitory complexes with chymotrypsin, Cathepsin G, and elastase. Addition of recombinant serpin-8-ΔN to *M. sexta* plasma suppressed proPO activation. Serpin-8-ΔN inhibits one of the serine proteinases (HP19) in proPO activating pathway by forming inhibitory complex with its catalytic domain. Serpin-8-HP14 inhibitory complex was detected in *M. sexta* hemolymph and serpin-8-ΔN formed complex

with *A. gambiae* HP14 catalytic domain. All of our results indicate that serpin-8-ΔN acts as a serine proteinase inhibitor with the specificity to inhibitor elastase- and chymotrypsin-like proteinases. *M. sexta* HP19 and HP14 are highly possible physiological targets of serpin-8.

Chapter IV reports the expression, purification and functional study of one clip domain serine proteinase in *M. sexta*. Two HP1 isoforms are present in *M. sexta* hemolymph. The two proteins share 90% amino acid sequence similarity. Recombinant HP1 zymogen forms, proHP1a and proHP1b, and catalytic domains, catHP1a and catHP1b were produced using baculovirus/insect cell system. Addition of zymogens or catalytic domains of HP1 into plasma resulted in proPO activation. Proteolytic cleavages of proHP6 and following proteolysis of proHP8 and proPAP-1 caused by HP6 activation were observed, when catHP1a alone was added into plasma. ProHP6 cleavage occurred within the catalytic domain when proHP6 was incubated with proHP1a in the presence of detergent. Some hemolymph factor(s) may contribute to the cleavage of proHP6 at its correct activation site, although the identity of such factor(s) is not yet known. HP1 was found to be regulated by *M. sexta* serpin-4 and serpin-5, and the inhibitory complex formed in an uncommon way.

REFERENCES

An, C., Ishibashi, J., Ragan, E.J., Jiang, H. and Kanost, M.R. (2009) (2009)Functions of Manduca sexta hemolymph proteinases HP6 and HP8 in two innate immune pathways. J. Biol. Chem. 284, 19716–19726.

An, C., Hiromasa, Y., Zhang, X., Lovell, S. and Michel, K. (2012) Biochemical Characterization of Anopheles gambiae SRPN6, a Malaria Parasite Invasion Marker in Mosquitoes. PLoS ONE. 7, e48689

Ashida, M. and Brey, P.T. (1997) Recent advances on the research of the insect prophenoloxidase cascade. Molecular Mechanisms of Immune Responses in Insects. Chapman and Hall, London, 135-172.

Beatty, K., Bieth, J. and Travis, J. (1979) Kinetics of association of serpin proteinases with native and oxidized α-1-proteinase inhibitor andα-1-antichymotrypsin. J. Biol. Chem. 255, 3931–3934.

Bidochka, M.J., Leder, R.J., Robert, D.W. (1997) Induction of novel proteins in *Manduca sexta* and *Blaberus giganteus*as a response to fungal challenge. J. Invertebr. Pathol. 70, 184-189.

Bohn, H., Barwig, B. (1984) Hemolymph clotting in the cockroach *Leucophaea maderae* (Blattaria) Influence of ions and inhibitors; isolation of the plasma coagulogen. J. Comp. Physiol. 154, 457-467.

Boman, H.G. (1991) Antibacterial peptides: Key components needed in immunity. Cell. 65, 205-207.

Boman, H.G. (1994) Cecropins: antibacterial peptides from insects and pigs. In Phylogenetic Perspectives in Immunity: The Insect Host Defense. 3–17.

Brey, P.T., Lee, W.J., Yamakawa, M., Koizumi, Y., Perrot, S., François, M. and Ashida, M. (1993) Role of the integument in insect immunity: epicuticular abrasion and induction of cecropin synthesis in cuticular epithelial cells. Proc. Natl. Acad. Sci. USA. 90, 6275-6279.

Buchon, N. and Lee, B.K. (2009) A single modular serine protease integrates signals from pattern-recognition receptors upstream of the Drosophila Toll pathway. Proc. Natl. Acad. Sci. USA. 106, 12442-12447.

Cerenius, L., Lee B.L. and Soderhall, K. (2008) The proPO-system: pros and cons for its role in invertebrate immunity. Trends. Immunol. 29, 263-271.

Christen, J.M., Hiromasa, Y., An, C. and Kanost. M.R. (2012) Identification of plasma proteinase complexes with serpin-3 in Manduca sexta. Insect. Biochem. Mol. Biol. 42, 946–955.

Coleman, S., Drahm, B., Petersen, G., Stolorov, J. and Kraus, K. (1995) A *Drosophila* male accessory gland protein that is a member of the serpin superfamily of proteinase inhibitors is transferred to females during mating. Insect. Biochem. Mol. Biol. 25, 203–207.

Cornet, B., Bonmatin, J.M., Hetru, C., Hoffmann, J.A., Ptak, M. and Vovelle, F. (1995) Refined three-dimensional solution structure of insect defensin A. Structure. 3, 435–448.

Decker, H. (2007) Similar enzyme activation and catalysis in hemocyanins and tyrosinases. Gene. 398, 183-191.

De Gregorio, E., Han, S.J., Lee, W.J., and Brey, P.T. (2002) An immune-responsive serpin regulates the melanization cascade in *Drosophila*. Dev. Cell. 3, 581–592.

Dimarcq, J.L., Hoffmann, D., Meister, M., Bulet, P., Lanot, R., Reichhart, J.M. and Hoffmann, J.A. (1994) Characterization and transcriptional profiles of a *Drosophila* gene encoding an insect defensin. Eur. J. Biochem. 221, 209–221.

Dunn, P.E. and Drake, D. (1983) Fate of bacteria injected into naïve and immunized larvae of the tobacco hornworm, *Manduca sexta*. J. Invertebr. Pathol. 41, 77-85.

Dushay, M. S., Asling, B. and Hultmark, D. (1996) Origins of immunity: Relish, a compound Rel-like gene in the antibacterial defense of *Drosophila*. Proc. Natl Acad. Sci. USA. 93, 10343–10347.

Dushay, M.S. (2009) Insect hemolymph clotting. Cell. Mol. Life. Sci. 66, 2643-2650.

Evans C.J., Hartenstein, V. and Banerjee, U. (2003) Thicker than blood: conserved mechanisms in *Drosophila* and vertebrate hemotopoiesis. Dev. Cell. 5, 673-690.

Fehlbaum, P., Bulet, P., Michaut, L., Lagueux, M., Broekaert, W.F., Hetru, C. and Hoffmann J.A. (1994) Insect immunity: septic injury of *Drosophila* induces the synthesis of a potent antifungal peptide with sequence homology to plant antifungal peptides of special interest. J. Biol. Chem. 269, 33159–33163.

Gettins, P.G. (2002) Serpin structure, mechanism, and function. Chem. Rev. 102, 4751–4804.

Gillespie, J.P. and Kanost, M.R. (1997) Biological mediators of insect immunity. Ann. Rev. of. Immunol. 42, 611-643.

Gorman, M.J., Wang, Y., Jiang, H. and Kanost, M.R. (2007) *Manduca sexta* hemolymph proteinase 21 activates prophenoloxidase-activating proteinase 3 in an insect innate immune response proteinase cascade. J. Biol. Chem. 282, 11742–11749.

Gottar, M., Gobert, V., Michel, T., Belvin, M., Duyk, G., Hoffmann, J.A., Ferrandon, D., and Royet, J. (2002) The *Drosophila* immune response against Gram-negative bacteria is mediated by a peptidoglycan recognition protein. Nature. 416, 640-644.

Gottar, M., Gobert, V., Matskevich, A.A., Reichhart, J.M., Wang, C. and Ferrandon, D. (2006) Dual detection of fungal infections in Drosophila through recognition of microbial structures and sensing of virulence factors. Cell. 127, 1425-1437.

Harlow, E. and Lane, D. (1988) Antibodies: A Laboratory Manual. Cold Spring Harbor Laboratory, Cold Spring Harbor, NY.

Hetru, C. Bulet, P., Cociancich, S., Dimarcq, J.L., Hoffmann, D., Hoffmann, J.A. (1994) Antibacterial peptides/polypeptides in the insect host defense: a comparison with

vertebrate antibacterial peptides/polypeptides. In Phylogenetic Perspectives in Immunity: The Insect Host Defense, 43–65.

Hoffman, J.A. (1995) Innate immunity of insects. Curr. Opin. Immunol. 7, 4-10.

Hoffman, J.A., Reichhart, J.M., Hetru. C. (1996) Innate immunity in higher insects. Curr. Opin. Immunol. 8, 8-13.

Hoffmann, J.A. and Reichhart, J.M. (2002) Drosophila innate immunity: an evolutionary perspective. Nat. Immunol. 3, 121-126.

Hoffman, JA. (2003). The immune response of *Drosophila*. Nat. 426, 33-38.

Huang, R., Lu, Z., Dai, H. and Jiang, H. (2007) The solution structure of clip domains from Manduca sexta prophenoloxidase activating proteinase-2. Biochem. 46, 11431-11439.

Hultmark, D. (1993). Immune reactions in *Drosophila* and other insects: a model for innate immunity. Trends. Genet. 9, 178-183.

Irving, J.A., Pike, R.N., Lesk, A.M. and Whisstock, J.C. (2000) Phylogeny of the serpin superfamily: implications of patterns of amino acid conservation for structure and function. Genome. Res. 10, 1845–1864.

Iwanaga, S. (1993b) The limulus clotting reaction. Curr. Opin. Immunol. 5, 74-82.

Iwanaga, S. and Lee, B.K. (2005) Recent advances in the innate immunity of invertebrate animals. J. Biochem. Mol. Biol. 38, 128-150.

Janeway, C.J. (1989) Approaching the asymptote? Evolution and revolution in immunology. Cold Spring Harbor, Symp. Quant. Biol. 54, 1-13.

Jang, I.H., Chosa, N., Kim, S.H., Nam, H.J., Lemaitre, B., Ochiai, M. and Lee, W.J. (2006) A spätzle-processing enzyme requires for Toll signaling activation in *Drosophila* innate immunity. Dev. Cell. 10, 45-55.

Jang, I.H., Nam H.J. and Lee, W.J. (2008) Clip-domain serine proteases in *Drosophila* innate immunity. J. Biochem. Mol.Biol. 41, 102-107.

Jiang, H., Wang, Y., Huang, Y., Mulnix, A.B., Kadel, J., Cole, K., and Kanost, M.R. (1996) Organization of serpin gene-1 from *Manduca sexta*: evolution of a family of alternate exons encoding the reactive site loop. J. Biol. Chem. 271, 28017-28023.

Jiang H., Wang, Y., Ma, C. and Kanost M.R. (1997) Subunit composition of pro-phenoloxidase from Manduca sexta: molecular cloning of subunit proPO-P1. Insect. Biochem. Mol. Biol. 27, 835-850.

Jiang, H. and Kanost, M.R. (1997a) Characterization and functional analysis of 12 naturally occurring reactive site variants of serpin-1 from *Manduca sexta*. J. Biol.Chem 272, 1082-1087.

Jiang, H., Wang, Y. and Kanost, M.R. (1998) (1998) Pro-phenol oxidase activating proteinase from an insect, *Manduca sexta*: A bacteria-inducible protein similar to Drosophila easter. Proc. Natl Acad. Sci. USA. 95, 12220–12225.

Jiang, H. and Kanost, M. R. (2000) The Clip-domain family of serine proteinases in arthropods. Insect. Biochem. Mol. Biol. 30, 95-105.

Jiang, H., Wang, Y., Yu, X.Q. and Kanost, M.R. (2003) Prophenoloxidase-activating proteinase-2 from hemolymph of *Manduca sexta*. J. Biol.Chem 278, 3552-3561.

Jiang, H., Wang, Y., Yu, X.Q. Zhu, Y. and Kanost, M.R. (2003) Prophenoloxidase-activating proteinase-3 (PAP-3) from *Manduca sexta* hemolymph: a clip-domain serine proteinase regulated by serpin-1J and serine proteinase homologs. Insect. Biochem. Mol. Biol. 33, 1049-1060.

Jiang, H., Ma, C. Lu, Z. and Kanost, M.R. (2004) β-1,3-glucan-recognition protein-2 (βGRP-2) from *Manduca sexta*, an acute-phase protein that binds β-1,3-glucan and lipoteichoic acid to aggregate fungi and bacteria. Insect. Biochem. Mol. Biol. 34, 89-100.

Jiang, H., Wang, Y., Gu, Y., Guo, X. and Kanost, M.R. (2005) Molecular identification of a bevy of serine proteinases in Manduca sexta hemolymph. Insect. Biochem. Mol. Biol. 35, 931-943.

Ji C., Wang, Y., Guo, X., Hartson S. and Jiang, H. (2004) A pattern recognition serine proteinase triggers the prophenoloxidase activation cascade in the Tobacco Hornworm, *Manduca sexta*. J. Biol. Chem. 279, 34101-34106.

Jung, S.H., Evans, C.J., Uemura, C. and Banerjee, U. (2005) The *Drosophila* lymph gland as a developmental model of hemotopoiesis. Development. 132, 2521-2533.

Kan, H., Kim, C., Kwon, H. and Lee, B.L. (2008) Molecular control of phenoloxidase-induced melanin systhesis in an insect. J. Biol. Chem. 283, 25316-25323.

Kang, D., Liu, G., Lundstrom, A., Gelius, E. & Steiner, H. (1998) A peptidoglycan recognition protein in innate immunity conserved from insects to humans. Proc. Natl Acad. Sci. USA. 95, 10078–10082.

Kanost, M. R. (1999) Serine proteinase inhibitors in arthropod immunity. Devel. Comp. Immunol. 23, 291-301.

Kanost, M. R., Jiang, HB., Yu, XQ. (2004) Innate immune responses of a lepidopteran insect, *Manduca sexta*. Immunol. Rev. 198, 97-105.

Kaufmann, S. (2008) Immunology's foundation: the 100-year anniversary of the Nobel Prize to Paul Ehrlich and Elie Metchnikoff. Nat. Immunol. 9, 705-712.

Kellenberger, C., Leone, P., Coguet, L., Jouenne, T., Reichhart, J.M. and Roussel, A. (2011) Structure-function analysis of grass clip serine protease involved in Drosophila Toll pathway activation. J. Biol. Chem. 286, 12300–12307.

Kim, T., Kim, Y.J., (2005) Overview of innate immunity in *Drosophila*. J. Biochem. Mol. Biol. 38, 121-127.

Kimbrell, DA., Beutler, B. (2001) The evolution and genetics of innate immunity. Nat. Rev. 2, 256-267.

Kruger, O., Ladewig, J., Koster, K. and Ragg, H. (2002) Widespread occurrence of serpin genes with multiple reactive centre-containing exon cassettes in insects and nematodes. Gene. 293, 97–105.

Ladendorff, N.E. and Konast, M.R. (1990) Isolation and characterization of bacteria-induced protein P4 from hemolymph of *Manduca sexta*. Arch. Insect. Biochem. Physiol. 15, 33-41.

Lee, S.Y., Moon, H.J., Kurata, S., Natori, S. and Lee, B.L. (1995) Purification and cDNA cloning of an antifungal protein from the hemolymph of *Holotrichia diomphalia* larvae. Biol. Pharm. Bull. 18, 1049–1052.

Lee, W.J., Lee, J.D., Kravchenko, V.V., Ulevitch, R.J., and Brey, P.T. (1996) Purification and molecular cloning of an inducible gram-negative bacteria-binding protein from the silkworm, *Bombyx mori*. Proc. Natl. Acad. Sci. USA. 93, 7888-7893.

Lee, S.Y., Kwon, T.H., Hyun, J.H., Choi, J.S., Kawabata, S.I., Iwanaga, S. and Lee, B.L. (1998) In vitro activation of pro-phenol-oxidase by two kinds of pro-phenol-oxidase-activating factors isolated from hemolymph of coleopteran, *Holotrichia diomphalia* larvae. Eur. J. Biochem. 254, 50-57.

Lee, K.Y., Horodyski, F.M., Valaitis, A.P. and Denlinger, D.L. (2002) Molecular characterization of the insect immune protein hemolin and its high induction during embryonic diapause in the gypsy moth, *Lymantria dispar*. Insect. Biochem. Mol. Biol. 32, 1457-1467.

Lee, M.H., Osaki, T., Lee, J.Y. and Lee, B.L. (2004) Peptidoglycan recognition proteins involved in 1,3-β-D-glucan-dependent prophenoloxidase activation system of insect. J. Biol. Chem. 279, 3218-3227.

Lemaitre, B., Nicolas, E., Michaut, L., Reichhart, J. M. and Hoffmann, J. A. (1996) The dorsoventral regulatory gene cassette spatzle/Toll/cactus controls the potent antifungal response in *Drosophila* adults. Cell. 86, 973–983.

Lemaitre, B., Hoffmann, JA. (2007) The host defense of *Drsophila melanogaster*. Annu. Rev. Immunol. 25, 697-743.

LeMosy, E.K., Hong, C.C. and Hashimoto, C. (1999) Signal transduction by a protease cascade. Trends. Cell. Biol. 9, 102-107

Leulier, F., Rodriguez, A., Khush, R.S., Abrams, J.M. and Lemaitre, B. (2000) The Drosophila caspase Dredd is requires to resist gram-negative baterial infection. EMBO. J. 1, 353-358.

Levashina, E.A., Langley, E., Green, C., Gubb, D., Ashburner, M., Hoffmann, J.A. and Reichhart, J.M. (1999) Constitutive activation of toll-mediated antifungal defense in serpin-deficient *Drosophila*. Science. 285, 1917–1919.

Li, Y., Wang, Y., Jiang, H. and Deng, J. (2009) Crystal structure of Manduca sexta prophenoloxidase provides insights into the mechanism of type 3 copper enzymes. Proc. Natl Acad. Sci. USA. 106, 17002–17006.

Ling, E. and Yu, X.Q. (2005) Prophenoloxidase binds to the surface of hemocytes and is involved in hemocyte melanization in *Manduca sexta*. Insect. Biochem. Mol. Biol. 35, 1356–1366.

Ligoxygakis, P., Pelte, N., Jiang, H., Hoffmann, J.A. and Reichhart, J.M. (2002) A serpin mutant links Toll activation to melanization in the host defence of *Drosophila*. EMBO J. 21, 6330–6337.

Liu, C., Xu, Z., Gupta, D., and Dziarski, R. (2001) Peptidoglycan recognition proteins: a novel family of four human innate immunity pattern recognition molecules. J. Biol. Chem. 276, 34686-34694.

Lowenberger, C., Bulet, P., Charlet, M., Hetru, C., Hodgeman, B., Christensen, B.M. and Hoffmann, J.A. (1995) Insect Immunity isolation of three novel inducible antibacterial defensins from the vector mosquito, *Aedes aegypti*. Insect. Biochem. Mol. Biol. 25, 867–873.

Lu Z. and Jiang H. (2008) Expression of Manduca sexta serine proteinase homolog precursors in insect cells and their proteolytic activation. Insec. Biochem. Mol. Biol. 38, 89-98.

Ma, C. and kanost, M.R. (2000) A β-1,3-glucan-recognition protein from an insect, *Manduca sexta*, agglutinates microorganisms and activates the prophenoloxidase cascade. J. Biol. Chem. 275, 7505-7514.

Meister, M. (2004) Blood cells of *Drosophila*: cell lineages and role in host defense. Curr. Opin. Immunol. 16, 10-15.

Michel, T., Reichhart, J.M., Hoffmann, J.A., and Royet, J. (2001) *Drosophila* Toll is activated by Gram-positive bacteria through a circulating peptidoglycan recognition protein. Nature. 414, 756-759.

Morishma, I., Horiba, T., Iketani, M., Nishioka, E., Horiba, T., Iketani, M., Nishioka, E. and Yamano, Y. (1995) Parallel induction of cecropin and lysozyme in larvae of the silkworm *Bombyx mori.* Dev. Comp. Immunol. 19, 357-363.

Ochiai, M. and Ashida, M. (1999) A pattern recognition protein for peptidoglycan: cloning the cDNA and the gene of the silk worm, *Bombyx mori.* J. Biol. Chem. 274, 11854-11858.

Osaki, T., Omotezako, M., Nagayama, R., Hirata, M., Iwanaga, S., Kasahara, J., Hattori, J., Ito, I., Sugiyama, H. and Kawabata, S. (1999) Horseshoe crab hemocyte-derived antimicrobial polypeptides, tachystatins, with sequence similarity to spider neurotoxins. J. Biol. Chem. 274, 26172-26178.

Park, J., Kim, C., Kim, J. and Lee, B.L. (2007) Clustering of peptidoglycan recognition protein-SA is required for sensing lysine-type peptidoglycan in insects. Proc. Natl. Acad. Sci. USA. 104, 6602-6607.

Pelte, N., Robertson, A.S., Zou, Z., Reichhart, J.M. and Gubb, D. (2006) Immune challenge induces N-terminal cleavage of the Drosophila serpin Necrotic. Insect. Biochem. Mol. Biol. 36, 37–46.

Perona, J.J. and Craik, C.S. (1995) Structural basis of substrate specificity in the serine proteases. Protein Sci. 4, 337-360.

Piao, S., Kim, S., Kim, J.H., Park, J.W., Lee, B.L. and Ha, N.C. (2007) Crystal structure of the serine protease domain of prophenoloxidase activating factor-I. J. Biol. Chem. 282, 10783–10791.

Ramet, M., Manfruelli, P., Pearson, A., Mathey-Prevot, B., and Ezekowitz, R.A. (2002) Functional genomic analysis of phagocytosis and identification of a *Drosophila* receptor for *E. coli.* Nature. 416, 644-648.

Rasmuson, T. and Boman, H.G. (1979) Purification and some properties of immune protein P4 from hemolymph of *Hyalophora cecropia* pupae. Insect. Biochem. 9, 259-264.

Ragan, E.J., An, C., Yang, C.T. and Kanost, M.R. (2010) Analysis of Mutually Exclusive Alternatively Spliced Serpin-1 Isoforms and Identification of Serpin-1 Proteinase Complexes in Manduca sexta Hemolymph. J. Biol. Chem. 285, 29642–29650.

Rizki, T.M. and Rizki, R.M. (1984). The cellular defense system of *Drosophila melanogaster*. Plenum New York, USA. 579-604.

Rizki, T.M. (1985) Genetics of a *Drosophila* phenoloxidase. Mol. Gen. Genet. 201, 7–13.

Robertson, A.S., Belorgey, D., Lilley, K.S., Lomas, D.A., Gubb, D. and Dafforn, T.R. (2003) Characterization of the necrotic protein that regulates the Toll-mediated immune response in *Drosophila*. J. Biol. Chem. 278, 6175-6180.

Shi, L., Li, B. and Paskewitz, S.M. (2006) Cloning and characterization of a putative inhibitor of melanization from *Anopheles gambiae*. Insect. Mol. Biol. 15, 313–320.

Shrestha, S. and Kim, Y. (2008) Eicosanoids mediate prophenoloxidase release from ooenocytoids in the beet armyworm *Spodoptera exigua.* Insect. Biochem. Mol. Biol. 38, 99–112.

Skinner, W., Dennis,P, Li, J., Summerfelt, R., Carney, R. and Quistad, G. (1991) Isolation and identification of paralytic peptides from hemolymph of the lepidopteran insects *Manduca sexta*, *Spodoptera exigua*, and *Heliothis virescens*. J. Biol. Chem. 266, 12873-12877.

Söderhäll, K. and Smith, V.J. (1983) Separation of the haemocyte populations of *Carcinus maenas* and other marine decapods, and prophenoloxidase distribution. Dev. Comp. Immunol. 7, 229–239.

Söderhäll, K., Corenius, L. and Johansson, M. (1996) The prophenoloxidase activating system in invertebrates. New Directions in Invertebrate Immunology. 229-254.

Sondergaard, L. (1993) Homology between the mammalian liver and the *Drosophila* fat body. Trends. Genet. 9, 193.

Soukup, S.F., Culi, J. and Gubb, D. (2009) Uptake of the Necrotic Serpin in Drosophila melanogaster via the Lipophorin Receptor-1. PLOS. 5, 1-13.

Steiner, H. (2004) Peptidoglycan recognition proteins: on and off switches for innate immunity. Immunol. Rev. 198, 83–96.

Strand, M.R., Pech, L.L. (1995) Immunological basis for compatibility in parasitoid-host relationships. Annu. Rev. Entomol. 40, 31-56.

Su, X.D., Gastinel, I.N., Vaughn, D.E., Faye, I., Poon, P. and Bjorkman, P.J. (1998) Crystal structure of hemolin: A horseshoe shape with implications for homophilic adhesion. Science. 281, 991-995.

Takehana, A. (2002) Overexpression of a pattern-recognition receptor, peptidoglycan-recognition protein-LE, activates imd/relish-mediated antibacterial defense and the prophenoloxidase cascade in *Drosophila* larvae. Proc. Natl. Acad. Sci. USA. 99, 13705-13710.

Tong, Y., Jiang, H. and Kanost, M.R. (2005) Identification of plasma proteases inhibited by *Manduca sexta* Serpin-4 and Serpin-5 and their association with components of the prophenoloxidase activation pathway. J. Biol. Chem. 280, 14932-14942.

Tzou, P, Ohresser, S., Ferrandon, D., Capovilla, M. and Reichhart J.M. (2000) Tissue-specific inducible expression of antimicrobial peptide genes in *Drosophila* surface epithelia. Immunity. 13, 737-748.

Vilmos, P. and Kurucz, E. (1998) Insect immunity: evolutionary roots of the mammalian innate immune system. Immunol. Letters. 62, 59-66.

Wang, Y., Jiang, H. and Kanost, M.R. (1999) Biological activity of *Manduca sexta* paralytic and plasmatocyte spreading peptide and primary structure of its hemolymph precursor. Insect. Biochem. Mol. Biol. 29, 1075-1086.

Wang, Y., Jiang, H. and Kanost, M.R. (2001) Expression and purification of Manduca sexta prophenoloxidase-activating proteinase precursor (proPAP) from Baculovirus-infected insect cells. Protein Expression and Purification. 23, 328-337.

Wang, Y., Jiang, H. (2006) Interaction of β-1,3-Glucan with its recognition protein activates hemolymph proteinase 14, an initiation enzyme of the prophenoloxidase activation system in *Manduca sexta*. J. Biol. Chem. 281, 9271-9278.

Wang, Y. and Jiang, H. (2007) Reconstitution of a branch of the Manduca sexta prophenoloxidase activation cascade in vitro Snake-like hemolymph proteinase 21 (HP21) cleaved by HP14 activates prophenoloxidase-activating proteinase-2 precursor. Insect. Biochem. Mol. Biol. 37, 1015-1025.

Wang Y. and Jiang, H. (2008) (2008)A positive feedback mechanism in the Manduca sexta prophenoloxidase activation system. Insect. Biochem. Mol. Biol. 38, 763-769.

Wang, Y., Sumathipala, N., Rayaprolu, S. and Jiang, H. (2011) Recognition of microbial molecular patterns and stimulation of prophenoloxidase activation byβ-1,3-glucanase-related protein in *Manduca sexta* larval plasma. Insect. Biochem. Mol. Biol. 41, 322-331.

Waterhouse, R.M. (2007) Evolutionary dynamics of immune-related genes and pathways in disease-vector mosquitoes. Science. 316, 1738-1743.

Weis, W.I., Taylor, M.E. and Drickarner, K. (1998) The C-type lectin superfamily in the immune system. Immunol. Rev. 163, 19-34.

Ye, S., Cech, A.L., Belmares, R., Bergstrom, R.C., Tong, Y., Corey, D.R., Kanost, M.R. and Goldsmith, E.J. (2001) The structure of a Michaelis serpin-protease complex. Nat. Struct. Biol. 8, 979-983.

Yoshida, H., Kinoshita, K. and Ashida, M. (1996) Purification of a peptidoglycan recognition protein from hemolymph of the silkworm, *Bombyx mori*. J. Biol. Chem. 271, 13854-13860.

Yu, X.Q., Gan, H. and Kanost, M.R. (1999) Immulectin, an inducible C-type lectin from an insect, *Manduca sexta*, stimulates activation of plasma prophenol oxidase. Insect. Biochem. Mol. Biol. 29, 585-597.

Yu, X.Q. and Kanost, M.R. (2000) Immunlectin-2, a lipopolysaccharide-specific lectin from an insect, *Manduca sexta*, is induced in response to Gram-negative bacteria. J. Biol. Chem. 275, 37373-37381.

Yu, X.Q., Zhu, Y., Ma, C., Fabrick, J.A. and Kanost, M.R. (2002) Pattern recognition proteins in *Manduca sexta* plasma. Insect. Biochem. Mol. Biol. 32, 1287-1293.

Yu, X.Q., Jiang, H., Wang, Y. and Kanost, M.R. (2003) Nonproteolytic serine proteinase homologs are involved in prophenoloxidase activation in the tobacco hornworm, *Manduca sexta*. Insect. Biochem. Mol. Biol. 33, 197–208.

Zhang, S., Gunaratna, R.T., Zhang, X., Najar, F., Wang, Y, Roe, B. and Jiang, H. (2011) Pyrosequencing-based expression profiling and identification of differentially regulated genes from *Manduca sexta*, a leipidopteran model insect. Insect. Biochem. Mol. Biol. 41, 733–746.

Zhao, P., Li J., Wang, Y. and Jiang, H. (2007) Broad-spectrum antimicrobial activity of the reactive compounds generated in vitro by Manduca sexta phenoloxidase. Insect. Biochem. Mol. Biol. 37, 952–959.

Zhu, Y., Wang, Y., Gorman, M. J., Jiang, H. and Kanost, M. R. (2003) *Manduca sexta* serpin-3 regulates prophenoloxidase activation in response to infection by inhibiting prophenoloxidase-activating proteinases. J. Biol. Chem. 278, 46556-46564.

Zou, Z. and Jiang, H. (2005) *Manduca sexta* serpin-6 regulates immune serine proteinases PAP-3 and HP8: cDNA cloning, protein expression, inhibition kinetics, and functional elucidations. J. Biol. Chem. 280, 14341-14348.

Zou, Z., Lopez, D.L., Kanost, M.R., Evans, J.D. and Jiang, H. (2006) Comparative analysis of serine protease-related genes in the honey bee genome: possible involvement in embryonic development and innate immunity. Insect. Mol. Biol. 31, 57-63.

APPENDICES

Expression of catalytic domains of hemolymph proteinases in *M. sexta*

Name	Primers (MfeI/XhoI)	PCR product (kb)	Predicted MW (kDa)	Sequencing result (correct clone in T vector)	Bacmid	Transfection	Expression
catHP1	+j586/-j587	704	26.63	HP1-1	HP1-2,3,4,5	Yes	dectected
catHP2	+j588/-j589	740	27.23	HP2-1	HP2-1,2	Yes	
catHP5	+j590/-j591	782	28.55	HP5-1	HP5-1,2	Yes	
catHP6	+j592/-j500	743	27.00	HP6-1(partial digestion)			
catHP8	+j593/-j501	779	28.55	HP8-5(partial digestion)	HP8-1,2,3,4		
catHP9	+j594/-j502	797	28.44	HP9-3	HP9-1,2,3,4	Yes	
catHP12n	+j595/-j596	839	30.93	HP12n-4	HP12n-1,2,3,4	Yes	
catHP13	+j597/-j516	746	27.64	HP13-2	HP13-1,2	Yes	

catHP15	+j598/-j504	824	30.40	HP15-1	HP15-1,2,3	Yes	dectected
catHP16	+j599/-j600	776	28.38	HP16-1	HP16-1,2,3,4	Yes	
catHP17	+j638/-j505	770	28.64	HP17-1	HP17-1	Yes	
catHP18	+j639/-j454	752	27.27	HP18-1	HP18-1,2,3,4	Yes	
catHP19	+j640/-j641	761	28.49	HP19-1	HP19-1,2,3	Yes	dectected
proHP20	+j642/-j643	932	34.21	proHP20-5	proHP20-1,2,3	Yes	dectected
catHP21	+j644/-j540	743	27.64	HP21-2	HP21-1,2,3	Yes	
catHP22	+j645/-j646	740	27.42	HP22-2(partial digestion)	HP22-1,2,3,4	Yes	
catHP23	+j647/-j648	818	30.69	HP23-2	HP23-1,2,3	Yes	dectected
catHP25	+j649/-j577	909	32.82	HP25-2	HP25-1,2	Yes	dectected
catPAP-1	+j395/-j396	770	28.03	PAP1-1(partial digestion)	PAP1-3,4,5,6	Yes	dectected

VITA

Fan Yang

Candidate for the Degree of

Doctor of Philosophy

Thesis: ROLES OF *MANDUCA SEXTA* SERPIN-8 AND HEMOLYMPH PROTEINASE-1 IN THE PROPHENOLOXIDASE ACTIVATION SYSTEM

Major Field: Entomology

Biographical:

Education:

Completed the requirements for the Doctor of Philosophy in Entomology at Oklahoma State University, Stillwater, Oklahoma in December, 2012.

Completed the requirements for the Master of Science in Microbial and Biochemical Pharmacy at East China University of Science and Technology, Shanghai, China in 2007.

Completed the requirements for the Bachelor of Science in Food Science and Engineering at East China University of Science and Technology, Shanghai, China in 2004.

Experience:

Graduate Research Assistant at Oklahoma State University from 2007-2012
Graduate Research Assistant at East China University of Science and Technology from 2004-2007